INVESTIGATION OF HEAT TRANSFER AUGMENTATION THROUGH USE OF INTERNALLY FINNED AND ROUGHENED TUBES (Final Summary Report)

A.E. Bergles
G.S. Brown, Jr.
R.A. Lee
R.R. Simonds
W.D. Snider

Report No. DSR 70790-69

F. W. French Tube Company
Newtown, Connecticut

Engineering Projects Laboratory
Department of Mechanical Engineering
Massachusetts Institute of Technology
Cambridge, Massachusetts 02139

August 1970

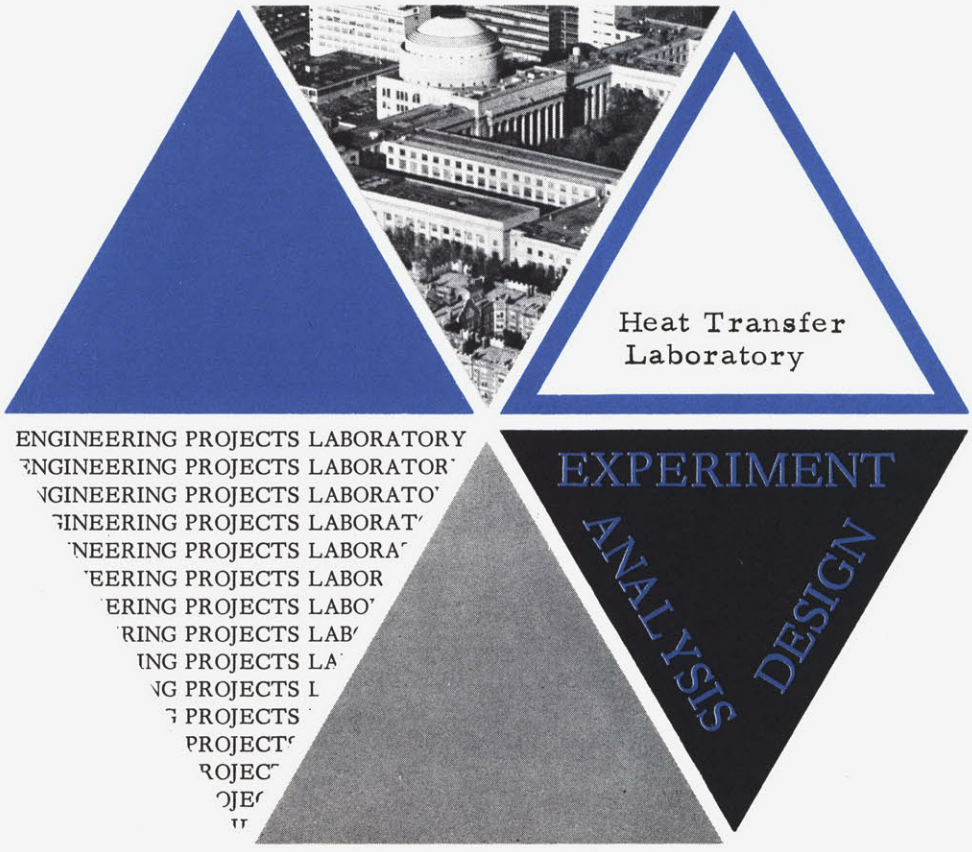

TECHNICAL REPORT NO. 70790-69

FINAL SUMMARY REPORT

INVESTIGATION OF HEAT TRANSFER AUGMENTATION THROUGH USE OF INTERNALLY FINNED AND ROUGHENED TUBES

A. E. Bergles
G. S. Brown, Jr.
R. A. Lee
R. R. Simonds
W. D. Snider

for

French Tube
Division of Noranda Metal Industries, Inc.
Prospect Drive
Newtown, Connecticut 06470

August, 1970

DSR Project 70790

Heat Transfer Laboratory
Engineering Projects Laboratory
Department of Mechanical Engineering
Massachusetts Institute of Technology
Cambridge, Massachusetts 02139

ABSTRACT

This report summarizes a three-year program concerned with obtaining basic design information for tubes having a random roughness on the inside wall (RID) and tubing having continuous internal fins (Forge Fin). Test apparatus and procedures were developed to obtain accurate heat-transfer and friction data for a wide variety of tube geometries using water as the test fluid.

For the random roughness the heat-transfer coefficient was above the smooth tube value, for comparable flow conditions, by over 60 percent at a Reynolds number of 30,000. Larger percentage improvements can be expected for higher Reynolds numbers and for fluids having higher Prandtl numbers. Improvements in performance, based on equal pumping power for augmented and smooth tubes, of about 50 percent were observed.

The heat-transfer characteristics for tape-generated swirl flow through rough tubes were investigated in order to determine the interaction of swirl flow and roughness effects. For the particular range of parameters covered, for equal flow rates, the maximum improvement in heat transfer with swirl flow in smooth tubes was 70 percent, whereas with swirl flow in rough tubes, the improvement was as much as 100 percent. The heat-transfer coefficient for rough tube swirl flow was accurately correlated by a modification of an additive expression previously suggested for prediction of smooth tube swirl flow data.

The test program for internally finned tubes established that short spiralled fins produce the greatest improvement in heat transfer. On the basis of equal flow conditions, the heat transfer was improved by over 200 percent; while at equal pumping power, the performance was as high as 170 percent. These improvements, which are attributed to increased area and turbulence promotion, appear to equal the improvements displayed by any of the schemes used to augment heat transfer inside tubes.

In order to bring the augmentation problem into perspective, a discussion of data for other types of roughness and finning is included.

ERRATA FOR REPORT 70790-69

Page	
vi	Ref. 42: Brouillette
4	Last heading for Table 1: (μ in.)
5	Delete not in last line
15	Line 17: protuberance
16	close brackets at end of Eq. (14)
20	Line 1: D_e-approach
25	Line 28: diamond
36	Line 23: presumed to be the same for both cases.
37	Eq. (A2-11): right handed side should have $Re_{a,h}$ Line 13: $(h_a/h_o)_p$
47	Line 28: Brouillette
52	Ref. 11, third line: Nucleaires
55	Ref. 38: Kolař Ref. 49: Maulbetsch

TABLE OF CONTENTS

LIST OF FIGURES

NOMENCLATURE

A	=	cross-sectional flow area
A_{eff}	=	effective internal heat-transfer area noted in Eq. (A2-7a)
C	=	constant
C_{min}	=	capacity rate defined in Eq. (A2-4)
c_p	=	specific heat at constant pressure
D	=	tube diameter
e	=	rms surface roughness
e_s	=	equivalent sand grain roughness
F	=	fin effect multiplier, defined by Eq. (9)
f	=	Fanning friction factor
G	=	mass velocity
g_c	=	conversion factor
h	=	heat-transfer coefficient
k	=	thermal conductivity
L_h	=	heated length of tube
L_p	=	length between pressure taps
Nu	=	Nusselt number = hD/k
P	=	wetted perimeter
ΔP	=	pressure drop
Pr	=	Prandtl number = $c_p \mu/k$
Q	=	volume flow rate
q	=	rate of heat transfer
q''	=	heat flux
Re	=	Reynolds number = $G D/\mu$
T	=	temperature
ΔT	=	wall minus fluid temperature, $T_w - T_b$
U	=	overall heat-transfer coefficient
V	=	mean axial fluid velocity
w	=	mass flow rate
y	=	tape twist ratio = inside diameters/180° of tape twist
y	=	distance normal to tube wall
y^+	=	dimensionless distance from tube wall = $(y/\nu)\sqrt{fV^2/2}$

α = geometric parameter defined by Eq. (11)

β = volumetric coefficient of thermal expansion

δ = distance from tube wall defined by Eq. (3)

ε = heat-exchanger effectiveness defined in Eq. (A2-5)

ε_H = eddy diffusivity for heat transfer

ρ = mean fluid density

μ = dynamic viscosity

ν = kinematic viscosity

SUBSCRIPTS

a = tube modified to augment heat transfer

b = bulk fluid condition

cc = centrifugal convection

di = diabatic conditions

iso = isothermal conditions

h = based on hydraulic diameter

i = based on internal (nominal) diameter

in = conditions at tube inlet

o = smooth tube without swirl tape

out = conditions at tube outlet

P = constant pumping power comparison

r = rough tube without swirl tape

rs = rough tube with swirl tape

s = smooth tube with swirl tape

sc = spiral convection

st = steam condition

w = tube inner wall condition

wo = tube outer wall condition

SUPERSCRIPT

- = average condition along length of heated tube

All fluid properties are evaluated at the bulk temperature unless otherwise indicated.

1. INTRODUCTION

Most of the extensive research in heat transfer has been devoted to understanding the process under normal conditions. In recent years, however, there has been increased emphasis on techniques which augment or intensify heat transfer. Laboratory verification has progressed to the point where many of the techniques can be considered seriously for application to heat exchange equipment on a commercial basis. The techniques which have been found to improve heat transfer to flow inside of tubes, usually at the expense of pumping power or external power applied to the system, include: 1) surface promoters, 2) displaced promoters, 3) vortex flows, 4) surface vibration, 5) fluid vibration, 6) electrostatic fields, and 7) fluid additives.

Recent surveys [1,2][1] considers these techniques in some detail. In general, the methods requiring external power, 4, 5, and 6, are difficult to apply to large-scale heat-exchange equipment. Information relating to the increased equipment cost and power requirements is generally lacking; however, it would appear that vibrations and electrostatic fields cannot be justified on an economic basis. The addition of small amounts of an additive is beneficial only in specific applications, such as pool boiling.

The methods which require no external power, 1, 2, and 3, can be incorporated in the design of new equipment or introduced into existing equipment. Displaced promoters are difficult to install inside tubes, and generally have very large friction factors. These promoters appear to be of real value only in flow bulk boiling where they force additional liquid to the heated surface. When practicality and effectiveness are considered, it appears that surface promoters and vortex flow are the most attractive candidates for commercial use at the present time.

Surface promoters range from selective finishing of the surface to increasing the surface area significantly by adding fins. The literature

---

[1]Numbers in brackets denote references listed beginning on p. 52.

reviews suggest that only special types of roughness will yield good performance[2]; many surface treatments produce a substantial reduction in heat-transfer performance. Unfortunately, the understanding of rough surface behavior is not yet to the point where friction and heat transfer can be predicted. The extensive research on surface promoters has yielded, rather on a trial-and-error basis, a number of efficient surfaces. However, many of the most effective surface finishes, such as the close-packed sand-grain roughness developed by Dipprey and Sabersky [3], cannot be mass-produced economically.

Finned surfaces have been extensively investigated for both single-phase and boiling conditions. The reported information is largely confined to studies of external fins. In recent years, however, new manufacturing techniques have made it possible to produce a wide variety of tubing with internal fins. Unfortunately, it has not been demonstrated that it is possible to utilize external-fin data or standard fin-efficiency computations to arrive at the performance of this tubing.

Vortex flow augmentation may assume many forms, including coiled tubes, propellers, inlet vortex generators, and twisted tapes. Twisted tapes appear to be the most suitable and effective for commercial equipment. A recent report [4] summarizes detailed tests with tube-tape assemblies which were produced in part by the French Tube Company. This technique is quite well established and would appear to require little additional research. It is noted that part of the improved performance of the twisted-tape inserts results from the fin effect of the tape. Now, integral internal fins can be spiralled to produce a vortex motion; furthermore, the fin effect with an integral fin is inherently superior to that obtained with any twisted tape insert. There is thus the possibility that spiralling internal fins represent a superior augmentative technique.

The research program described in this report was inititated in

---

[2]Performance might be defined as the increase in heat-transfer coefficient of the augmented channel over the regular channel at equal pumping power. This is discussed more fully in Section 2.5.

1967 in response to a request by the French Tube Company to evaluate their Rough Inside Diameter (RID) tubing and their Forge Fin tubing. The RID tubing has an interior finish resembling a close-packed sand-grain roughness, and can be produced at a small premium above standard tubing. The Forge Fin process produces tubing having integral internal fins which can be spiraled. The four master's theses completed in connection with this program [5-8] were concerned not only with obtaining the basic design information for these two types of tubing, but also with understanding the mechanism of heat and momentum transfer in tubes having these complex geometrical configurations.

2. ROUGH TUBE STUDIES

2.1 Scope of Research

Several typical samples of the RID tubing were chosen for the initial test program. The dimensions of this tubing and a standard reference tube are given in Table 1. Water was chosen as the working fluid; Reynolds numbers up to 50,000 could be obtained with the Laboratory water loop (Appendix 1). In view of the unfavorable electrical characteristics of the test sections, the Laboratory electrical supply could not be used, and heating was provided by steam. A special enclosure was constructed to provide steam heating over a test-section length of 3 ft (Appendix 2). Heat fluxes up to 100,000 $Btu/hrft^2$ could be obtained with this method of heating; however, the flow rate and temperature level were adjusted so that no boiling occurred. A description of the test procedure for this series of experiments is included in Appendix 2. Further details can be found in [7].

TABLE 1

DESCRIPTION OF TEST SECTIONS

Tube	Heated Length (ft)	O.D. (ft)	I.D. (ft)	Surface RMS Roughness (in.)
Standard Copper Tube No. 1	3.20	0.0520	0.0449	100.0-130.0
RID Copper Tube No. 2	3.22	0.0312	0.0262	100.0-200.0
RID Copper Tube No. 6	3.20	0.0312	0.0262	175.0-275.0

2.2 Friction Factor Results

Isothermal friction factors were obtained for all three tubes in a Reynolds number range between 500 and 25,000, and are presented in Fig. 3.

In the laminar flow region the results for all three tubes essentially agreed with the classical analytical prediction. The scatter is largely due to experimental errors incurred in measuring the very small pressure drops associated with laminar flow. Agreement was to be expected, since many previous investigators have shown that the laminar flow friction factor is independent of relatively small scale surface roughness.

The turbulent flow smooth tube data were somewhat above the line presented by Moody [9] to represent the performance of commercially smooth tubes. The deviation, however, was not over two percent. The data for RID Tube No. 2 were slightly above the smooth tube data, but by not more than five percent. RID Tube No. 6 showed friction factor increases over the smooth tube of twelve and twenty-five percent at Reynolds numbers of 8,000 and 25,000, respectively.

When all the isothermal, turbulent flow, rough tube friction factor data were compared with the isothermal friction factor data of Nikuradse [10] and Moody [9], as shown in Fig. 4, it appeared that the RID tubes performed more like the tubes tested by Moody than those investigated by Nikuradse. This was in contrast to the results of Dipprey and Sabersky [3], who were able to duplicate the results of Nikuradse by using tubes formed over a sand-coated mandrel. Nikuradse originally coated tubes with various size sand-grains to achieve different degrees of roughness and denoted the levels by a representative (e_s/D) value. Moody experimented with commercially rough tubes, and by comparing their performance with that of the sand-grain-coated tubes in the fully rough friction region, assigned (e_s/D) values to his results. By looking at Fig. 4, it is apparent that even though a commercially rough tube and a sand-grain-coated tube exhibited the same friction factor in the fully rough region, they behaved quite differently in the region preceding the fully rough zone. This disparity prevented the categorical establishment of the reprsentative (e_s/D) values for the RID tubes tested because all the data obtained lay in the disparate region. It would be necessary to perform more experiments at higher Reynolds numbers to properly evaluate the appropriate (e_s/D) value of each tube.

The influence of heating on friction factors in rough tubes has not

not been well established. A viscosity ratio correction has been found adequate for liquids in smooth tubes

$$f_{di} = f_{iso} \left\{ \frac{\mu_w}{\mu_b} \right\}^n \qquad (1)$$

Where n is dependent on the Reynolds number [11]. For water flowing in a tube roughened with rolled protuberances, Kalinin et al. [12] suggest that n is below the smooth tube value of 1/3.

As shown in Fig. 5 the data for the commercially smooth tube suggested that n = 0.35 for Re = 7,000 - 20,000; this value is identical to that obtained in a previous study in this laboratory [13]. The data for RID Tube No. 2 are in very good agreement; however, the data for RID Tube No. 6 do not correlate as neatly. It is probable that both Reynolds number and roughness are also required to accurately correlate diabatic friction factors. The provisional recommendation is to use the smooth tube value, n = 0.35, for tubes having this type of roughness.

2.3 Heat-Transfer Results for Turbulent Flow

The turbulent heat-transfer coefficient results are presented in Fig. 6. The McAdams correlation is the conventional reference for smooth tube results; however, it has been established that for water at Re < 10,000 the constant should be 0.025 instead of 0.023 [14]. The present smooth tube results are in excellent agreement with the modified McAdams equation. This reference check lends confidence to the reliability of the rough tube results obtained.

The data for the two RID tubes were above the smooth tube data by over sixty percent at a Reynolds number of 30,000, and a larger percentage improvement is suggested at higher Reynolds numbers. It is not possible to make a meaningful comparison of these data with other data for "sand-grain" surfaces, e.g. Dipprey and Sabersky [3], since the roughness type is not exactly identical. The general characteristics are similar, however, in that the effectiveness of the rough surface increases as the Reynolds number increases.

The physical reasons for the improved heat transfer in rough tubes can be seen by considering the usual expression for apparent heat flux in turbulent flow [15]:

$$\frac{q''}{\rho\, c_p\, \nu} = -\left[\frac{\varepsilon_H}{\nu} + \frac{1}{Pr}\right]\frac{\partial T}{\partial y} \tag{2}$$

It can be seen from this expression that for low Pr the second term is significant, and since it does not depend on the distance from the wall, the resistance to heat flow would be distributed all over the cross-section. On the other hand, for large Pr, the first term would be predominant, and since it does depend on the distance from the wall, being zero at the wall, this suggests that nearly the whole resistance occurs near the wall. It can thus be concluded that for fluids which do not have a very low Pr, the coefficient of heat transfer could be increased if the resistance to the heat flow near the wall could be decreased. Essentially it means that thinning of the zone where low ε_H/ν occurs increases heat transfer. The zone of low ε_H/ν could be defined as $y^+ = C$, where $C = 5$, for example. The distance from the wall where ε_H/ν is low is then given by

$$\delta = \frac{C\nu}{V\sqrt{f/2}} \tag{3}$$

It can be seen from Eq. 3 that δ can be reduced by increasing either friction coefficient or the average velocity V. From extensive experimental data it is evident that increasing roughness increases the friction factor, due to the increases in friction and form drag. Hence, it would be expected that there is an increase in heat transfer with increase in roughness, and furthermore the effect would be greater for higher Pr. The heat-transfer coefficient for rough tubes should also increase above the smooth tube value with increasing Reynolds number since the ratio of protuberance height to laminar sublayer thickness increases as Reynolds number increases.

2.4 Heat-Transfer Results for Transitional and Laminar Flow

Although it is apparent that the RID tubes are effective only at highly turbulent Reynolds numbers, it is of interest to examine the heat-transfer behavior at lower Reynolds numbers. This situation may occur in practice under off-design conditions; furthermore, the effect of small-scale roughness on laminar and transitional flow is of fundamental interest.

The results of the low flow rate runs are presented in Fig. 7. At first glance, it seems hard to explain the behavior of the data below an average bulk Reynolds number of 3,000. However, if some thought is given to the nature of the test apparatus and the method of plotting the results, it becomes clear why the data appear as they do.

A very significant factor influencing the results was that the total heat flux into the test-section could not be controlled since the outside steam temperature remained constant. This meant that there was a large fluid temperature change between inlet and outlet for low flow rates. This variation caused the Reynolds number to change correspondingly. In essence, this meant that an inlet Reynolds number, based on the average bulk fluid temperature, of about 4,500 was necessary to insure that the flow conditions were turbulent throughout. From looking at Fig. 7 it can be seen that only at this level did the Nusselt number plot begin to correlate with the conventional turbulent flow results. For all flow conditions below this Reynolds number level, the fluid entered the heated length in either a laminar or transitional flow pattern and then became turbulent downstream.

The same high level of heat flux that caused the flow pattern to become turbulent downstream produced in the first portion of the tube a very high radial temperature variation in the fluid. All the data were acquired with an inlet water temperature between 50°F and 80°F and a uniform wall temperature of about 215°F. This temperature difference produced a very high Grashof number, based on tube diameter, on the order of 10^6 in the first portion of the tube. For the lowest flow rate, then, the heat transfer in the first portion of the tube was dominated by the transverse free convection superimposed on the axial forced convection. The free convection decreases along the tube due to the decreasing $T_w - T_b$, and is of little importance once turbulence is established. The relative

length over which each mode predominated is difficult to determine and no real effort was made to precisely establish it.

Presented below is a more qualitative than quantitative evaluation of the heat-transfer results that could be expected under the low flow rate conditions being considered. To make this evaluation more understandable, the data from a specific run will be considered.

Run 233, RID Tube No. 2

entrance conditions	exit conditions
Re = 605	Re = 2415
Pr = 8.83	Pr = 1.90
T_b = 53.6°F	T_b = 196.4 °F
T_w = 219.0°F	T_w = 219.0°F

From the results of Brown and Thomas [16], it is possible to determine what the probable heat-transfer coefficient might have been in the laminar flow, high Grashof number portion of the tube. Their results are essentially for the case of fully-developed secondary flow, but in view of the very low Reynolds number at the entrance, are probably applicable. The simplest assumption regarding how the fluid temperature might increase with axial length would be linear. Assuming a linear temperature gradient, the flow might become transitional about half-way down the tube. If the transitional region is considered very short, the flow pattern could be assumed essentially one-half predominately secondary flow and one-half turbulent flow. The average Grashof number for the first portion of the tube would be 9.7×10^5, and the average bulk Prandtl number about 5.5. The data of Brown and Thomas predict a Nusselt number of between 25 and 28 for these conditions. The average Nusselt number for the second half of the tube, determined from the standard McAdams correlation and based on average bulk fluid temperature, would be 17.5. The overall Nusselt number divided by Prandtl number to the 0.4 power based on the average bulk temperature for the entire tube, would be about 15.5. The experimental result obtained was actually about 13.5.

An examination of the data for all three tubes tested lends credence to the discussion just presented. Smooth Tube No. 1 had an I.D. of 0.0449 ft, while both RID tubes were 0.0262 ft I.D. Therefore, for the same difference between the fluid bulk temperature and the wall temperature, the

Grashof number would be five times greater for Tube No. 1. The data for the smooth tube lie well above the RID tube data as expected. The rougher RID tube also exhibited a lower heat-transfer coefficient in this low flow rate region than did the smoother RID tube. This indicates that perhaps the rougher surface tended to reduce the secondary-flow effect and thereby diminish the gain observed for smoother tubes.

A more comprehensive examination of the problem of combined forced and free convection in horizontal tubes (uniform heat flux) is given in [7].

2.5 Performance Evaluation

A useful comparison of augmentative schemes can be made by comparing the augmented heat-transfer coefficients with conventional smooth tube heat-transfer coefficients at equal pumping power. The pumping power is usually considered when selecting an augmentative scheme since it is relevant to the operating cost. This is only one factor which enters into the decision, however, since rough swirl tubes are more expensive to manufacture than conventional smooth tubes, and may be more difficult to maintain in certain circumstances. In any event, a constant pumping power comparison can be readily developed from the information presented here, as described in Appendix 2.

The results of the constant pumping power analysis are presented in Fig. 8. The improvement in the heat-transfer performance of the smoother RID tube over the commercially smooth tube was over 50 percent at a Reynolds number level of 27,000. The improvement observed for the rougher RID tube was only 30 percent at the same level. This was due to the fact that the rougher RID tube exhibited much the same heat-transfer coefficient as the smoother tube but had a higher friction factor. It was necessary to exceed a Reynolds number of 14,000 before any improvement was obtained over the smooth tube with either RID tube. This is to be expected in view of the qualitative explanation of the mechanism given in the preceding section.

3. HEAT TRANSFER AND PRESSURE DROP IN ROUGH TUBES WITH TAPE-GENERATED SWIRL FLOW

3.1 Introduction

It has been established that rough surfaces and swirl flow are among the most effective and practical methods for augmenting single-phase heat transfer in tubes. The effectiveness of the RID surface, in particular, has been demonstrated in Section 2 of this report.

Swirl flow is another technique that has been used to augment heat transfer in tubes. Swirl generation is usually accomplished by means of twisted-tape inserts which run the full length of the tube. Comprehensive experimental and analytical studies [19-22] have clarified the mechanism of heat transfer in tape-generated swirl flow of single-phase fluids, and have produced general correlations. In general, the elevated heat-transfer coefficients in swirl flow can be described by three effects: a) increased fluid velocity and secondary flow due to the longer spiral path, b) increased circulation created with heating due to the large centrifugal force, and c) fin effects due to the presence of the tape. In a recent study, Lopina and Bergles [4,22] developed an accurate prediction equation for water by simple superposition of these three effects. The heat-transfer coefficients in swirl flow can be 100 percent above those in straight flow under comparable flow and heat flux conditions, and over 20 percent greater for constant pumping power.

Thus, there is considerable evidence that surface roughness and swirl flow induced by twisted tapes, when applied separately, are very effective augmentative techniques. It is reasonable to assume that a combination of swirl flow and roughness would be superior to either technique utilized separately. At any rate, there is no particular redundancy in the mechanisms which would suggest that this might not be likely to happen. In general, it appears that little has been done to exploit the possibilities of compound augmentation; the only noteworthy example seems to be use of twisted tapes with gas-solid suspensions [23]. An investigation was performed to

determine how surface roughness and swirl flow interact when applied simultaneously or, equivalently, how the extensive experimental results for each technique can be used to predict the behavior when the two techniques are combined.

3.2 Scope of Research

Electrically heated test sections were prepared for use with the water loop described in Appendix 1. Four types of test sections were employed: smooth, smooth with twisted-tape inserts, rough, and rough with twisted tape inserts. The nominal test-section specifciations are shown in Table 2.

TABLE 2

TEST-SECTION SPECIFICATIONS

Smooth tubing: Cold drawn DHP copper
- Wall thickness = 0.022 in.
- Internal roughness = 30 μ in. (Talysurf rms)
- D_i = 0.248 in.
- L_h/D_i = 59-85

Rough tubing: ROUGH ID cold drawn DHP copper
- Wall thickness = 0.020 in.
- Internal roughness = 300 μ in.
- D_i = 0.250 in.
- L_h/D_i = 54-79

Swirl tapes: Inconel, INCO Alloy 600
- Thickness = 0.0186 in.
- Roughness = 15 μ in.
- y values = 2.5, 4.2, 6.0

Details of the test-section fabrication, test procedure, and data reduction are given in Appendix 3. A more detailed description of this investigation is given in [6].

3.3. Pressure Drop Results

Isothermal and heated friction factors for straight flow and swirl flow in smooth tubes are given in Fig. 10. The isothermal straight

flow data are in good agreement with the usual approximation for commercially smooth tubes

$$f_o = 0.046/Re^{0.2} \tag{4}$$

The isothermal swirl flow friction factors are in reasonable agreement with the expression

$$f_{s,h}/f_o = 2.75\ y^{-0.406} \tag{5}$$

which was found to correlate a variety of swirl data to within about ± 20 percent [22]. The heated friction factors were corrected to isothermal conditions by use of the viscosity ratio multiplier $(\mu_b/\mu_w)^{0.35}$ for straight flow, in agreement with the results of Section 2.2, and $(\mu_b/\mu_w)^{0.35}\ D_h/D_i$ for swirl flow [22]. These correction factors appear to be accurate for the present conditions ($T_b \sim 90$ °F, ΔT = 8-50 °F).

Isothermal and heated friction factors for straight flow and swirl flow in the rough tubes are given in Fig. 11. The isothermal straight flow data are considerably higher than the commercially smooth prediction. Gambill and Bundy [24] suggested an equation for predicting isothermal swirl flow friction factors for tubes having varying degrees of rms roughness:

$$f_{rs,h} = f_{s,h(y=\infty)} + 0.0525y^{1.31}\ (Re_h/2000)^n$$

where

$$n = 0.81\ \exp\ (-1700\ e/D_h) \tag{6}$$

As seen from Fig. 11, the average deviation of the present data from this prediction is about ± 20 percent, which is approximately the same scatter noted in the original correlation. However, the correlation consistently overpredicts the data at high Reynolds numbers.

The influence of heating on friction factors in rough tubes, either

swirl or straight, does not appear to have been examined previously. The heated friction factors shown in Fig. 11 were accurately corrected to isothermal conditions by application of the same viscosity ratio multipliers as were used for smooth tubes. This is of considerable importance in designing for high heat fluxes since the friction factor is significantly below that given by isothermal predictions.

3.4 Heat-Transfer Results

The experimental heat-transfer results are presented in Figs. 12-14 on the coordinates of $Nu_i/Pr^{0.4}$ versus Re_i. By basing the coordinates on the inside diameter rather than the hydraulic diameter, it is possible to directly show the improvement in h obtainable with swirl flow over a comparable empty tube for a given mass velocity. As shown in Fig. 12, the smooth tube, straight flow reference data are in general agreement with the conventional McAdams equation

$$Nu_o = 0.023\ Re^{0.8}\ Pr^{0.4} \tag{7}$$

in the region of fully turbulent flow. The constant tends to be somewhat higher as noted in Section 2.3.

The data with twisted-tape inserts indicate that improvements in h of up to 70 percent on the basis of equal Re were obtained with swirl flow in smooth tubes. These data were compared with the additive prediction equation developed by Lopina and Bergles [22] for swirl flow heat transfer in smooth tubes:

$$h_s = F\ (h_{sc} + h_{cc}) \tag{8}$$

where

$$F = \frac{q_{total}}{q_{total} - q_{fin}} \tag{9}$$

The spiral convection h was obtained by adjusting the conventional smooth tube correlation to account for the velocity increase due to tape twist. The centrifugal convection h was obtained by applying a standard correlation

for a horizontal hot plate facing up, where the gravitational acceleration is replaced by the actual acceleration assuming a rotating slug flow model. The final expression was found to be

$$h_s = \frac{k}{D_h} F \left[0.023(\alpha Re_h)^{0.8} Pr^{0.4} + 0.193 \left\{ \left(\frac{Re_h}{y} \right)^2 \frac{D_h}{D_i} \beta \Delta T \ Pr \right\}^{1/3} \right] \quad (10)$$

where

$$\alpha = \frac{1}{2y} (4y^2 + \pi^2)^{1/2} \quad (11)$$

According to the analysis given in [4], which assumes perfect tube-tape contact, the fin effect multiplier, F, for the present conditions ranged from 1.045 to 1.155 depending on the value of h. As shown in Fig. 12 the prediction was typically in good agreement with the data. The presence of contact resistance between the tube and the tape could account for the fact that the prediction was slightly higher than the average of the data.

A general presentation of the rough tube data is given in Fig. 13. The rough tube, straight flow data are seen to be substantially above the smooth tube data, with the improvement approaching 40 percent at the highest Re considered. As indicated in Section 2.3 the increased improvement with increasing Re would be expected since the ratio of the proturberance height to the laminar sublayer thickness increases as Re increases. The data for rough tubes can be correlated as follows:

$$Nu_r = 0.0088 \ Re^{0.915} \ Pr^{0.4} \quad (12)$$

It must be emphasized, however, that this expression is only applicable for system variables used in this work; changes in roughness and Pr would be expected to influence both the constant and Re-exponent. These effects have been demonstrated in the extensive studies of Dipprey and Sabersky [3] and Gowen and Smith [25].

As noted in Fig. 13 the rough tube, swirl flow data are elevated above the rough tube, straight flow data, with the tightest tape twist showing the greatest improvement. Figure 14 indicates conclusively that

rough tube, swirl flow data are significantly above the corresponding smooth tube, swirl flow data. The improvement at equal Re is as much as 35 percent for the present conditions, and would be expected to be even greater at higher Reynolds number[3]. The improvement over the conventional smooth tube h is then in excess of 100 percent.

In view of the previous success with an additive correlation technique for smooth tube swirl flow, it was thought appropriate to attempt correlation of the rough tube, swirl flow data in a similar manner. Assuming no cross-coupling, the desired heat-transfer coefficient is given by

$$h_{rs} = F\,(h_{sc,r} + h_{cc}) \tag{13}$$

Utilizing the present correlation for rough tube, straight flow as given in Eq. (12), Eq. (13) can be transformed, in a manner analogous to that represented in Eq. (10), to the following:

$$h_{rs} = \frac{k}{D_h} F \left[8.8 \times 10^{-3} \,(\alpha\, Re_h)^{0.915}\, Pr^{0.4} + 0.193 \left\{ \left(\frac{Re_h}{y}\right)^2 \frac{D_h}{D_i}\, \beta \Delta T\, Pr \right\}^{1/3} \right] \tag{14}$$

As seen from Fig. 13 this equation provides an excellent prediction of the present data for swirl flow in rough tubes.

As more data for rough tube swirl flow become available it is possible that slight modifications of Eq. (14) may be necessary. It is probable that the constant in the centrifugal convection term should be elevated to reflect the surface roughness; however, this could only be determined by conducting experiments at very high ΔT so that centrifugal convection contributes more than 15 percent to h_{rs}, as was the case here.

---

[3] It is evident from these results that tube roughness could explain some of the discrepancy which is frequently observed between swirl data for apparently similar geometries and flow conditions from different laboratories.

In addition, when the fin effect becomes large ($F > 1.15$), it would be necessary to develop more accurate expressions for F in which account for large differences in h between the rough tube and the smooth fin.

3.5 Performance Evaluation

Typical values of $(h_a/h_o)_P$ were calculated for the tubes used in this study for $T_b = 80°F$ and $\Delta T = 50°F$. The performance evaluation for these tubes was based on essentially the same procedure as outlined in Appendix 2. The empty rough tube friction data from Fig. 11 (corrected for viscosity variation) were used together with the correlation given in Eq. (12); the smooth swirl data were taken from Eqs. (5) and (10); and the rough swirl friction data from Fig. 11 (corrected for viscosity variation) were used in combination with the correlation given in Eq. (14).

The results plotted in Fig. 15 indicate that all three arrangements yield substantial improvements in heat-transfer coefficient; however, the improvement is strongly dependent on Re_o, or pumping power level. At low Re_o, the clear choice would be a smooth swirl tube; but at higher Re_o, the rough tubes out-perform the smooth swirl tube. The rough swirl tube is clearly the top performer at high Re_o, and it would be expected that improvements well above the 25 percent maximum recorded here could be obtained at $Re_o > 10^5$. It should be emphasized, though, that these comparative data apply to the present tests. Different roughness configurations, tube-tape assemblies, fluids, and operating conditions would be expected to influence the form and possibly the relative position of these performance curves.

4. HEAT TRANSFER AND PRESSURE DROP IN INTERNALLY FINNED TUBES

4.1 Introduction

Perhaps the most direct method of reducing the thermal resistance on the inside of heat exchanger tubes is to provide internal longitudinal fins. It appears, however, that very few studies of heat transfer in internally finned tubes have been reported. Hilding and Coogan [26] presented data for ten specially fabricated test sections (copper tubes with brass fins). The data were taken for heating of air over a range of transition and turbulent Reynolds numbers. In order to facilitate comparison of their work with the present data, their data have been transcribed and replotted in Figs. 28-34. For continuous finned, open core tubes, improvements in Nusselt number, based on nominal diameter and area, were as large as 170 percent for a tube having nearly 3 times the nominal surface area (Fig. 34). For turbulent flow the Nusselt numbers, based on effective area and equivalent diameter, were always below the smooth tube result.

Among other studies reported in the open literature, the Russians have used tubing with internal longitudinal fins for industrial superheaters, however, detailed tests results have been reported for only the friction factor [27]. Studies of two-phase heat transfer with inner fin tubing are reported in [28].

The present tests were directed toward obtaining a further assessment of the heat-transfer performance of inner fin tubing. Some guidelines regarding the number and height of fins were desired. A topic of special interest was the effect of fin spiral on heat transfer. Finally, the influence of surface roughness was to be examined.

The characteristics of the Forge-Fin tubes used in this study are given in Table 3, Appendix 4. Accurate internal measurements were made by photographically enlarging an ink stamping of the cross-section. A typical tube cross-section is shown in Fig. 16. Test-section fabrication and test

procedures are given in Appendix 2. Experimental results of this investigation are presented in Figs. 17-24.

4.2 Heat-Transfer Results

4.2.1 General Improvement in Heat Transfer

One of the more direct indications of heat transfer effectiveness of the inner fin tubes is given in Fig. 17. In defining the Nusselt number for this figure, the nominal heat-transfer area of the tube and the inside diameter were used. The Reynolds number was also based on the inside diameter. This method of presentation was employed because it indicates the improvement to be expected on the tube side of an existing heat exchanger if the smooth tubes originally in the exchanger are replaced by finned tubes. Since the tubes must fit in the same tube sheet, they muat have the same inner diameter, assuming constant wall thickness, and the same nominal heat transfer area.

The heat-transfer data for the smooth tube were found to be slightly higher than would be expected from the McAdams correlation (dashed line), as would be expected from the discussion in Section 2.3. The heat-transfer results presented on a nominal basis in Fig. 17 have a range of improvement over the smooth tube results of about 50 to over 200 percent. It is noted from Table 3 that Tubes 3 and 5, which exhibit the greatest improvement, have only about a 60 percent increase in surface area. Other tubes, however, have far more surface area with less improvement in heat transfer. Some reasons for this behavior are examined in the following discussion.

4.1.2 Influence of Fin Geometry on Improvement in Heat Transfer

An attempt was made to correlate all of the data by using the traditional approach of the hydraulic diameter and the effective surface area. The data plotted in this fashion are shown in Figs. 18 and 19, with a composite of best-fit curves being given in Fig. 20. Although the number of test sections was necessarily limited, the following trends are suggested by the data: The hydraulic diameter is effective for correlation only when the fins are straight and of moderate height (Tube 4). If the fins are short, any rifling of the fins raises heat-transfer coefficients above the smooth tube value (Tubes 3 and 5). More severe rifling is necessary to elevate the

coefficients when the fins are moderately high (Tube 13). The D -approach overpredicts the data when the fin height is large (Tube 15). This last observation is in general agreement with the results reported by Hilding and Coogan, since their data for fins of comparable height-to-tube-diameter ratio were below the smooth tube value. See Figs. 28 and 32. This effect is worth further consideration since it has a bearing on the manner in which extra surface area is provided in inner fin tubing.

One possible explanation for this behavior is that little heat is transferred from the unfinned surface and the fin area near the base. Consider an enlarged tube cross-section as shown in Fig. 16, and examine the trough formed by two fins and the tube wall. In this trough the fluid velocity would average much less than it would in the free stream. The laminar sublayer thickness would be very large at the bottom of the trough over the unfinned area, and would steadily decrease as it went up the side of the fin to a relatively small thickness over the fin tip. Therefore, the aggregate thermal resistance through the fin and its associated laminar sublayer would be much less than the aggregate resistance through the laminar sublayer over the unfinned area, and most of the heat would flow from the finned area to the fluid rather than from the unfinned area to the fluid. An attempt was made to check this hypothesis by replotting the data in terms of a heat-transfer coefficient defined using the total fin area. The results of this transformation were inconclusive as might be expected, since there is always some heat transfer through the unfinned area, and with large fins the fin area near the base is not very effective. With these complex geometries there is clearly a wide variation in heat-transfer coefficient from base to fin tip, an effect which cannot be accounted for in simple fashion.

4.2.3 Influence of Fin Spiralling

As noted in the previous section the general effects of fin spiralling were related to fin height. Tubes 4, 12, and 13 were chosen with the intent of ascertaining the effect of fin spiralling on heat transfer.

Tubes 12 and 13 were meant to be identical with Tube 4, except that Tube 12 was to have spiralled fins and Tube 13 was to have more tightly spiralled fins. It was thought that this would help clarify the effect

of fin spiralling. In actual fact, the fin dimensions of these three tubes varied, but not enough to completely obscure the effect of fin spiralling. The results for Tube 13 with tightly spiralled fins (y = 5.62) did lie above the results for Tube 12 with less tightly spiralled fins (y = 9.27). However, on the average the results for Tube 12 essentially coincide with the results for the straight finned tube (Tube 4). Therefore, it must be concluded that either the spiralling of the fins had no effect and some other parameter was the cause of the data for Tube 13 being higher, or that the fins must be spiralled to a certain degree of tightness before any significant twist effect is observed. The latter explanation is probable in view of the strong effect of fin height. The fins are expected to act as turbulence promoters; the core flow exhibits negligible rotation, but there is separation as the flow passes over the oblique protuberances. The more nearly transverse the fins are, the better the chance is for the disturbances to penetrate into the troughs between fins. It is interesting to note that the fin spiralling has an effect which is in the same general direction is that observed by Hilding and Coogan for discontinuous fins (Figs. 28 and 30). The discontinuous fins are, however, very difficult to manufacture.

When the fin height is small, as with Tubes 3 and 5, any spiralling improves heat transfer since there is no problem with flow stagnation in the troughs. These fins are clearly superior to the deeper finned tubes from the standpoint of performance and weight. The "optimum" internally finnned tube developed by Heeren and Wegscheider [29] also has relatively short fins which are stratigically tapered and spaced to minimize the low velocity region between fins. Detailed data are unavailable for a direct comparison with results of this study; however, it is clear that even the short fins must be shaped and spaced to avoid stagnation regions between fins. More work should be done with the present trapezoidal and triangular shaped fins to establish optimum spacing.

4.2.4 Influence of Tube Roughness

Tubes 14 and 15 were specified in an attempt to determine the superimposed influence of wall roughness on heat transfer. The roughness for Tube 15 was of the RID type and comparable to that produced for the

tubes in Section 2. Since the roughness is only in the region where the heat transfer is poor, for these deep finned tubes, there was no favorable effect of the roughening; in fact, from Figs. 19 and 20 it can be seen that data for Tube 15 lie below those for Tube 14, apparently due to the slightly higher fins.

4.3 Pressure Drop Results

Adiabatic pressure drop results are presented in Figs. 21 and 22, while the diabatic data are shown in Figs. 23 and 24. In these figures the Fanning friction factor and Reynolds number are evaluated using the equivalent diameter. The reference curve in the figures is the generally accepted curve for a smooth circular tube [9]. For Reynolds number definitely in the turbulent region ($Re \sim 10^4$), all data are reasonably close to the accepted curve. This suggests that the equivalent diameter is an acceptable correlating parameter for friction data for inner fin tubing. The data of Hilding and Coogan (Figs. 29, 31, 33) lie above the smooth tube curve, however, these data would be brought closer to the smooth tube value by application of a viscosity ratio correction for air.

The diabatic pressure drop results shown in Figs. 23 and 24 are generally slightly lower than the adiabatic results. This would be expected from the experience with smooth and rough tubes noted in Sections 2 and 3. An attempt to determine the viscosity ratio exponent was rather inconclusive as shown in Fig. 25. There is some suggestion that the usual exponent $n = 0.35$ should be reduced for finned tubes; however, more measurements would be required to confirm this. The present apparatus yielded an average value of the friction factor which cannot be considered generally valid on a local basis. As noted in Section 2.4 the effects of laminar-turbulent transition and free convection would be particularly pronounced at low Reynolds numbers, as is in fact indicated by the scatter in Fig. 23. Free convection, in particular, would cause the derived value of n to be lower.

One of the significant features of both the adiabatic and diabatic friction data is the general tendency for transition to take place at relatively low values of Reynolds number. This same effect is evident in the data of Hilding and Coogan. The tubes with spiralling fins would be

expected to exhibit earlier transition, due to interruption of the flow as it passes across the fins.

4.4 Performance Evaluation

The data were further reduced to give the constant pumping power comparison, where $(h_a/h_o)_P$ was based on the nominal heat-transfer area as noted in Appendix 2. In general, it should be noted that these reduced data should not be extrapolated beyond the ranges indicated without extending the range of the basic heat-transfer and friction data. The results given in Fig. 26 indicate that all seven tubes performs quite well; however, particularly good performance is exhibited by Tubes 3 and 5. These data further reinforce the conclusion that short, spiralling fins are most desirable.

The data of Hilding and Coogan for continuous fins were reduced in similar fashion and plotted in Fig. 27. The general range of improvement is somewhat below that indicated in the present study, even though much more internal surface area was used in several of their tubes.

5. REVIEW OF OTHER DATA FOR INTERIOR TURBULENCE PROMOTERS

This study has considered a limited number of the possible geometrical configurations within the broad areas of surface promoters and swirl flow. A number of the configurations tested have been found to be effective under typical flow conditions, from the standpoint of both elevated heat-transfer coefficient and constant pumping power comparison. It is appropriate to compliment this discussion of present results with a brief account of the improvements which might be expected with other configurations. Only a typical sampling of results for four different types of turbulence promoters will be presented [4]. The first type was tubes with random roughness, which were defined as tubes in which the roughness elements were randomly arranged on the tube wall. The second type was tubes with machined roughness which were defined as tubes in which the internal roughness was produced by machining, resulting in a regular arrangement of the roughness elements. The third type was tubes with transverse protuberances which were defined as tubes in which were placed protuberances primarily perpendicular to the fluid flow. The fourth type was fluted tubes which were defined as tubes with the tube wall indented in spiral fashion. Tubes with twisted tapes inserted were not considered, since they have been treated extensively elsewhere. Tubes with displaced promoters or gross inserts, such as cylindrical cores, were also not treated since they do not appear to be of great practical importance.

The results of each investigation were presented in plots of $Nu/Pr^{0.4}$ vs. Re for the heat-transfer results and the Fanning friction factor, f, vs. Re for the pressure drop results. The diameter used in defining the Nusselt number, the Reynolds number, and the friction factor, and the area used in defining the heat transfer coefficient are included with the description of each investigation given in Appendix 5. Also

---

[4] A bibliography which does more justice to the extensive literature in this area is given in [30].

listed in the appendix are the test fluid, Reynolds number range, heating type, and type of tubing tested. All fluid properties were evaluated at the bulk temperature unless otherwise noted by means of a subscript on the dimensionless quantities. Friction factors are indicated as diabatic or adiabatic by subscripts when the type is definitely known. All data were approximated by best-fit lines before presentation. The dashed reference lines in the majority of the figures accompanying this section are McAdams correlation ($Nu = 0.023\ Re^{0.8}\ Pr^{0.4}$) for the heat transfer performance of smooth tubes, and the data of Moody for the pressure drop in smooth tubes.

5.1 Tubes with Random Roughness

Relatively few studies have considered surfaces with random roughness for augmentation of heat transfer. A study of the heat-transfer and friction characteristics of commercially produced pipes having appreciable natural roughness is given by Nunner [31] and Smith and Epstein [32]. In general, these tubes exhibit modest increases in heat-transfer coefficient, but display substantial increases in friction factor. They have not been found effective on a performance basis.

Dippery and Sabersky [37] reported an extensive study of heat transfer in tubes with artificial random roughness. Their data are shown in Figs. 35 and 36, where the heat-transfer curves represent averaged data over the Prandtl number range 1.20-5.94. This particular type of roughness is very effective over certain ranges of velocity level as demonstrated in Fig. 37.

5.2 Tubes with Machined Roughness

A number of investigators have machined the inner surface of a tubular test section in order to achieve a regular roughness. The data of Cope [33] for daimond knurling are shown in Figs. 38 and 39, and a performance comparison is given in Fig. 40. Included on Fig. 40 are data of Sams [34] which indicate a moderate effect of the heating rate on performance. In general, the coarse roughness seems to produce increases in heat transfer which are not commensurate with the increase in friction.

Additional data for thread-form roughening are presented in Figs. 41 and 42 for Brouillette et al. [35] and in Figs. 43 and 44 for Teverovskii [36]. Other studies which have been performed include those of Sutherland and Miller [37] and Kolař [38].

5.2 Tubes with Transverse Protuberances

Transverse protuberances with appreciable spacing maybe of the attached or integral type. In the former category are found the ring-type inserts studied by Nunner [31]. The data for rings of various profile, height, and spacing are given in Figs. 45 and 46. The performance data in Fig. 47 suggest substantial improvements for certain geometries and velocity levels. A subsequent study by Koch [39] was concerned with relatively large loose fitting ring-type inserts held in place with axial supports. Aside from being rather impractical, these inserts produced extremely large friction factors which overshadowed the improvements in heat transfer.

Kalinin et al. [40] tested a variety of tubes which were internally roughened by rolling ridges into the tube wall. Their data are transcribed in Figs. 48 and 49. In general, these tubes give substantial increases in heat transfer for relatively small increases in pressure drop. A detailed investigation of ribbed tubes was recently completed by Webb [41]. His heat-transfer and pressure drop data are summarized in Figs. 50-53. The rather substantial increase in heat-transfer coefficient with Prandtl number is evident from the first three figures of this set.

Data for wire coil inserts have been reported by Nagaoka and Watanabe [42], Seigel [43], and Sams [44]. Representative heat-transfer and friction data of Sams are included in Figs. 54 and 55.

5.4 Spirally Indented or Fluted Tubes

A geometry which is currently enjoying popularity with workers in the field are the spirally indented or fluted tubes. Lawson et al. [45], Kidd [46], Withers and Young [47], and Eissenberg [48] have reported data for spirally indented or "rope" tubes having a variety of indentation depths and pitches. Typical data of Eissenberg and shown in Figs. 56 and 57.

Fluted tubes having a rather gross distortion are currently being manufactured. Maulbetsch [49] has furnished test results for several convoluted tubes. A similar tube tested as an incidental part of the present study is described as Tube 10 in Table 3, Appendix 4. Data for both of these tests are summarized in Figs. 58 and 59.

5.5 Summary of Review

An examination of the typical data included in this brief summary indicates rather clearly that substantial improvements in heat transfer can be realized from a variety of surface promoters. The random roughness developed by Dipprey and Sabersky (Fig. 35) is very effective, with the heat-transfer coefficient being improved about 150 percent over the smooth tube value at equal flow conditions. On the basis of constant pumping power, the coefficient is improved as much as 90 percent (Fig. 37).

Improvements in heat-transfer coefficient of about 100 percent can be realized with a variety of machined roughness (Figs. 38, 41, 43), yet the performance at constant pumping power seems to be quite poor (Fig. 40).

Certain arrangements of transverse protuberances are very effective, with a variety of them exhibiting over 100 percent improvement over the smooth tube value (Figs. 45, 48, 54). A particularly effective combination seems to have been found by Webb since his high Prandtl number results exhibit increases well above 200 percent. Performance evaluations are not available for all of these tubes.

The spirally indented tubes produce improvements in the 100 percent range (Fig. 56), while somewhat larger improvements are reported for a fluted tube (Fig. 58).

6. CONCLUSIONS

This research program has produced basic design information for tubes having a random roughness on the inside wall (RID) and tubing having continuous internal fins (FORGED FIN). These tubes represent two important classes of heat-transfer augmentation by alteration of the heat-transfer surface. The interest in these tubes is practical as well as academic since they can be mass-produced.

Studies with tubes having random roughness established that the heat-transfer coefficient was above the smooth tube value, for comparable flow conditions, by over 60 percent at a Reynolds number of 30,000. Larger percentage improvements are to be expected for higher Reynolds numbers and for fluids having higher Prandtl numbers than water ($Pr \sim 4$). Improvements in performance, based on equal pumping power for augmented and smooth tubes, of about 50 percent were observed. These improvements are below the gains reported by Dipprey and Sabersky [3] for a special randomly rough tube; however, the present tubes have the advantage of being commercially practical. In general, the randomly rough tubes seem to be superior to tubes having machined roughness. Tubes with certain types of transverse protuberances are to be regarded as competitors of the randomly rough tubes, from the standpoint of both performance and suitability for mass production. This test series pointed out the importance of superimposed free convection for horizontal tubes in laminar and transitional flow.

From the experimental results of this investigation it is evident that the augmentative techniques of surface roughening and swirl flow can be effectively combined. At the highest Reynolds numbers considered in this study, the heat-transfer coefficient for swirl flow in rough tubes was 35 percent above that for swirl flow in smooth tubes at equal Reynolds number. The rough swirl flow improved the conventional smooth tube coefficients by as much as 100 percent. At equal pumping power, the rough swirl tube exhibited a maximum improvement of 25 percent in the heat-transfer coefficient above the conventional smooth tube value. However, greater improvements would be expected at higher Reynolds numbers, and with fluids of higher Prandtl number.

Accurate correlation of the rough swirl flow heat-transfer coefficient was achieved by utilizing the correlation for rough straight flow in an

additive correlation previously suggested for smooth swirl flow. This makes it possible to predict rough tube swirl flow for any roughness configuration for which the basic heat-transfer data are available.

A detailed test program with internally finned tubes was carried out. The Nusselt number for the internally finned tubes was found to be improved 50 percent to 200 percent over the smooth tube when compared using the inner diameter and the nominal heat transfer area. The equivalent diameter and effective heat-transfer area were not found to be acceptable correlating parameters for heat transfer, even though the friction data were reasonably well correlated by the hydraulic diameter. It is felt that any successful correlation scheme will have to be based more directly on the physics of the fluid flow.

Of the various fin configurations tested, those having rather short spiralled fins produce the greatest improvements in heat transfer. These fins are superior to the higher fins from the standpoints of both performance and weight. Roughening of the base surface (RID) produced no noticeable improvement in heat transfer. The constant pumping power comparison indicated that Forge Fin performance ranged from 25-170 percent above the smooth tube. These results are substantially higher than those inferred from the data of Hilding and Coogan [26] for air. This improvement appears to equal that displayed by any of the schemes used to augment heat transfer inside tubes.

As with all augmentative techniques, some caution should be exercised in extending the extrapolation of these results beyond the present test conditions. As usual, the ultimate decision to adopt augmentation will be based not only on the heat-transfer performance but will also consider such factors as manufacturing costs, susceptibility to corrosion and ease of cleaning.

ACKNOWLEDGMENTS

This investigation was sponsored by the F.W. French Tube Company, Newtown, Connecticut. The personal interest and assistance of Mr. F.W. French, II during all phases of the investigation is gratefully acknowledged. G.S. Brown, Jr. and R.R. Simonds were supported by the contract as research assistants during their graduate study. W.D. Snider's attendance at M.I.T. was sponsored by the U.S. Coast Guard. R.A. Lee's graduate study was supported by the Research Laboratories of General Motors Corporation.

The assistance of Prof. B.B. Mikic is appreciated. Mr. Fred Johnson provided valuable assistance in apparatus construction.

APPENDIX 1

DESCRIPTION OF WATER LOOP

The flow loop used in this study is located in the M.I.T. Heat Transfer Laboratory. A schematic layout of the facility is shown in Fig. 1. It is closed-loop system limited to pressure levels of about 200 psia. Circulation of distilled water was provided by a two-stage regenerative pump, driven by an induction motor. The flow circuit consisted of a bypass and test-section line, both preceeded by a nitrogen accumulator to reduce any pressure fluctuations.

In the test-section line, water flowed through a Fisher-Porter flowrator followed by a preheater and metering valve, then through the test-section (shown here as the electrically heated tube), after which it merged with the flow from the bypass line. The rate of flow and the test-section inlet pressure were controlled by adjusting the metering valves at both the test-section inlet and exit, and at the bypass line valve.

The loop was equipped with filters and an ion-exchange demineralizer to maintain as low a level of dissolved minerals and undesirable foreign matter as possible. In order to insure a minimum of dissolved air in the system, a degassing tank was provided with electrical immersion heaters to degas a bypassed portion of the main flow. This tank also served as a surge tank and make-up water tank. Above the degassing tank was a fill-tank fed by a small Hypro pump. A heat exchanger employing city water as the cooling fluid was located before the pump to remove the heat introduced to the flow in the test section. Due to seasonal fluctuations in the temperature of city water supply, the minimum operating temperature of the water entering the test section varied between 50°F in winter and 80°F in summer.

APPENDIX 2

APPARATUS AND PROCEDURE FOR STEAM-HEATED TEST SECTIONS

Steam Jacket

The steam-heated test apparatus designed and constructed by Snider [8] is shown schematically in Fig. 2. The apparatus was essentially a shell-and-tube condenser with a shell diameter of 4 in., a heated length of 3 ft, and a capability of accepting test sections up to 1.100 in. O. D. The description given by Sachs [18] for a similar apparatus was used as a guide in design. Steam at 25-40 psig from the building steam supply was used and reduced to the desired pressure by a Spence Type EW regulating valve before entering the condenser. The steam inlet pipe is a 1/4-in. copper tube with 16 holes (No. 50 drill) in its upper surface. The pipe runs axially along the length of the condenser near the top of the condenser shell. Condensate passed out of the shell through a drain fitted with a thermostatic trap. A Pyrex sight port was installed to permit visual observations of the condensate to determine the mode of condensation. The apparatus was mounted on a portable test stand which could be quickly connected to the water loop.

Test Section

After detailed inspection and measuring, the required length of test tubing was prepared for insertion in the steam jacket. Bushings were attached to the tube where it passed through the condenser shell and where it joined with the mixing chamber. Pressure taps were placed at the inlet and exit regions of the heated length. These were made from 1/4-in. N.P.T. reducers soldered to the tube wall. Five thermocouples were attached to the tube at equal intervals. Small depressions in the outer tube wall were made with a drill. Due to the thinness of the tube walls, however, these depressions were not large enough to accomodate the entire thermocouple junction (1/32-in. bead diameter). Therefore, the beads essentially rested in the depressions while solder was put over them, attaching them to the wall.

After soldering, the thermocouple wires leading from the bead were covered with Hysol epoxy to prohibit any possible contact of the bare lead wires. The thermocouple wires were then led out through the inlet header through a Conax fitting containing a lava sealant.

Prior to installation, the test sections were cleaned to insure that the dropwise condensation promoter would adhere properly. A chemical promoter, a two-percent (by weight) solution of di-n-octadecyl disulfide in carbon tetrachloride was selected. Past use of this promoter in the Laboratory suggested that it would be suitable. It was initially applied rather liberally to the tube, but during operation, all excess promoter washed off, presumably leaving only a monolayer thickness.

Instrumentation was provided to monitor the pressure, flow rate, and temperature of the water entering and leaving the test-section, as well as the outside tube wall temperatures along the heated length. All fluid and tube wall temperatures were measured by 30 gauge copper-constantan thermocouples. The thermocouples were connected to a common ice bath through a Leeds and Northrup 12-position thermocouple selection switch, and the millivolt output was indicated on a Minneapolis-Honeywell, Brown recorder on the 0 - 6 millivolt range. The test-section inlet temperature was measured by a thermocouple inserted through a Conax fitting in a pipe tee ahead of the test-section calming length. The test-section outlet temperature was measured by a thermocouple at the exit of a mixing chamber attached to the test-section exit. Tests were run to substantiate the presumed assumption that the measured exit temperature was indeed the water mixed-mean temperature. These tests showed that after the water passed through the mixing chamber there was no appreciable thermal stratification, even at very low flow rates.

Bourdon-tube gauges were used to measure the bypass line pressure and Helicoid 8-1/2 in. gauges were used to measure the inlet and exit test-section and condenser-shell steam pressures. The pressure drop across the test section was measured with a 60-in. Meriam U-tube manometer filled with either Meriam fluid No. 3 (specific gravity of 2.95) or mercury.

Fischer-Porter flowrators, with overlapping ranges from 15 to 4,000 lbm/hr, were used to measure the flow rate through the test section.

Test Procedure

After the test section was in place and all instrumentation connected, the system was filled with distilled water from the degassing and supply tanks. Air was bled from the high points of the system, and the preparatory degassing procedure was completed.

The inlet pressure and the flow rate through the test section were controlled by the main loop throttle valve and the metering valve at the test-section inlet. The test-section inlet water temperature was controlled by adjusting the heat exchanger and preheaters. The temperature of the cooling water to the heat exchanger determined the minimum level of the inlet water temperature.

During isothermal pressure drop runs, the inlet pressure, pressure drop across the test-section, flow rate,and inlet water temperature were recorded. As wide a range of flow rates as possible was run for all tubes. It was necessary to switch between the two manometers available depending on the pressure-drop level.

To begin the heating runs, the steam was cut in after the flow rate and entrance pressure had been fixed. The steam regulating valve was adjusted to maintain about 2-1/2 psig pressure which produced a shell temperature of around 220°F. Sufficient movement of the steam inside the shell, to prevent the collection of noncondensible gases near the test section was obtained by maintaining a steady efflux of steam out of the side vent. After the exit, inlet, and five wall thermocouple readings had become steady, these and the flow rate, pressure drop, and inlet pressure were recorded. The steam temperature inside the shell was also recorded.

Data Reduction

The pressure drop data were used to compute the Fanning friction factor, defined in the usual fashion:

$$f = \frac{\Delta P}{4(L_p/D_h)(\rho V^2/2g_c)} \qquad \text{(A2-1)}$$

The nominal inside diameter was used for the equivalent diameter of the

RID tube, while the hydraulic diameter for the FORGE-FIN tubes was computed from the ususal definition.

$$D_h = \frac{4A}{P} \tag{A2-2}$$

Since the test rig had only a single steam jacket, it was possible to obtain only the average inside heat-transfer coefficient for the 3-ft nominal test length. The standard expression for the overall heat-transfer coefficient is given as

$$\bar{U}_i = - \frac{C_{min}}{A_{i,eff}} \ln (1 - \varepsilon) \tag{A2-3}$$

where

$$C_{min} = wc_p \tag{A2-4}$$

$$\varepsilon = \frac{T_{out} - T_{in}}{T_{st} - T_{in}} \tag{A2-5}$$

$$A_i = 2 \pi r_i L_h \tag{A2-6}$$

The desired inside coefficient is contained in the expression for the overall coefficient

$$\frac{1}{U_i} = \frac{1}{h_i} + \frac{\ln(D_{wo}/D)A_{i,eff}}{2 \pi k L_h} + \frac{1}{(A_{wo}/A_{i,eff})h_{st}} \tag{A2-7}$$

The effective heat-transfer area is defined by the equation:

$$A_{eff} = A_u + \eta A_f \tag{A2-7a}$$

where: A_u is the unfinned heat-transfer area

A_f is the finned heat-transfer area

η is the fin efficiency.

To be more specific:

$$A_u = (\pi D_i - Nb') \times L$$

$$A_f = \left(\frac{2c}{\cos \theta} + a'\right) \times NL$$

$$\eta = \frac{\tanh[(2h/kt)^{1/2}(c' + (t/2))]}{[(2h/kt)^{1/2}(c' + (t/2))]}$$

where: N is the number of fins

c is the vertical length of one side of a fin

b' is the measured fin width at its base

a' is the measured fin width at its top

$$\sin \theta = \frac{\pi}{(\pi^2 + 4y^2)^{1/2}}$$

c' is the true fin height $\simeq$ c

t is the average true fin width.

This calculation of the fin efficiency assumes that the heat-transfer coefficient is constant over the entire heat-transfer area and that the fins may be approximated by rectangular fins. All quantities that are indicated as measured are measured from a tube cross-section that is perpendicular to the length of the tube.

For purposes of calculating the fin efficiency, all of the fins were approximated by trapezoidal fins, and then the width of the top and the bottom of the fin were averaged so that calculations could be made as for a rectangular fin. Any error introduced in this manner is probably small, due to the high thermal conductivity of the tube material (copper) and the consequently high fin efficiencies. An average heat-transfer coefficient, h, calculated with an assumed efficiency was used in the fin

efficiency calculations. In many steam-heated systems the steam-side coefficient is so large that the last term in Eq. (A2-7) can be neglected. In effect, a constant outer tube wall temperature replaces T_{st} in the expression for ε above. In the present tests, the measured wall temperature was reasonably constant, except at the highest flow rates where a maximum variation of 30°F from inlet to outlet was observed. This of course, was indicative of the increase in water-side coefficient with increasing Reynolds member. Unfortunately there was no way to accurately estimate the average steam-side coefficient so as to be able to back-out the water-side coefficient. The only alternative was then followed whereby the measured average outer wall temperature was used in the expression for ε.

All fluid properties used in forming dimensionless groups were evaluated at the linear average of the inlet and outlet water temperatures. The actual water temperature profile lies somewhere between the log profile suggested by a constant tube wall temperature and the simple linear profile. However, for determination of the average temperature, the linear profile is considered to be adequate since the temperature variation between inlet and outlet was generally not large.

Constant Pumping Power Comparison

Consider heat exchanger tubes of fixed diameter and length, either commercially smooth or augmented by means of roughness. The fluid transport properties are presumed to be for both cases. For constant pumping power

$$(Q\ \Delta P)_o = (Q\ \Delta P)_a \tag{A2-8}$$

Incorporating friction factors and Reynolds numbers, this becomes

$$(Af_i Re_i^3)_o = (Af_i Re_i^3)_a \tag{A2-9}$$

The pumping power level is established by picking $Re_{a,i}$ and reading off $f_{a,i}$. By use of a correlation for the smooth tube friction factor, the

smooth tube Reynolds number can be calculated. For instance if $f_o = 0.046/Re_i^{0.2}$ and the same viscosity ratio correction applies to smooth and augmented tubes, the following equation applies:

$$Re_{o,i} = [21.7(A_a/A_o)(Re_{a,i})^3 f_{a,i}]^{0.357} \qquad \text{(A2-10)}$$

This Reynolds number can then be used in the conventional smooth tube correlation to calculate the heat-transfer coefficient, h_o. The ratio $(h_a/h_o)_P$ can then be plotted versus a Reynolds number, chosen here as Re_o, to give an indication of the performance at various velocity (or pumping power) levels.

Internally finned tubes were handled the same way; however, it should be noted that the hydraulic diameter counterpart of equation (A2-10) is

$$Re_{o,h} = [21.7(A_a/A_o)(D_o/D_{a,h})^4(Re_{a,i})^3 f_{a,h}]^{0.357} \qquad \text{(A2-11)}$$

The final ratio, $(h_a/h_o)P$ is based on the nominal heat transfer area, which is the appropriate basis since the finned tube replaces a smooth tube of the same nominal area.

APPENDIX 3

APPARATUS AND PROCEDURE FOR ELECTRICALLY HEATED TEST SECTIONS

Test Sections

Heat-transfer and pressure drop data for a variety of tubular test sections were taken on the low pressure water system described in Appendix 1. Low voltage, direct current power was supplied to the test sections and a series dummy load, which was required to stabilize the motor-generator power supply.

The general arrangement of the electrically heated test sections is shown in Fig. 9. Power was supplied through brass bushings brazed to the copper tubes; the heated length was defined to be the distance between the inner faces of these bushings. The pressure taps were 0.0135 in. holes which were drilled through the power bushings and tube wall. Since d-c heating was employed, the six wall temperature thermocouples were isolated from the tube wall by a layer of insulating tape. For the swirl test sections, both pressure taps and thermocouple junctions were located (with the aid of X rays) at a circumferential point 90 degree from the tube-tape juncture. A guard shield, consisting of a segmented brass tube wound with insulated heater wire, surrounded the entire test section in order to minimize the radial heat loss and insure accurate wall temperature indications. Thermocouples were also fastened on the inside wall of the guard shield at six locations.

The test sections were fabricated from cold drawn copper tubing supplied by the F. W. French Tube Co. The smooth tubes were drawn in standard commercial fashion, while the rough tubes were made by the RID process.

The twisted tapes were fabricated by suspending approximately 70 lb of weights on the end of sheared strips of Inconel which were supported at the top by a clamp. The weights were then rotated to produce the desired tape twist. To insure uniform contact between the tape and the tube wall,

the tubes were redrawn over the twisted tapes. The tape width, tube dimensions, and size of the sinking die were such that the redrawing caused about a 0.002 in. penetration of the tape into the tube wall. X-rays of the tube-tape assemblies verified the uniformity of tape twist and tube wall penetration.

Operating Procedure

The dissolved gas content in the loop was maintained below 0.5 cc/liter by continuous degassing, and the purity was maintained at 2 meg ohm-cm by continuous demineralization.

For each series of runs, isothermal pressure drop data were first determined. The preheaters were used to vary the temperature of the water for several different flow rates, and the overall test-section pressure drop was recorded. Pressure drop data were also recorded during each heating run.

For the runs with heat addition, the desired flow conditions were established and power was applied to the test section. The average bulk temperature was maintained at approximately 90°F by adjusting the inlet segments of the guard shield were then heated so that their inner wall temperatures were within 2°F of the average of the corresponding test-section wall temperatures. With this procedure the probable wall temperature error was estimated to be less than 1°F. At equilibrium, data were recorded concerning test-section flow rate, inlet and exit fluid temperatures, current voltage drop, tube wall temperatures, exit pressure, and pressure drop.

Data Reduction

All data were reduced by means of a digital computer. The average friction factor was found from

$$f_i = \frac{\Delta P \, D_i \rho}{2 L_p G^2} \qquad \text{(A3-1)}$$

where it was assumed that the pressure gradient in the short sections between pressure taps and the heated length was identical to that in the heated section.

The heat input was determined by enthalpy rise and power input measurements. These independent results were required to agree within 10 percent for the data to be accepted; however, agreement was generally well within this figure. The average heat flux for both axial and swirl tests was defined in terms of the nominal inside surface area:

$$q'' = q/\pi D_i L_h \tag{A3-2}$$

Use of the total heat input in this expression is justified since heat generation in the tape was less than 2.5 percent of the total heat input to the fluid. Due to the small temperature gradient along the tube, the deviation of the average heat flux from the local heat flux was less than 2 percent; hence the average heat flux was used to compute local heat-transfer coefficients. The temperature drop through the copper tube wall was neglected since it was below 0.25°F for all tests. The bulk temperature at each position was computed assuming a linear variation along the heated length. The local heat-transfer coefficient is then given by

$$h = \frac{q''}{T_w - T_b} \tag{A3-3}$$

Local values for Nu, Pr, and Re were computed on the basis of fluid properties corresponding to the bulk fluid temperature. Averages obtained by numerical integration were used in developing the plots presented in this paper.

A more complete description of the experimental procedure and data reduction can be found in [6].

APPENDIX 4, Table 3

CHARACTERISTICS OF THE TUBES OF THIS STUDY

(all dimensions in ft or ft^2, as appropriate)

Tube number	1	3	4
Type	Smooth	Spiral Fin	Straight Fin
Material	Copper	Copper	Copper
Total tube length	5.80	5.37	5.96
Heated length, L/D_i	3.01 67.1	3.01 36.6	3.01 65.1
Unheated entrance length, L/D_i	2.28 50.8	1.86 22.6	2.42 52.5
Inner diameter	0.0449	0.0822	0.0462
Outer diameter	0.0520	0.0884	0.0520
Tube wall thickness	0.00368	0.00308	0.00300
External surface area, heated	0.490	0.835	0.490
Cross-sectional flow area ($x10^3$)	1.575.	4.921	1.664
Wetted perimeter	0.141	0.434	0.232
Equivalent diameter	0.0449	0.0458	0.0287
Fin number and shape	---	16 trapezoidal	10 trapezoidal
Fin efficiency, average	---	0.961	0.964
Effective surface area, heated	0.424	1.263	0.685
Unfinned area A_u	0.424	0.525	0.317
Finned area A_f	---	0.767	0.381
Nominal surface area, heated	0.424	0.776	0.436
Fin height	---	0.00651	0.00500
Fin width	---	0.00391	0.00326
Fin twist, y	---	5.69	---

Table 3 (continued)

Tube number	5	10	12
Type	Spiral Fin	Convol-uted	Spiral Fin
Material	Copper	Copper	Copper
Total tube length	5.96	5.20	5.95
Heated length, L/D_i	3.01 62.2	3.01 50.1	3.01 64.7
Unheated entrance length, L/D_i	2.42 50.0	1.11 18.5	2.49 53.5
Inner diameter	0.0484	0.0600	0.0465
Outer diameter	0.0520	0.0652	0.0520
Tube wall thickness	0.00175	0.00260	0.00284
External surface area, heated	0.490	0.682 (est.)	0.490
Cross-sectional flow area ($x10^3$)	1.746	1.74	1.51
Wetted perimeter	0.246	0.188	0.210
Equivalent diameter	0.0284	0.0371	0.0289
Fin number and shape	30 triangu-lar	4 flutes	10 trape-zoidal
Fin efficiency, average	0.971	---	0.963
Effective surface area, heated	0.722	0.565	0.692
Unfinned area A_u	0.232	---	0.334
Finned area A_f	0.505	---	0.372
Nominal surface area, heated	0.456	0.621	0.439
Fin height	0.00250	0.0110	0.00472
Fin width	0.00125	---	0.00310
Fin twist, y	10.26	1.55	9.27

Table 3 (continued)

Tube number	13	14	15
Type	Spiral Fin	Spiral Fin	Spiral Fin & RID Wall
Material	Copper	Copper	Copper
Total tube length	5.94	5.90	4.75
Heated length, L/D_i	3.01 66.1	3.01 66.7	3.01 68.1
Unheated entrance length, L/D_i	2.46 54.0	2.34 51.9	1.25 28.4
Inner diameter	0.0455	0.0451	0.0441
Outer diameter	0.0520	0.0518	0.05175
Tube wall thickness	0.00325	0.00335	0.00382
External surface area, heated	0.490	0.490	0.489
Cross-sectional flow area ($x10^3$)	1.44	1.347	1.242
Wetted perimeter	0.214	0.306	0.336
Equivalent diameter	0.0271	0.01775	0.01473
Fin number and shape	10 trapezoidal	12 trapezoidal	12 trapezoidal
Fin efficiency, average	0.940	0.804	0.779
Effective surface area, heated	0.712	0.886	0.938
Unfinned area A_u	0.314	0.305	0.304
Finned area A_f	0.424	0.724	0.814
Nominal surface area, heated	0.430	0.426	0.417
Fin height	0.00548	.0078-.0105	0.0106
Fin width	0.00310	0.00228	0.00226
Fin twist, y	5.62	55.9	123.0

APPENDIX 5 - Table 4

CHARACTERISTICS OF THE INVESTIGATIONS INCLUDED IN THE SURVEY

Investigation	Tube type	Test fluid	Re range ($x10^{-3}$)	Type of heating	Area base of h	Diam. used	Reference
Hilding & Coogan	F	air		CSt	E	E	[26]
Dipprey & Sabersky	R	water	14-500	Elec	N	V	[3]
Brouillette, Myers, & Mifflin	Th	water	30-175	CSt	T	I_{av}	[35]
Cope	Kn	water	2-60	S&THX	N	V	[33]
Sams	Th	air	1-350	Elec	N	V	[34]
Teverovskii	Th	air	24-327	St	N	V	[36]
Kalinin, Dreitser, & Yarkho	Rib	water-glycerine	2-100	Elec	N	I	[40]
Nunner	Rib, R	air	0.5-100	CSt	N	I	[31]
Sams	WC	air	6-100	Elec	N	I	[44]
Webb	Rib	air, water, n-Butyl alcohol	6-140	Elec	N	I	[41]
Eissenberg	SpInd	water	16-105	CSt	O	O	[48]
Maulbetsch	Fl	water	47-127	S&THX	T	E	[49]

The abbreviations used in this part are as follows:

Tube type:
- F = finned
- R = rough
- Th = threaded
- Kn = knurled
- Rib = ribs, transverse to flow
- WC = wire coils inserted
- SpInd = spirally indented
- Fl = convoluted

Heating type:
- CSt = condensing steam
- Elec = electrical
- S&THX = shell-and-tube heat exchanger

Area base of h:
- E = effective (ie. fin efficiencies taken into account)
- T = total
- N = nominal ($=\pi DL$)
- O = original (ie. that of tube before augmentation)

Diameter used:
- E = equivalent

$$D_E = \frac{4 \times (\text{flow area})}{\text{wetted perimeter}}$$

- I = inside
- V = volumetric

$$D_V = (4 \times \text{vol. of tube}/\pi L)^{\frac{1}{2}}$$

- O = original (as for area base)

DESCRIPTION OF TEST CONDITIONS FOR OTHER INVESTIGATORS

Hilding and Coogan [26]

Hilding and Coogan tested a variety of finned tubing produced by brazing strips inside plain tubing. All tubes had straight fins of width 0.010 in. which were evenly spaced around the circumference of smooth tubes of inner diameter 0.550 in. and wall thickness 0.0375 in. Details of these tubes are given below.

Tube	Description
1	plain smooth tube, no fins
2 (A)	two fins meeting in tube center (i.e., strip extending full width of tube)
3 (B)	four fins meeting in tube center (i.e., two perpendicular strips extending full width of tube)
4 (C)	four fins, 0.200 in. high
5 (D)	eight fins, 0.200 in. high
6	four fins, 0.200 in. high, straight for 3 in. of length, rotated 45 deg., then straight for 3 more inches of length, etc.
7	two fins meeting in tube center (i.e., strip extending full width of tube) straight for 6 in., rotated 90 deg., straight for another 6 in., etc.
8	same as Tube 7, except fin discontinuites every 3 in. instead of every 6 in.
9 (E)	eight fins, 0.100 in. high
10 (F)	six fins meeting in tube center (i.e., three strips extending full width of tube)
11 (G)	concentric tube of 0.190 in. I.D. and 0.250 in. O.D. and between the two tubes, 8 fins, (i.e., fins in the annular section)

Dipprey and Sabersky [3]

Dipprey and Sabersky tested tubing with varying degrees of roughness on the inner surface. This roughness was of the sand-grain type and was produced by nickel-plating a sand covered mandrel and then dissolving the mandrel. The tube dimensions were as given below:

Tube	D - (in.)	e_s - (in.)	e_s/D
1	0.377	smooth	
2	0.384	0.00092	0.0024
3	0.393	0.0054	0.0138
4	0.399	0.0195	0.0488

where D is the internal diameter of the tube tested and e_s is the sand-grain roughness size.

Cope [33]

Cope investigated tubes which were artificially roughened to varying degrees by a special knurling process which produced a series of pyramids of height, e, on the inside of the tubes. All tubes were of 3/4 in. internal diameter and had roughnesses as indicated in Fig. 40.

Sams [34]

Sams investigated three tubes which were internally roughened by means of a rectangular thread. The test sections had an inner diameter of 1/2 in., grooves of depth, e, width, w, and spacing (pitch - width), s. The tubes are further described below:

Tube	e - (in.)	w - (in.)	s - (in.)
A	0.0065	0.0047	0.0047
B	0.0095	0.0085	0.0110
C	0.0042	0.0047	0.0047

Brouillette, Mifflin, and Myers [35]

Brouilette and co-workers investigated tubes which were internally roughened by means of machining the inner surface of the tube. This machining produced a series of V-shaped (60 deg) protuberances of height,

e, on the tube wall. The tubes tested are described below:

Tube	I. D. - (in.)	e/D	fins/in.
1	1.003	0.009	32
2	1.011	0.017	24
3	1.021	0.027	14
4	1.046	0.050	8
5	1.007	0.013	12
P	0.994	smooth	

Teverovskii [36]

Teverovskii investigated a variety of tubes which were roughened by triangular metric threads cut on the inner wall. Some characteristics of the test sections are given below:

Tube	$\frac{\text{thread height}}{\text{tube radius}}$
A	0.0201
B	0.0267
C	0.0530
D	0.0654
E	0.0785

Nunner [31]

Nunner tested several smooth tubes with piston-ring-like orifices inserted into them, and several commercially rough tubes. The rings were of height, k, and spacing, L. The details of these tubes are given below:

	Tube	Ring shape	k - (mm)	L - (mm)	I. D. - (mm)
	1	smooth			50.06
(A)	2	rectangular	2	40.9	49.82
(B)	3	half-round (r = 2mm)	2	163.5	49.95
(C)	4	"	2	40.9	49.82
(D)	5	partly-round (r = 18mm)	2	163.5	49.82
(E)	6	half-round (r = 4 mm)	4	81.7	49.5
(F)	7	"	4	40.9	48.92
(G)	8	"	4	20.4	47.78
(H)	9	"	4	8	43.85

Kalinin, Dreitser, and Yarkho [40]

Kalinin et al. tested a variety of tubes which were internally roughened by rolling ridges into the tube wall. This formed semi-circular protuberances inside the tube and depressions in the tube wall outside the tube. These protuberances were of height, e, and pitch, t. The tubes had an inner diameter, D, of 9.6 $\pm$ 0.01 mm. Although both air and a water-glycerine mixture were used as test fluids, only the results for water-glycerine are reported, due to difficulties in test section identification for the air tests. The test section particulars for the heat transfer tests with water-glycerine are given below:

Tube	e/D	t/D
1	0.025	0.5
2	0.015	1.0
3	0.025	1.0
4	0.025	2.5
5	0.050	2.5
6	0.050	1.0
7	0.035	1.0
P	smooth	

The test-section particulars for the pressure drop tests with water-glycerine are given below:

Tube	e/D	t/D
a	0.0285	0.5
b	0.027	1.0
c	0.017	0.5
d	0.0085	0.5

All of the protuberances were transverse to the fluid flow, and extended around the whole circumference of the tube.

Webb [41]

Webb investigated the performance of smooth tubes with ribs inserted transverse to the fluid flow. These orifice-like ribs were of height, h, and axial spacing, s. All of the tubes tested had an inner diameter, D, of 1.45 in. Pressure drop data were taken with air only. The details of the test sections are given below:

Tube	h/D	s/h
1	0.010	10
2	0.020	10
3	0.040	10
4	0.020	20
5	0.020	40
6	smooth	

Sams [44]

Sams tested smooth tubes with wire coiled on the inner wall to promote tubulence. All of the tubes tested had an inner diameter of 1/2 in. The details of each test section are given below:

Tube	Wire diameter - (in.)	Coil pitch - (in.)	$(T_w/T_b)_{max}$
1	smooth		1.86
2	0.026	1.63	1.38
3	0.026	1.03	1.34
4	0.026	0.49	1.55
5	0.026	0.26	1.28
6	0.026	0.13	1.64
7	0.026	0.026	1.40
8	0.019	0.62	1.34
9	0.019	0.26	1.28
10	0.019	0.10	1.26
11	0.019	0.019	1.38
12	0.013	2.18	1.40
13	0.013	1.19	1.38
14	0.013	0.69	1.35
15	0.013	0.49	1.35
16	0.013	0.27	1.29

Eissenberg [48]

Eissenberg investigated, among other things, the performance of a spiral indented, or rope, tube (Tube A). It had a diameter of 1 in., an indentation depth of 0.030 - 0.033 in., and an indentation pitch of 0.5 in.

Maulbetsch [49]

Maulbetsch and Praught tested several convoluted tubes manufactured by Ionics, Inc., Windsor, Connecticut. The details of the convoluted tubes are given below:

Tube	$I.D._{nom}$ - (in.)	flute depth -(in.)	flute pitch - (in.)	No. of flutes
S	0.777	1/8	7/16	3
L	1.295	1/4	7/8	4

REFERENCES

1. Bergles, A. E., and Morton, H. L., "Survey and Evaluation of Techniques to Augment Convective Heat Transfer," M.I.T. Engineering Projects Laboratory Report No. 5382-34, February 1965.

2. Bergles, A. E., "Survey and Evaluation of Techniques to Augment Convective Heat and Mass Transfer," Int. J. Heat Mass Transfer Series, Progress in Heat and Mass Transfer, Vol. 1, 1969, pp. 331-424.

3. Dipprey, D. F., and Sabersky, R. H., "Heat and Momentum Transfer in Smooth and Rough Tubes at Various Prandtl Numbers," Int. J. Heat Mass Transfer, Vol. 6, 1963, pp. 329-353.

4. Lopina, R. F., and Bergles, A.E., "Heat Transfer and Pressure Drop in Tape Generated Swirl Flow," M.I.T. Engineering Projects Laboratory Report No. 70281-47, June 1967.

5. Brown, G. S., Jr., "Augmenting Forced Convection Heat Transfer by Means of Internally Finned and Roughened Tubes", S. M. Thesis in Mech. Eng., M.I.T., February 1970.

6. Lee, R. A., "Heat Transfer and Pressure drop in Swirl Flow Through Rough Tubes," S. M. Thesis in Mech. Eng., M.I.T., August 1968.

7. Simonds, R. R., "An Investigation of Heat Transfer in Smooth and Rough Tubes," S. M. Thesis in Mech. Eng., September 1968.

8. Snider, W. D., "Investigation of Heat Transfer Augmentation Through Use of Internally Finned Tubes," S. M. Thesis in Mech. Eng. and S. M. Thesis in Naval Arch. and Marine Eng., M.I.T., May 1968.

9. Moody, L. F., "Friction Factors for Pipe Flow," Trans. ASME, Vol. 66 1944, pp. 671-684.

10. Nikuradse, J., "Laws for Flow in Rough Pipes," VDI - Forschungsheft 361, Series B, Vol. 4, 1933; NACA TM 1292, 1950.

11. LaFay, J., "Mesure du Coefficient de Frottement Avec Transfert de Chaleur en Convection Forcee dans un Canal Circulaire," Centre D' Etudes Nucleares de Grenoble, Service des Transferts Thermiques Note TT No. 275, 1967.

12. Kalinin, E. K., Dreitser, G. A., and Yarkho, S. A., "The Experimental Study of the Heat Transfer Intensification Under Conditions of Forced

One-and Two-Phase Flow in Channels," Proceedings of the Sessions on Augmentation of Convective Heat and Mass Transfer, ASME Winter Annual Meeting, November 1970.

13. Bergles, A. E., and Dormer, T., Jr., "Subcooled Boiling Pressure Drop with Water at Low Pressure," Int. J. Heat Mass Transfer, Vol. 12, 1969, pp. 459-470.

14. Bergles, A. E., and Rohsenow, W. M., "The Influence of Temperature Difference on the Turbulent Forced-Convection Heating of Water," J. Heat Transfer, Vol. 84, 1962, pp. 268-270.

15. Rohsenow, W. M., and Choi, H. Y., Heat, Mass and Momentum Transfer, Prentice-Hall, Inc., Englewood Cliffs, New Jersey, 1961.

16. Brown, A. R., and Thomas, M. A., "Combined Free and Forced Convection Heat Transfer for Laminar Flow in Horizontal Tubes," J. Mech. Eng. Sci., Vol. 7, 1965, pp. 440-448.

17. McAdams, W. M., Heat Transmission 3rd Edition, McGraw-Hill, 1954.

18. Sachs, P., "Modified Correlation for the Rate of Heat Transfer to Water Flowing in a Tube," J. Mech. Eng. Sci., Vol. 4, 1962, pp. 78-84.

19. Gambill, W. R., Bundy, R. D., and Wansbrough, R. W., "Heat Transfer Burnout, and Pressure Drop for Water in Swirl Flow Through Tubes with Internal Twisted Tapes," Chem. Engng. Prog. Symp. Ser., Vol. 57, No. 32, 1961, pp. 127-137.

20. Smithberg, E., and Landis, F., "Friction and Forced Convection Heat Transfer Characteristics in Tubes with Twisted Tape Swirl Generators," Journal of Heat Transfer, Vol. 86, 1964, pp. 39-49.

21. Thorsen, R. S., and Landis, F., "Friction and Heat Transfer Characteristics in Turbulent Swirl Flow Subjected to Large Transverse Temperature Gradients," J. Heat Transfer, Vol. 90, 1968, pp. 87-98.

22. Lopina, R. F., and Bergles, A. E., "Heat Transfer and Pressure Drop in Tape-Generated Swirl Flow of Single-Phase Water," J. Heat Transfer, Vol. 91, 1969, pp. 434-442.

23. Schluderberg, D. C., Whitelaw, R. L., and Carlson, R. W., "Gaseous Suspensions -- A New Reactor Coolant," Nucleonics, Vol. 19, No. 8, 1961, pp. 67-76.

24. Gambill, W. R., and Bundy, R. D., "An Evaluation of the Present Status of Swirl Flow Heat Transfer," ORNL 61-4-61, 1961; also ASME Paper No. 62-HT-42, 1962.

25. Gowen, R. A., and Smith, J. W., "Turbulent Heat Transfer from Smooth and Rough Surfaces," AIChE Preprint 32 for Tenth National Heat Transfer Conference, 1968.

26. Hilding, W. E., and Coogan, C. H., Jr., "Heat Transfer and Pressure Loss Measurements in Internally Finned Tubes," Symposium on Air-Cooled Heat Exchangers, ASME, 1964, pp. 57-85.

27. Lipets, A. U., Zholudov, Y. S., Antonov, A. Y., and Gromov, G.V., " The Temperature Regime and Hydraulic Resistance of Tubes with Internal Longitudinal Fins," Heat Transfer-Soviet Research, Vol. 1, No. 5, 1969, pp. 86-94.

28. Lavin, J. G., and Young, E. H., "Heat Transfer to Evaporating Refrigerants in Two-Phase Flow,: AIChE Preprint 21e for National Meeting, 1964.

29. Heeren, H., and Wegscheider, J. J., "Internally Finned Tubes, a Design Tool to Improve Condenser Performance," ASME Paper No. 67-WA/CT-2, 1967.

30. Bergles, A. E., and Webb, R. L., "Bibliography of Techniques to Augment Heat and Mass Transfer," Proceedings of the Sessions on Augmentation of Convective Heat and Mass Transfer, ASME Winter Annual Meeting, November 1970.

31. Nunner, W., "Waermeuebergang und Druckabfall in Rauhen Rohren, "VDI - Forschungsheft 455, Series B, vol. 22, 1956, pp. 5-39. Also AERE Lib./Trans. 786, 1958.

32. Smith, J. W., and Epstein, N., "Effect of Wall Roughness on Convective Heat Transfer in Commercial Pipes," AIChE Journal, vol. 3, 1957, pp. 241-248.

33. Cope, W. F., "The Friction and Heat Transmission Coefficients of Rough Pipes," Proc. Instn. Mech. Engrs., vol. 145, 1941, pp. 99-105.

34. Sams, E. W., "Experimental Investigation of Average Heat-transfer and Friction Coefficients for Air Flowing in Circular Tubes Having Square-thread-type Roughness," NACA RME52D17, 1952.

35. Brouillette, E. C., Mifflin, T. R., and Myers, J. E., "Heat Transfer and Pressure Drop Characteristics of Internal Finned Tubes," ASME Paper No. 57-A-47, 1957.

36. Teverovskii, B. M., "The Influence of Surface Roughness on the Resistance to Flow of Liquids and on Convective Heat Exchange," TRG Inf. Ser. 291(W), 1963.

37. Sutherland, W. A., and Miller, C. W., "Heat Transfer to Superheated Steam , 2. Improved Performance with Tubulence Promoters," GEAP-4749, 1964.

38. Kolar, V., "Heat Transfer in Turbulent Flow of Fluids Through Smooth and Rough Tubes," Int. J. Heat Mass Transfer, vol. 8, 1965, pp. 639-653.

39. Koch, R., "Druckverlust und Waermeuebergang bei Verwirbelter Stroemung," VDI - Forshungsheft 469, Series B, vol. 29, 1958, pp. 1-44.

40. Kalinin, E. K., Dreitser, G. A., and Yarkho, S. A., "Experimental Study of Heat Transfer Intensification Under Conditions of Forced Flow in Channels," ASME 1967 Semi-International Symposium.

41. Webb, R. L., "Turbulent Heat Transfer in Tubes Having Two-dimensional Roughness, Including the Effect of Prandtl Number," Ph.D. Thesis, Univ. of Minnesota, Sept., 1969.

42. Nagaoka, Z., and Watanabe, A., "Maximum Rate of Heat Transfer with Minimum Loss of Energy," Proceedings 7th International Congress on Refrigeration, Hauge/Amsterdam, vol. 3, No. 16, 1936, pp. 221-245.

43. Seigel, L. G., "The Effect of Turbulence Promoters on Heat Transfer Coefficients for Water Flowing in Horizontal Tubes," Heating, Piping, and Air Conditioning, vol. 18, No. 6, June, 1946, p. 111.

44. Sams, E. W., "Heat Transfer and Pressure Drop Characteristics of Wire-coil Type Turbulence Promoters," TID-7529, Pt. 1, Book 2, 1957.

45. Lawson, C. G., Kedl, R. J., and McDonald, R. E., "Enhanced Heat-transfer Tubes for Horizontal Condensers with Possible Applications in Nuclear Power Plant Design," ANS Trans., vol. 9, No. 2, Oct.-Nov., 1966, pp. 565-566.

46. Kidd, G. J., Jr., "The Heat Transfer and Pressure Drop Characteristics of Gas Flow Inside Spirally Corrugated Tubes," ASME Paper No. 69-WA/HT-3, 1969.

47. Withers, J. G., and Young, E. H., "Investigation of Steam Condensing on Vertical Rows of Horizontal Corrugated and Plain Tubes," Symposium on Enhanced Tubes for Desalination Plants, Office of Saline Water, U. S. Department of the Interior, 1969.

48. Eissenberg, E. M., "The Multitube Condenser Test," Symposium on Enhanced Tubes for Desalination Plants, Office of Saline Water, U. S. Department of the Interior, 1969.

49. Maulbelsch, J. S., Dynatech R/D Company, Personal Communication January 1970.

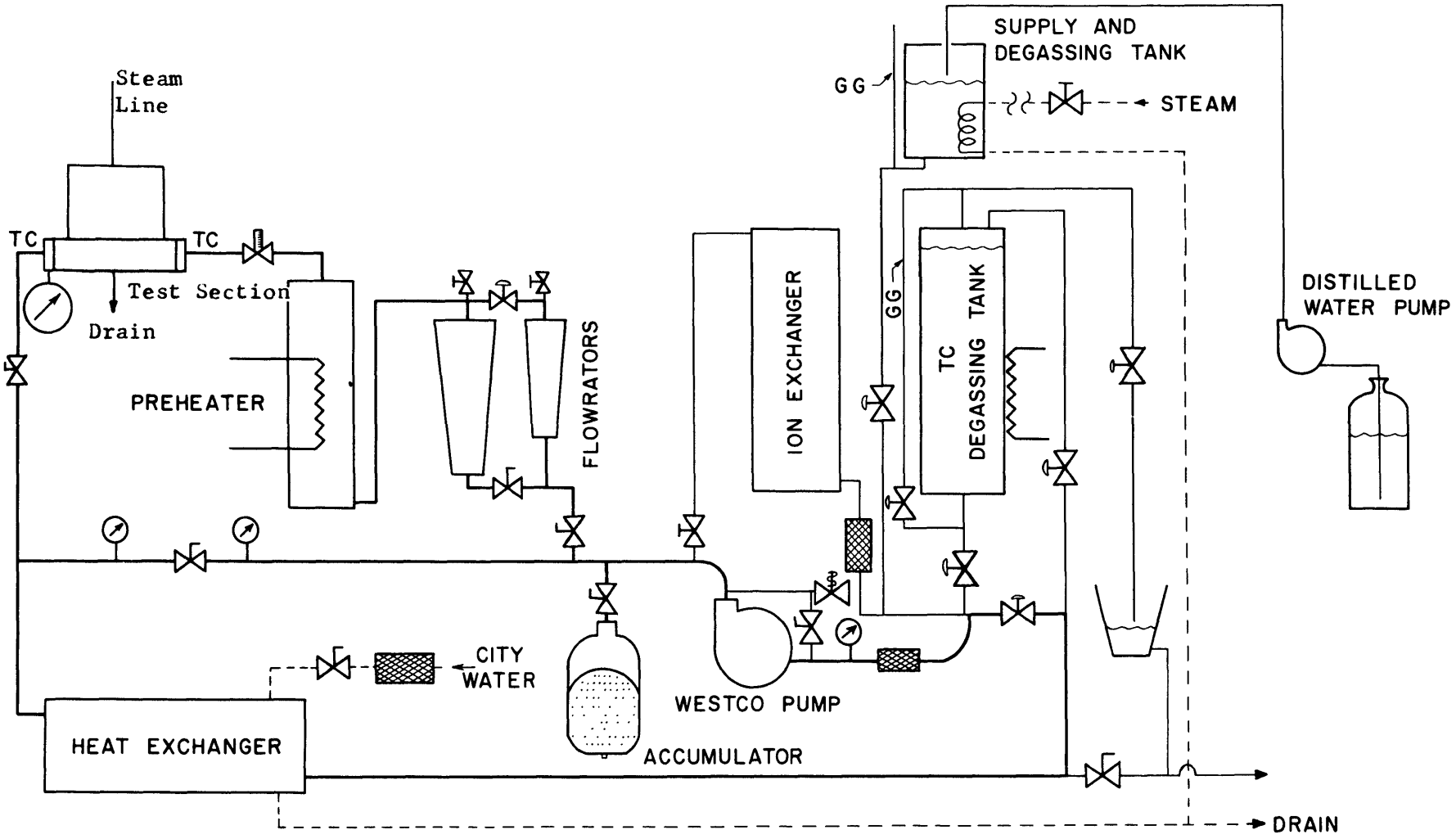

Fig. 1. Schematic of Water Test Loop

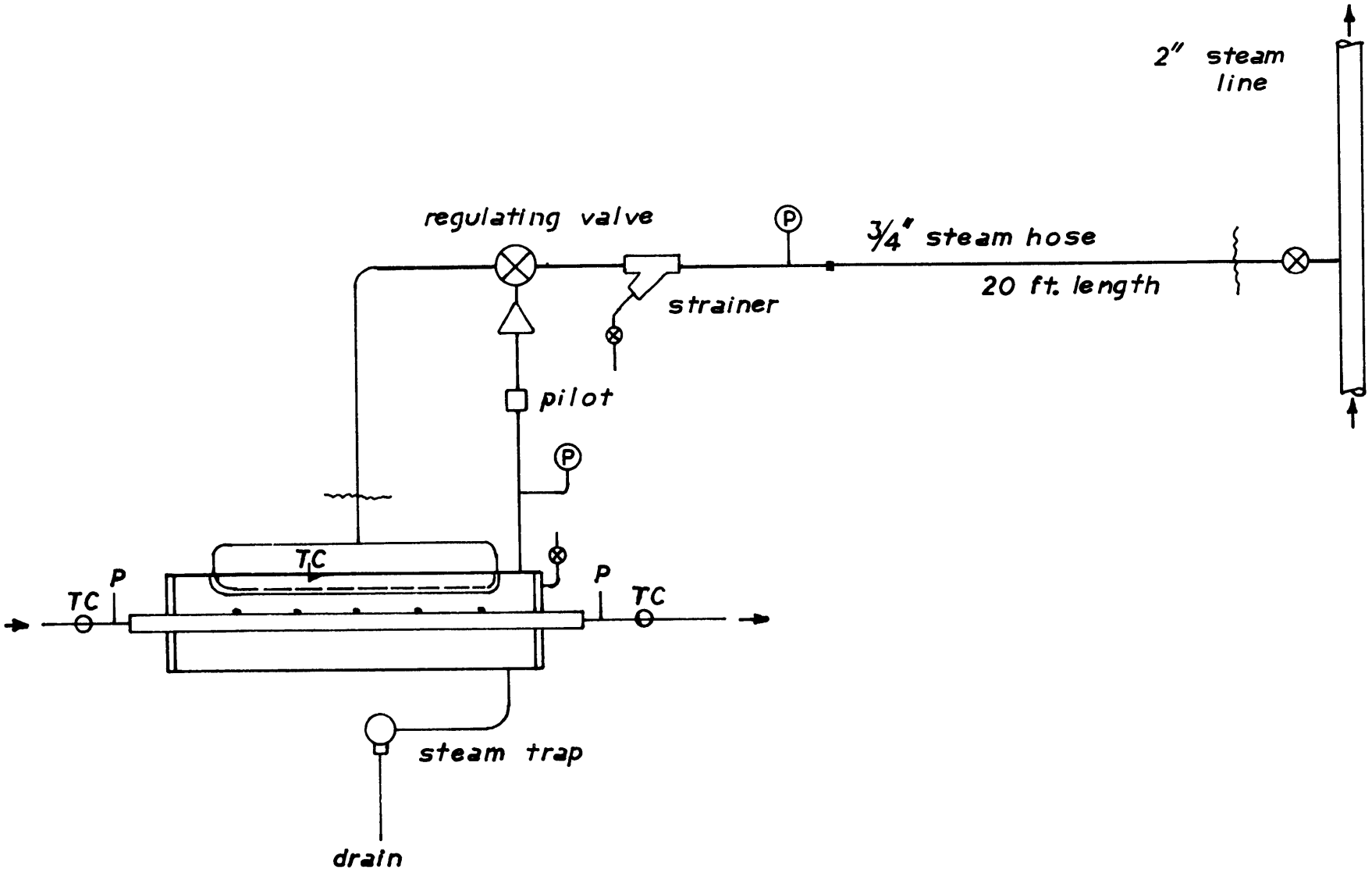

Fig. 2 Schematic of Steam Condensation Apparatus

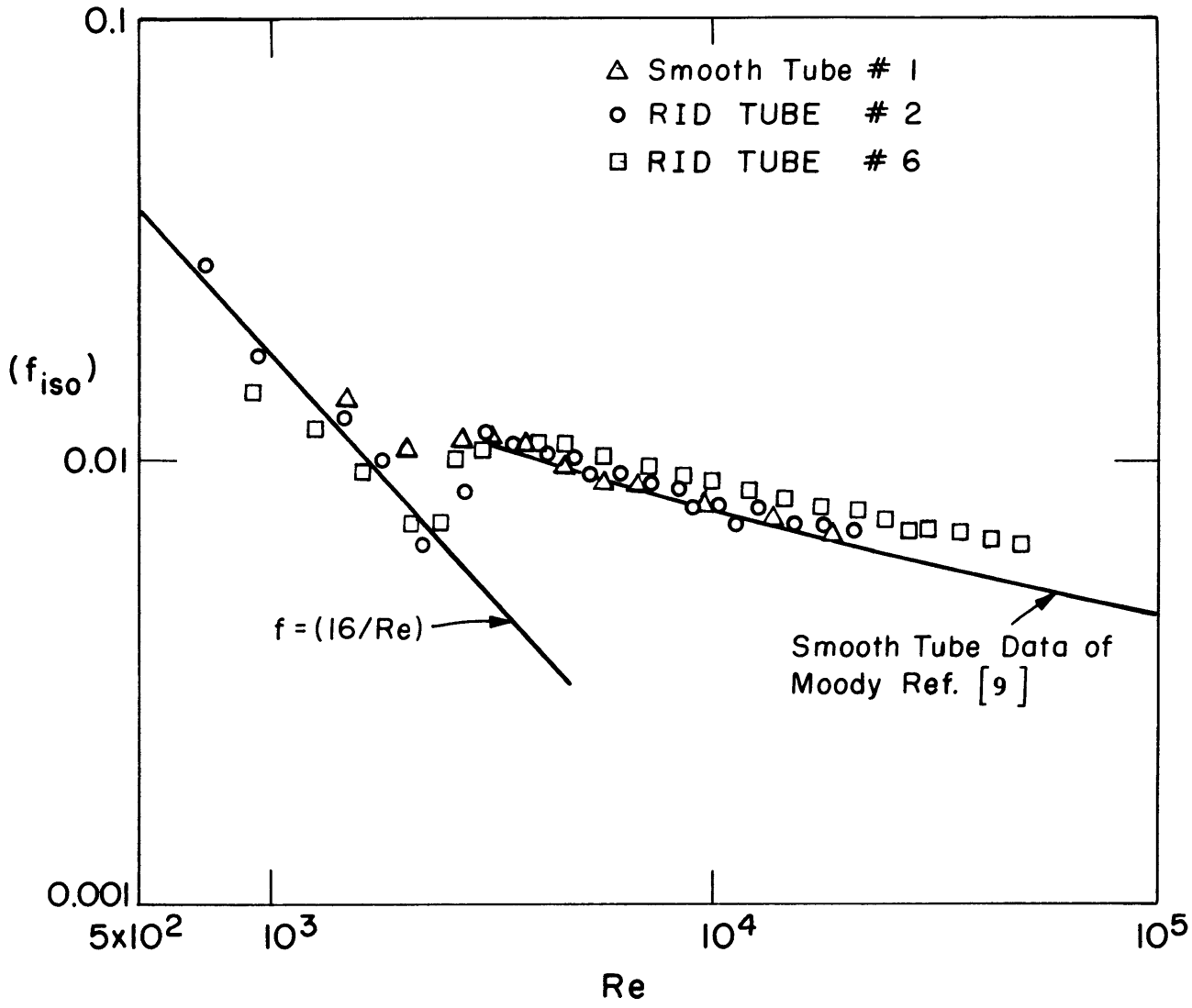

Fig. 3 Isothermal Friction Factors for Smooth and RID Tubes

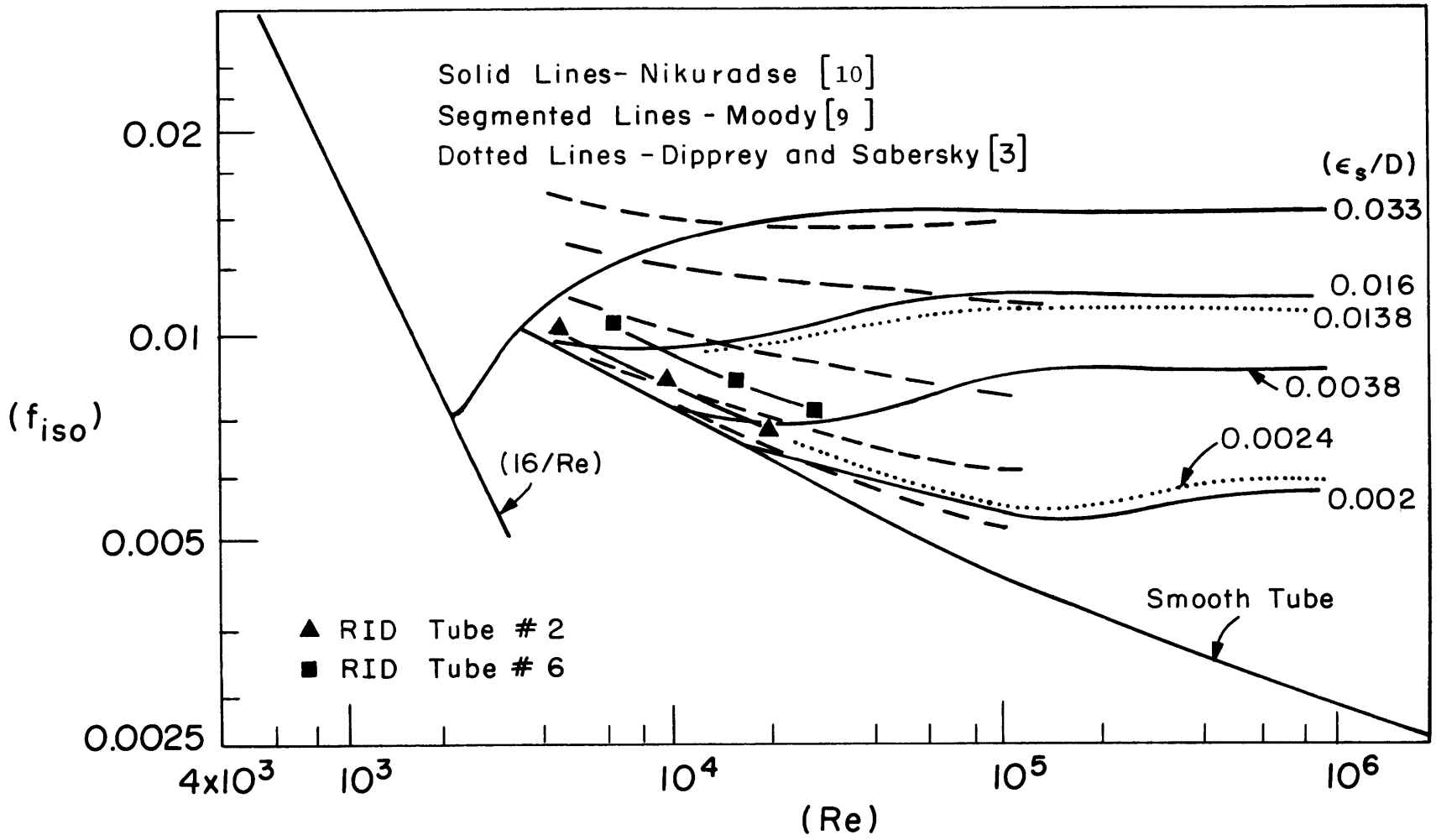

Fig. 4 Comparison of Friction Factor Results with Classical Results

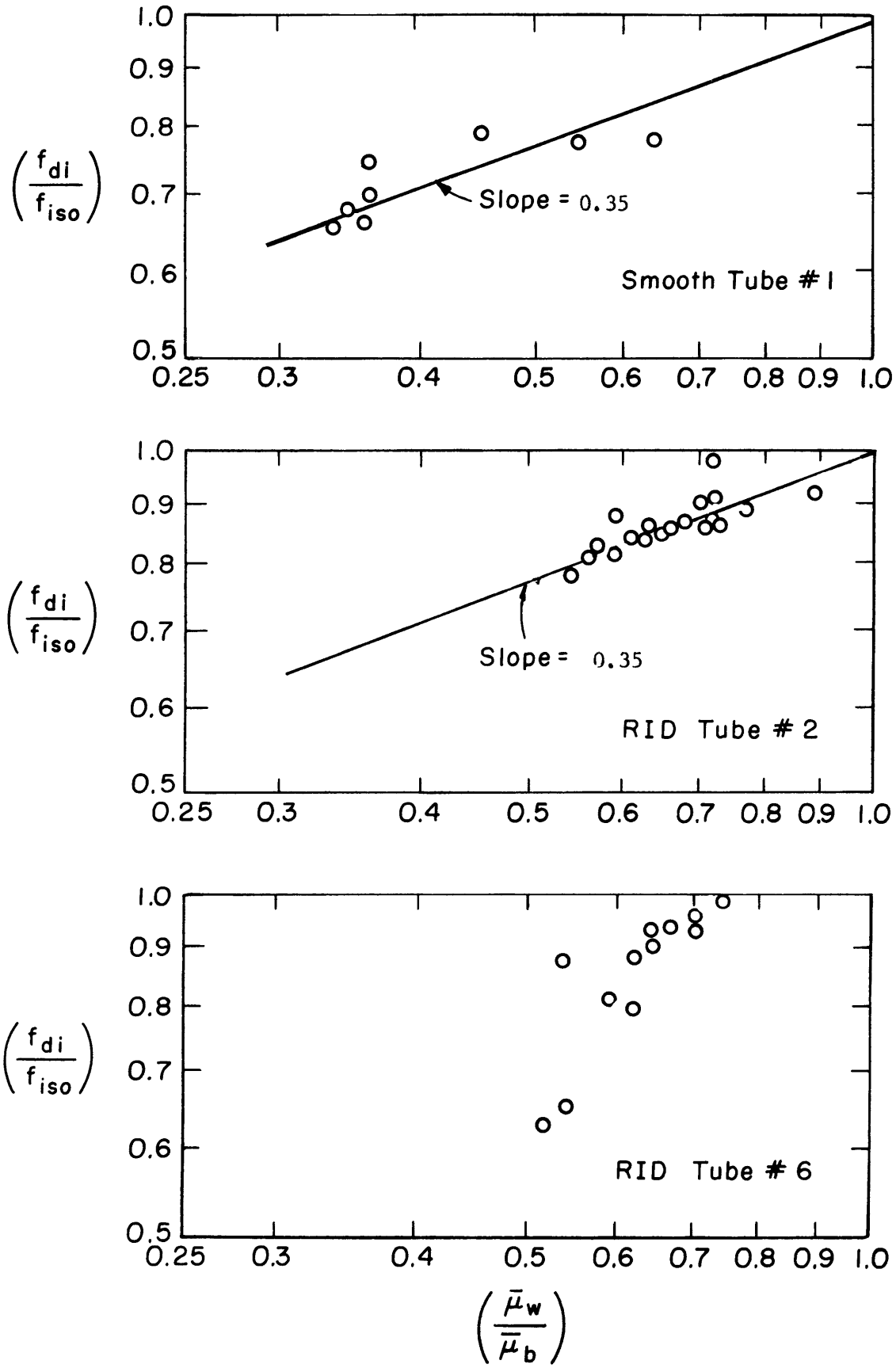

Fig. 5 Correlation of Diabatic Friction Factors for Smooth and RID Tubes

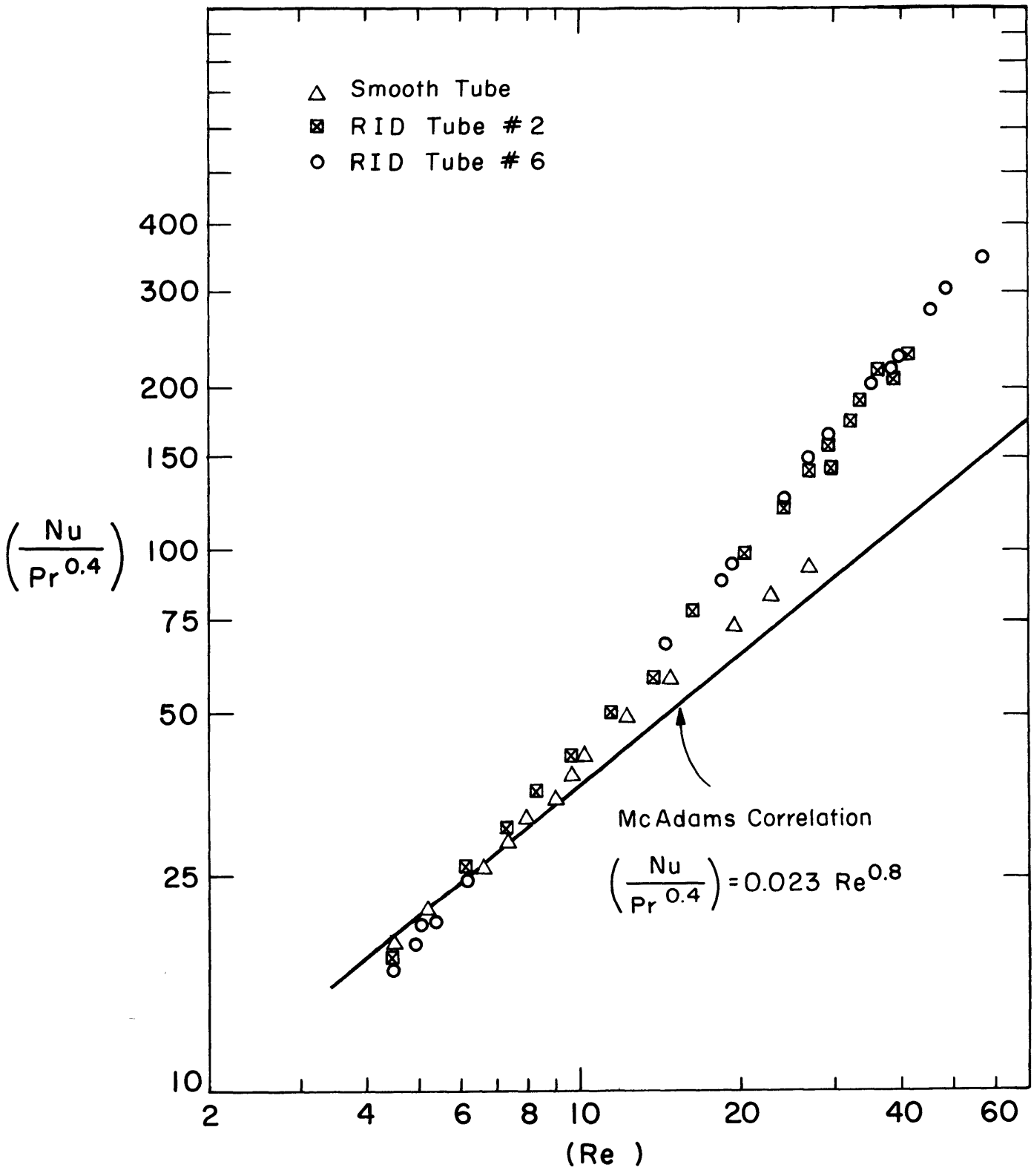

Fig. 6 Heat Transfer Data for Smooth and RID Tubes in Turbulent Range

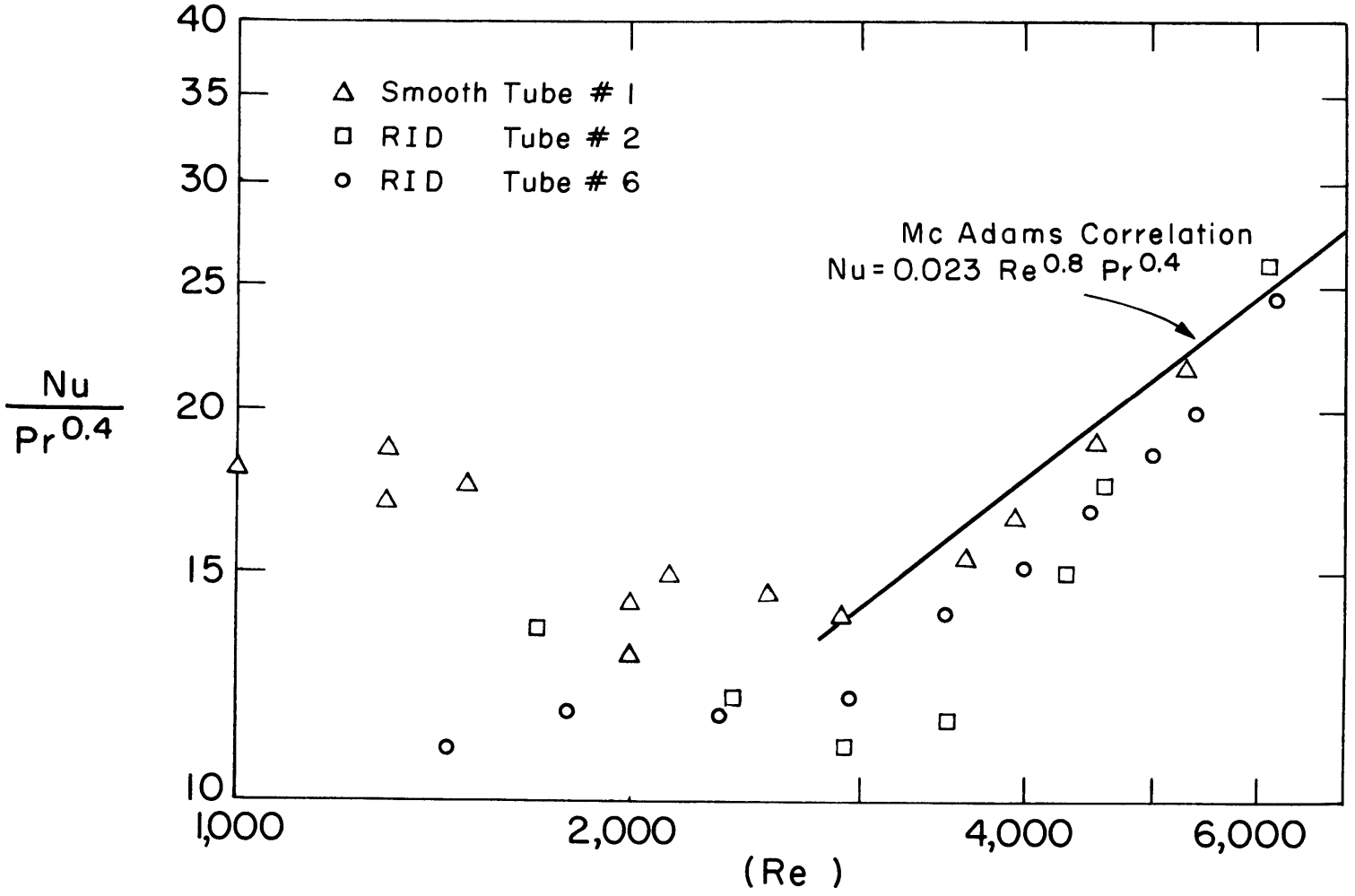

Fig. 7 Heat Transfer Data for Smooth and RID Tubes in Laminar and Transitional Range

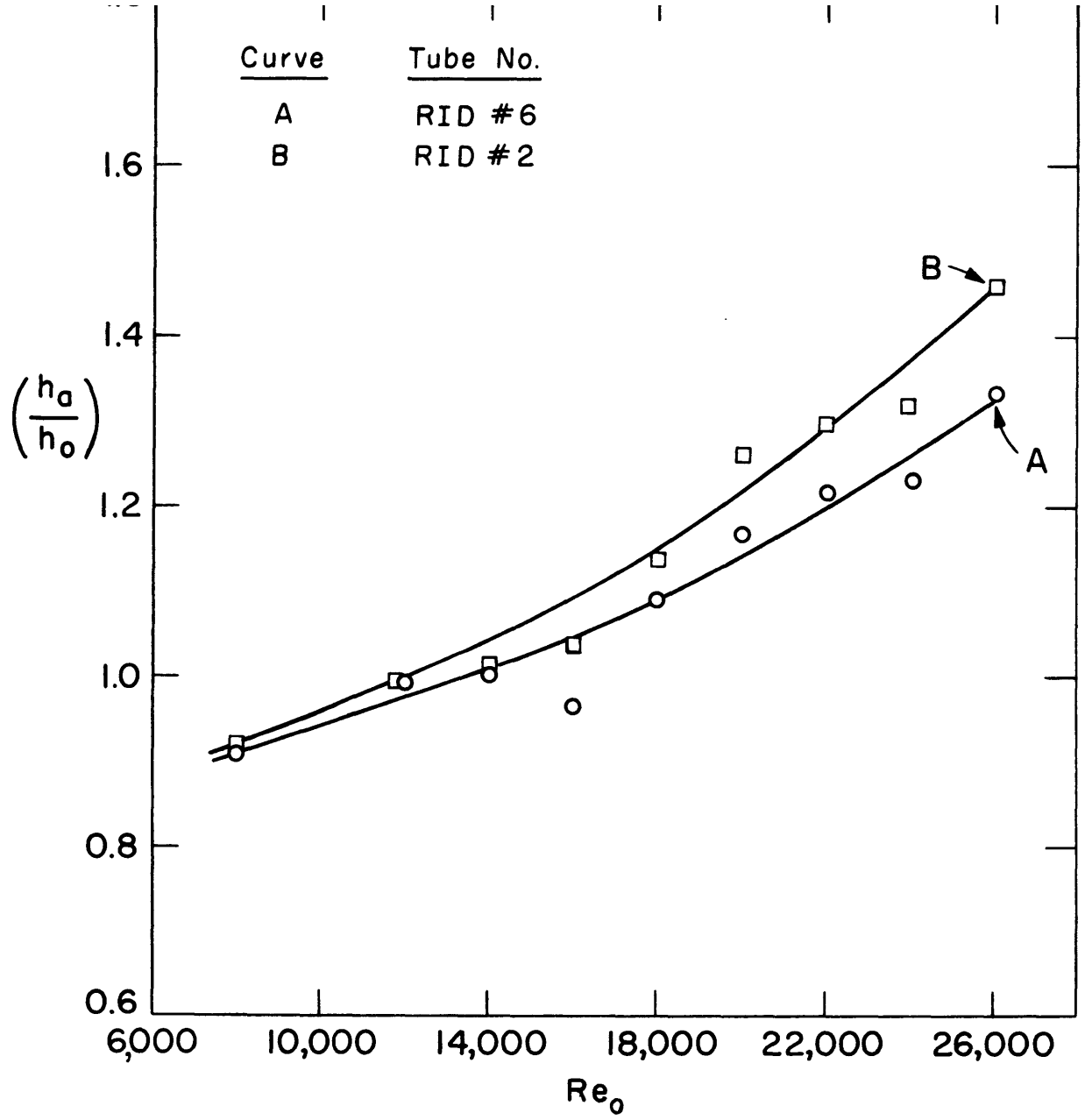

Fig. 8 Constant Pumping Power Comparison for RID Tubes

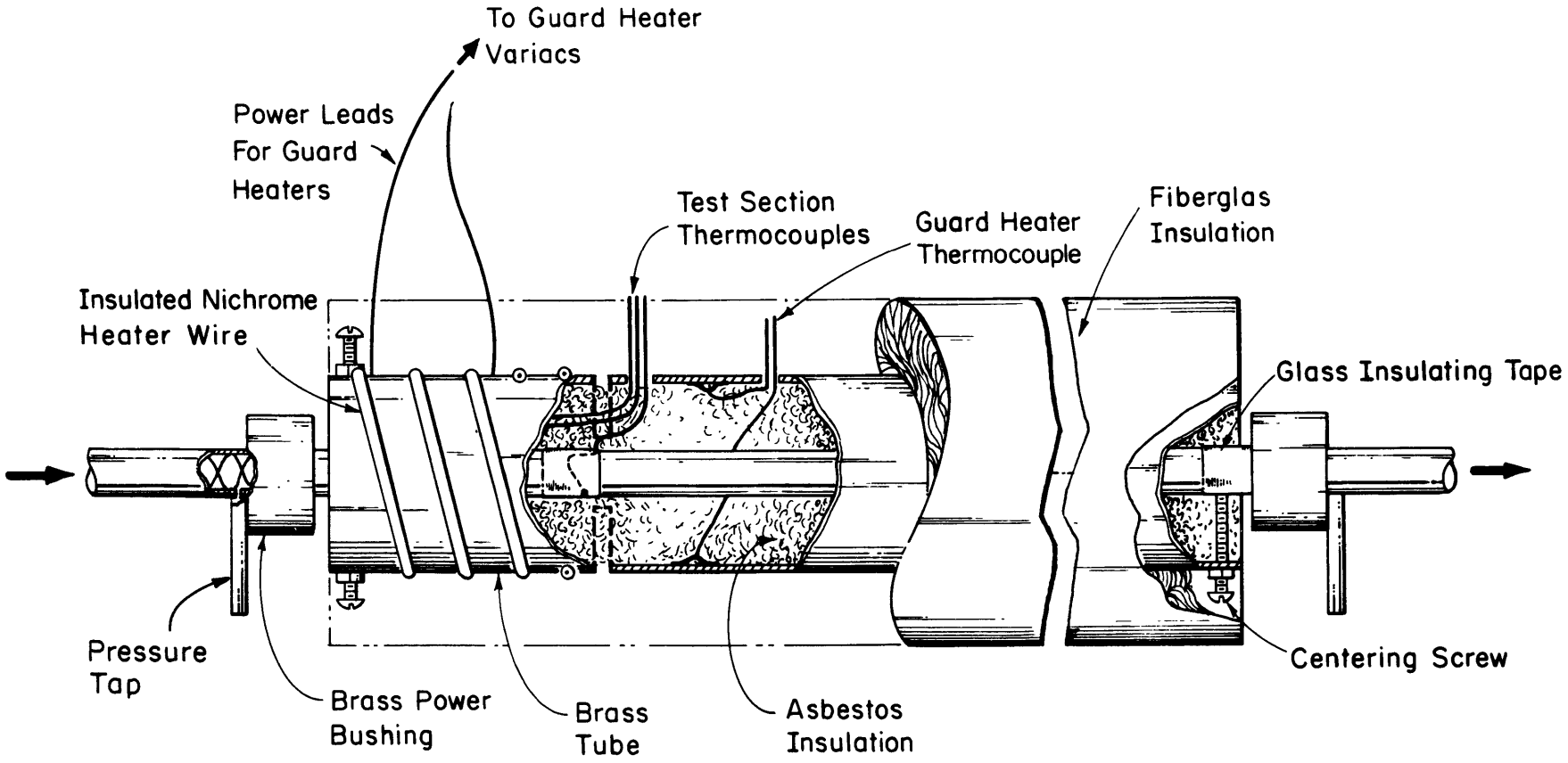

Fig. 9 Test Section Assembly for Electrically Heated Tubes

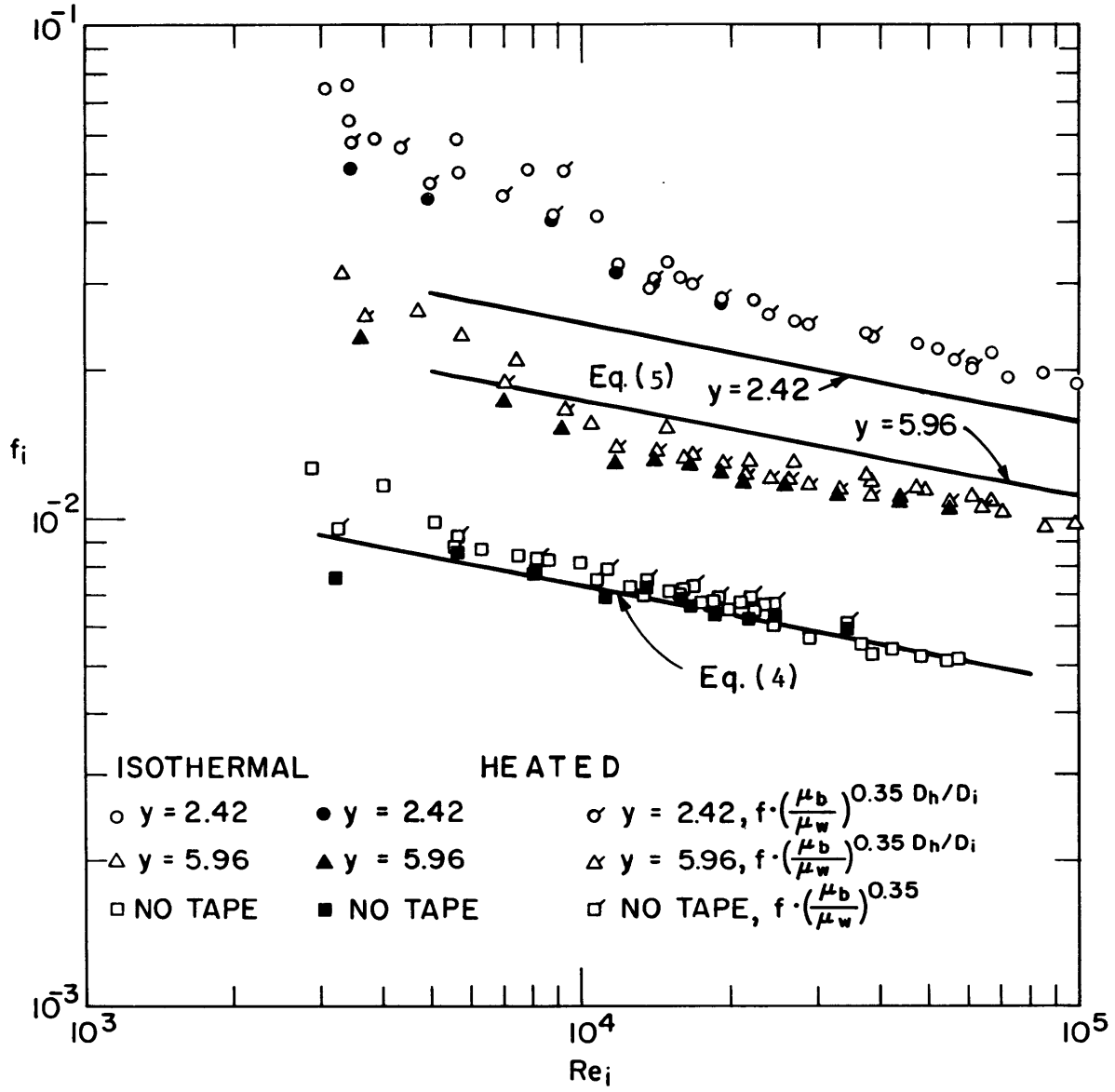

Fig. 10 Friction Factors for Straight and Swirl Flow in Smooth Tubes

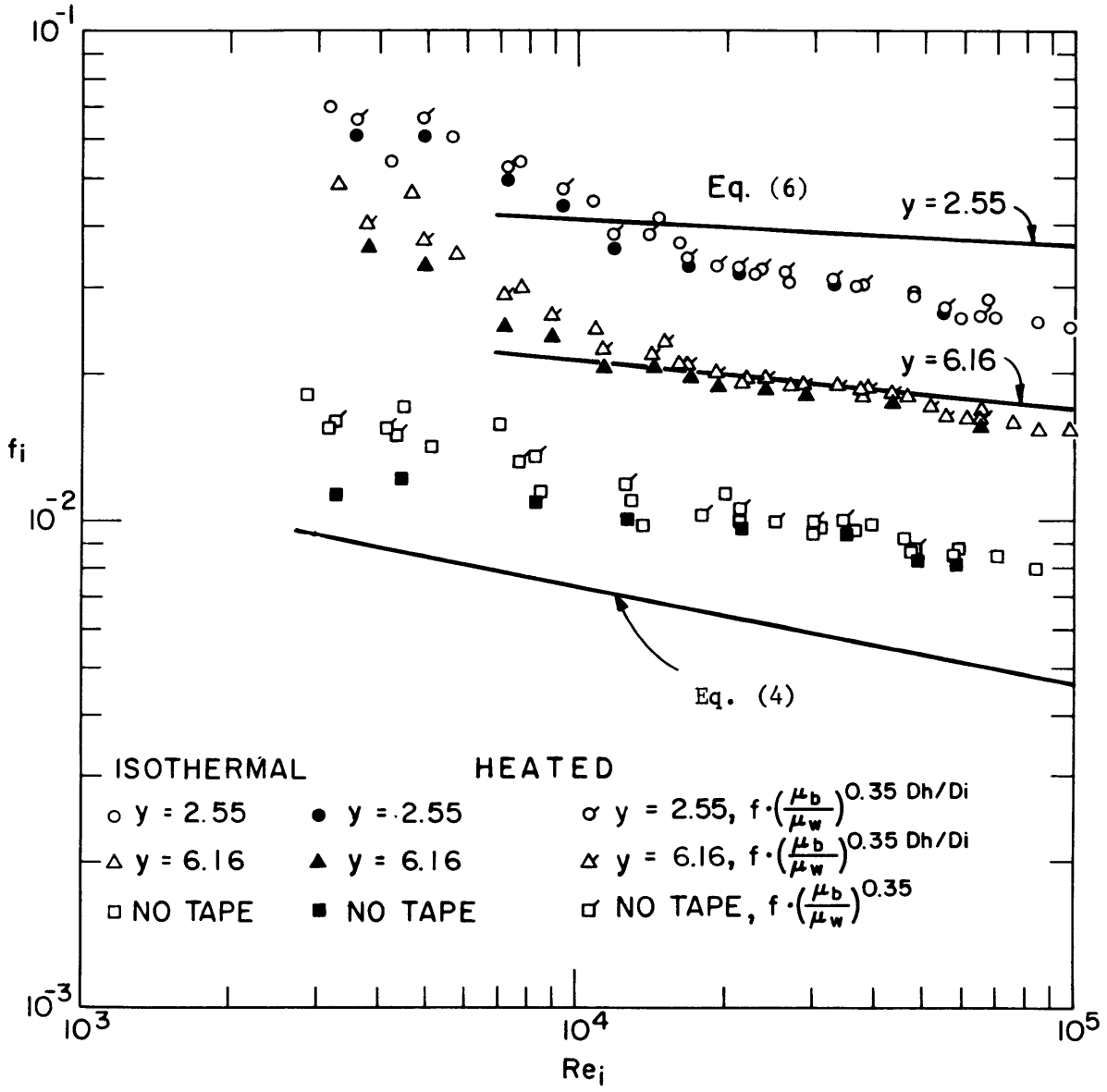

Fig. 11 Friction Factors for Straight and Swirl Flow in Rough Tubes

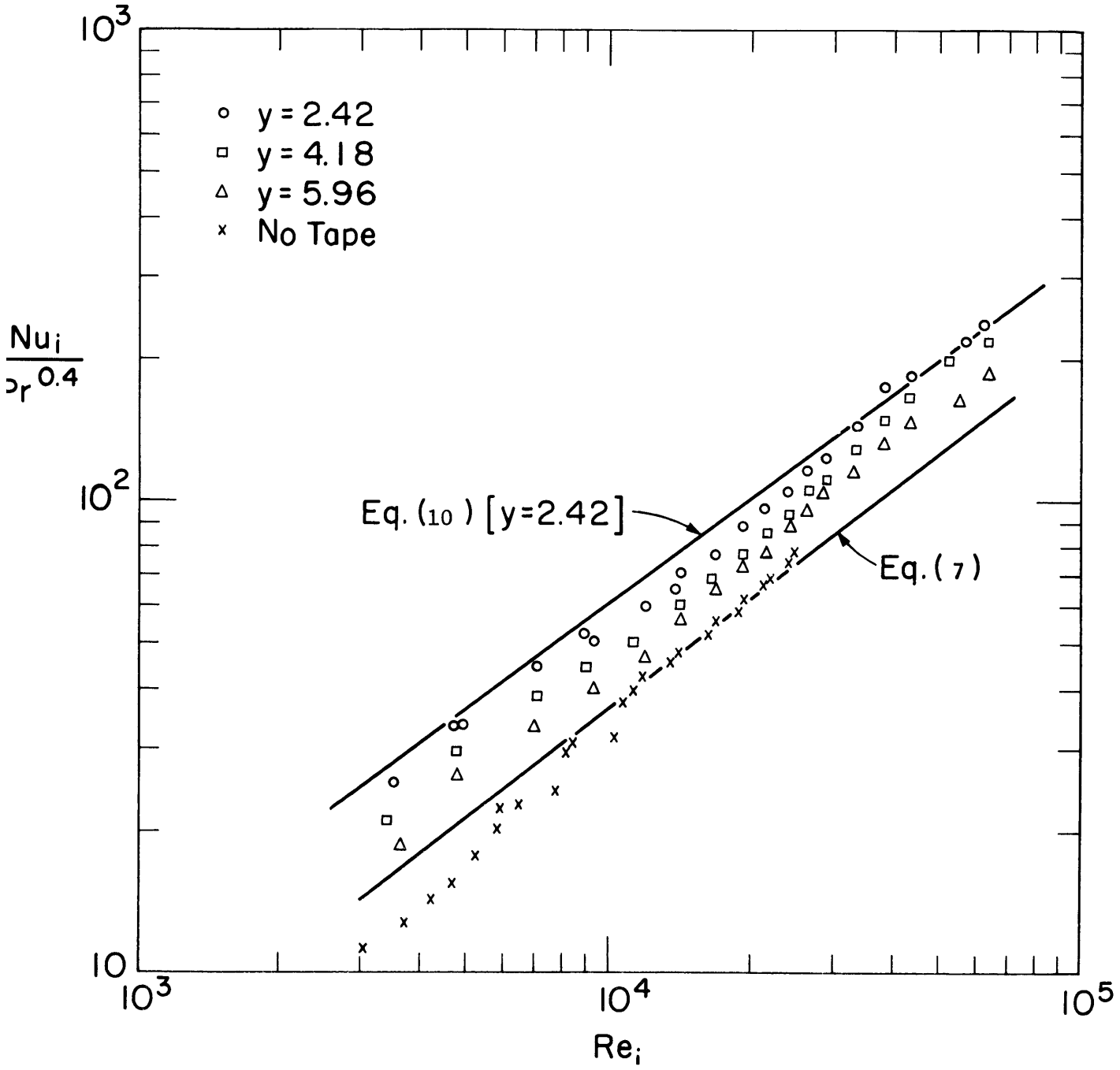

Fig. 12 Heat-Transfer Data for Straight and Swirl Flow in Smooth Tubes

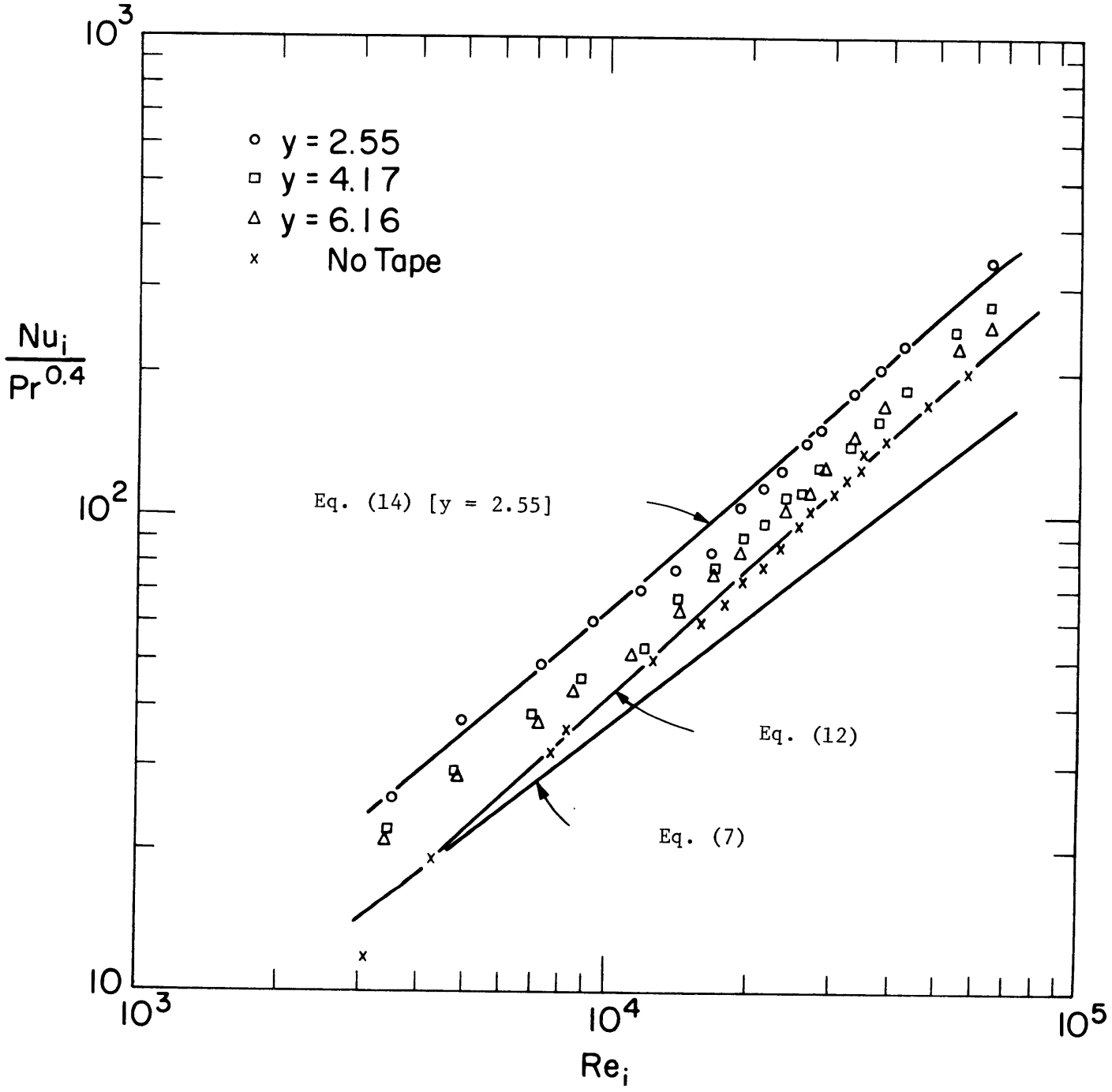

Fig. 13 Heat-transfer Data for Straight and Swirl Flow in Rough Tubes

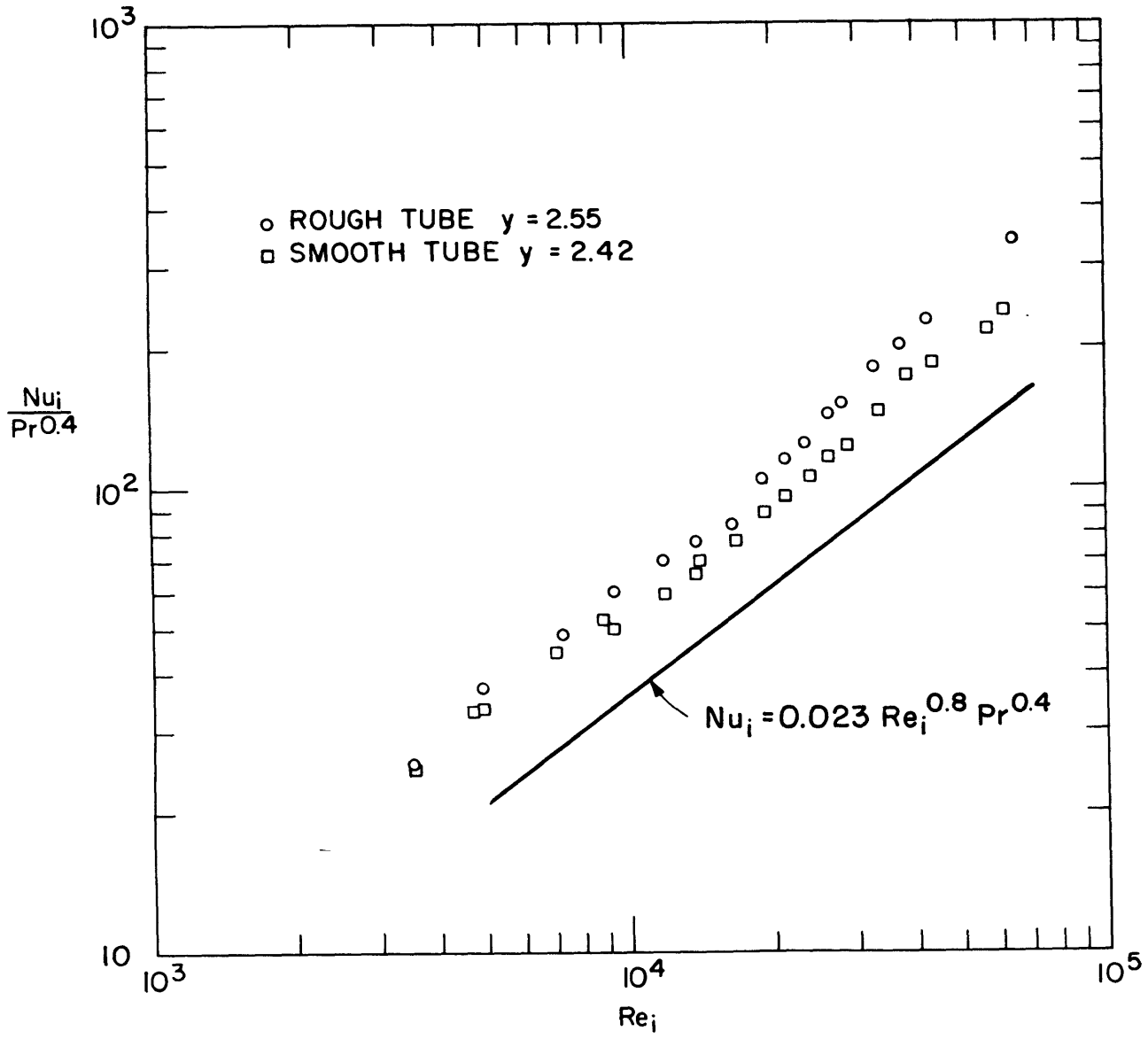

Fig. 14 Comparison of Heat-transfer Data for Swirl Flow in Smooth and Rough Tubes

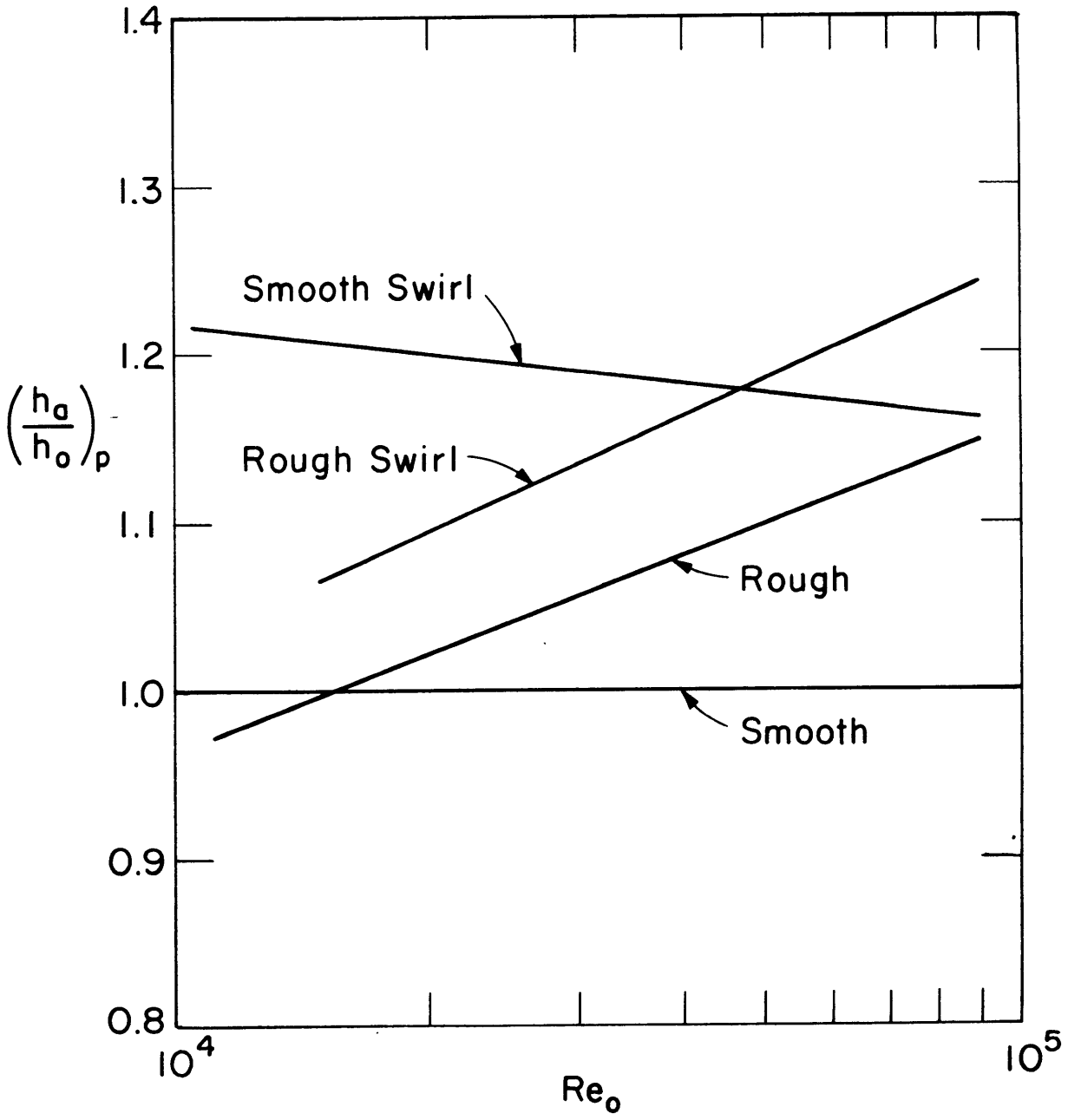

Fig. 15 Ratio of Augmented and Non-augmented Heat-transfer Coefficients at Constant Pumping Power

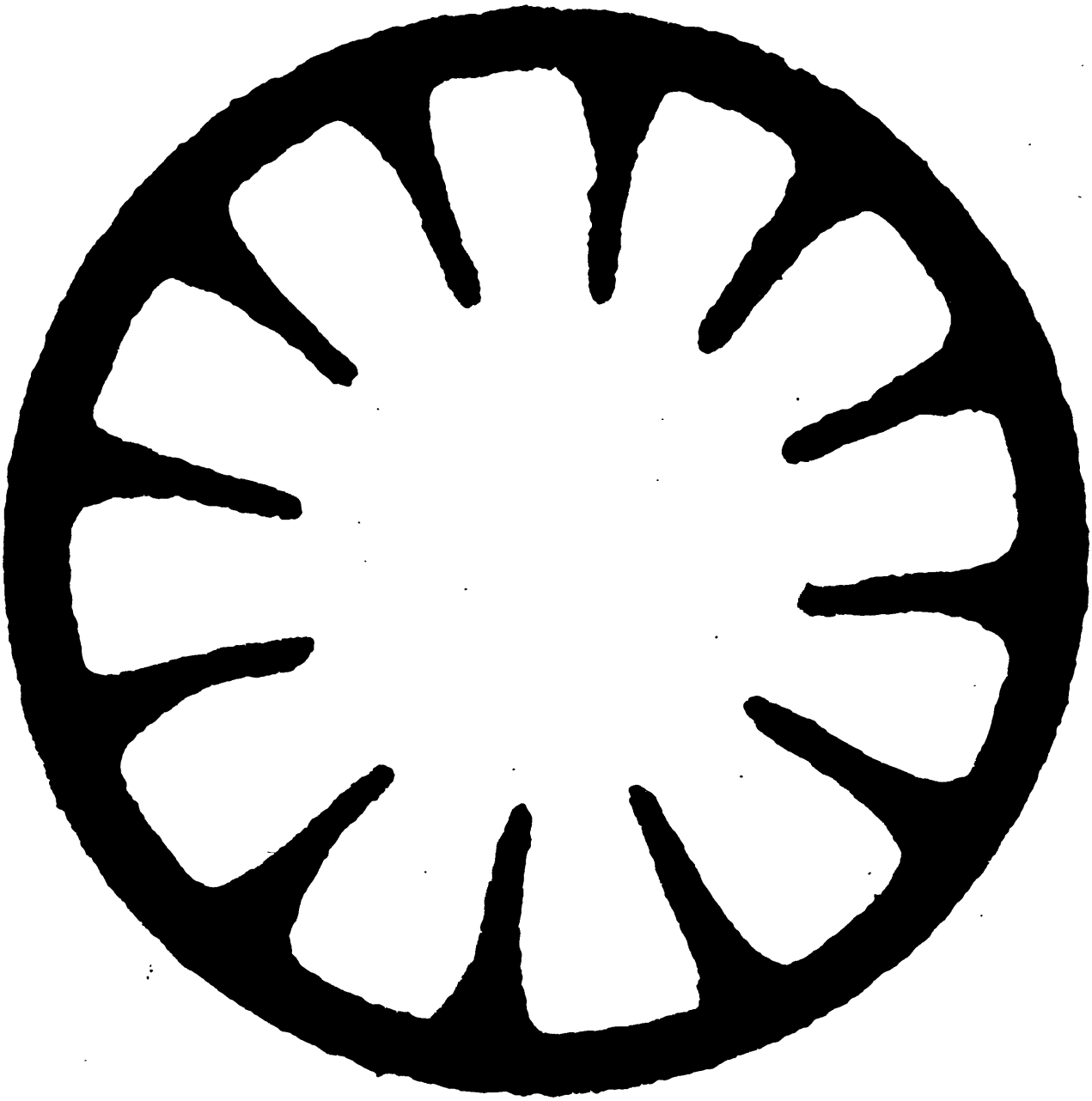

Fig. 16 Enlarged Cross-section of a Typical Internally Finned Tube (Tube 14)

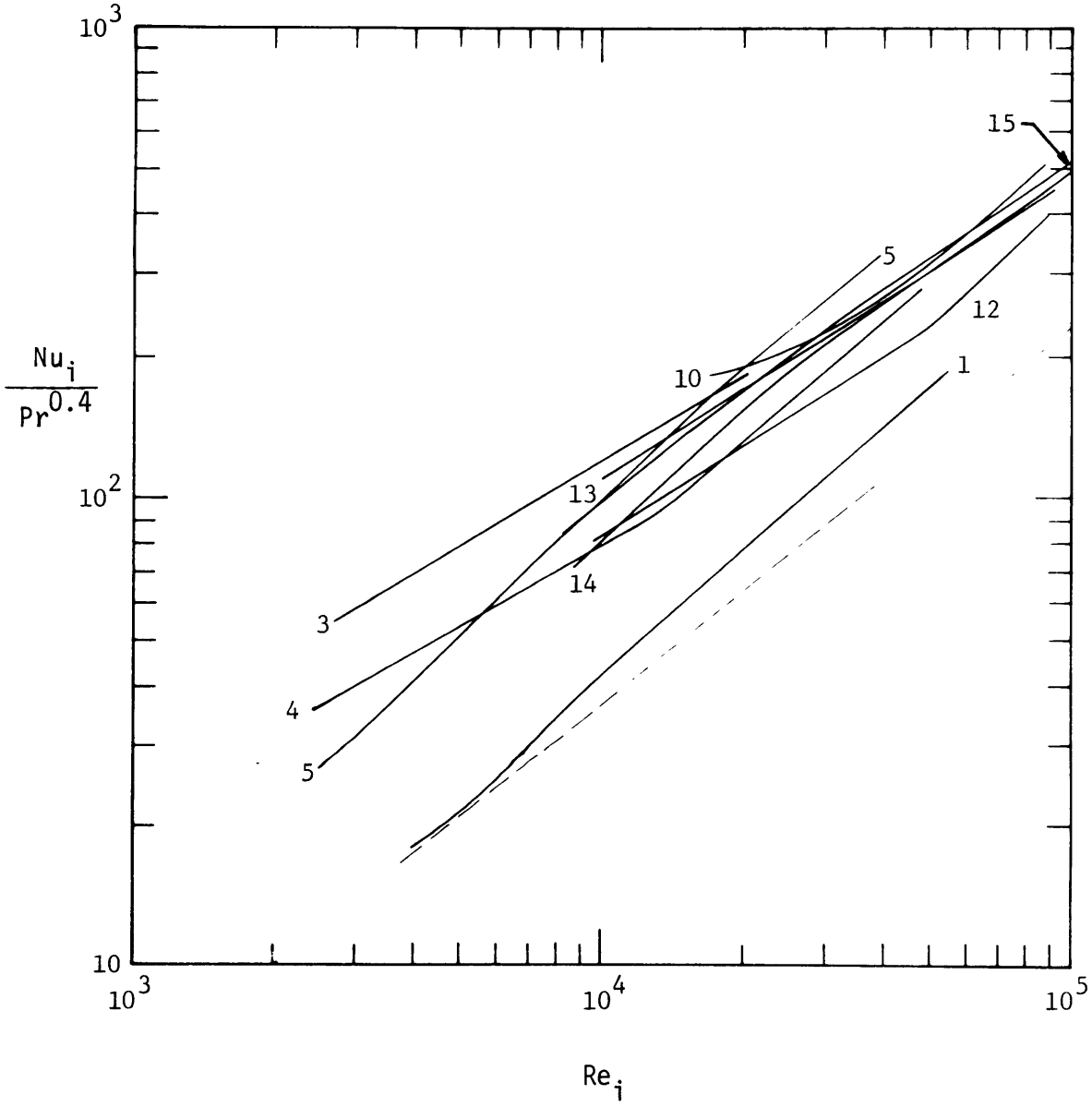

Fig. 17 Composite of Heat-transfer Data for Internally Finned Tubes Based on Nominal Diameter and Heat-transfer Area

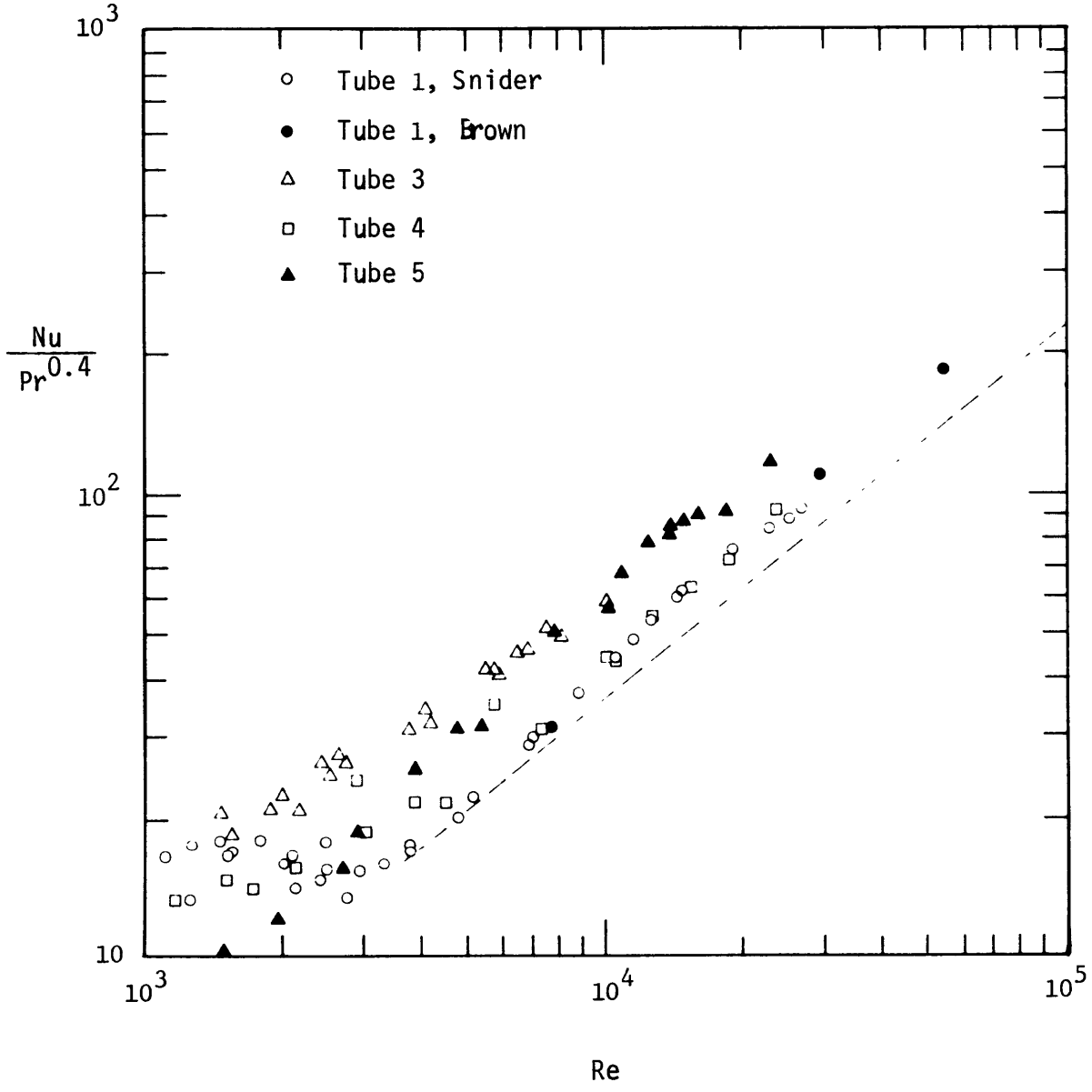

Fig. 18 Heat-Transfer Data for Internally Finned Tubes

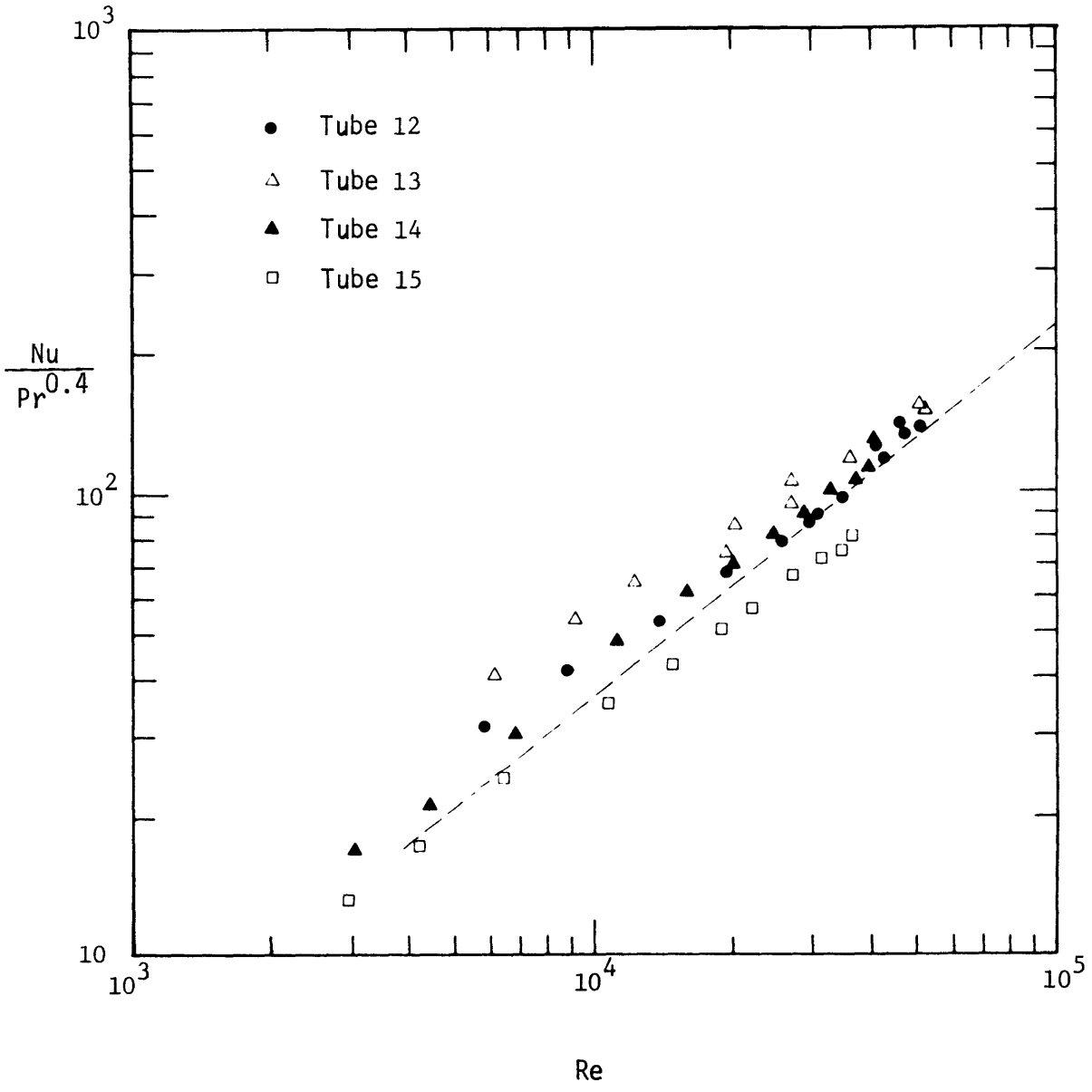

Fig. 19 Heat-Transfer Data for Internally Finned Tubes

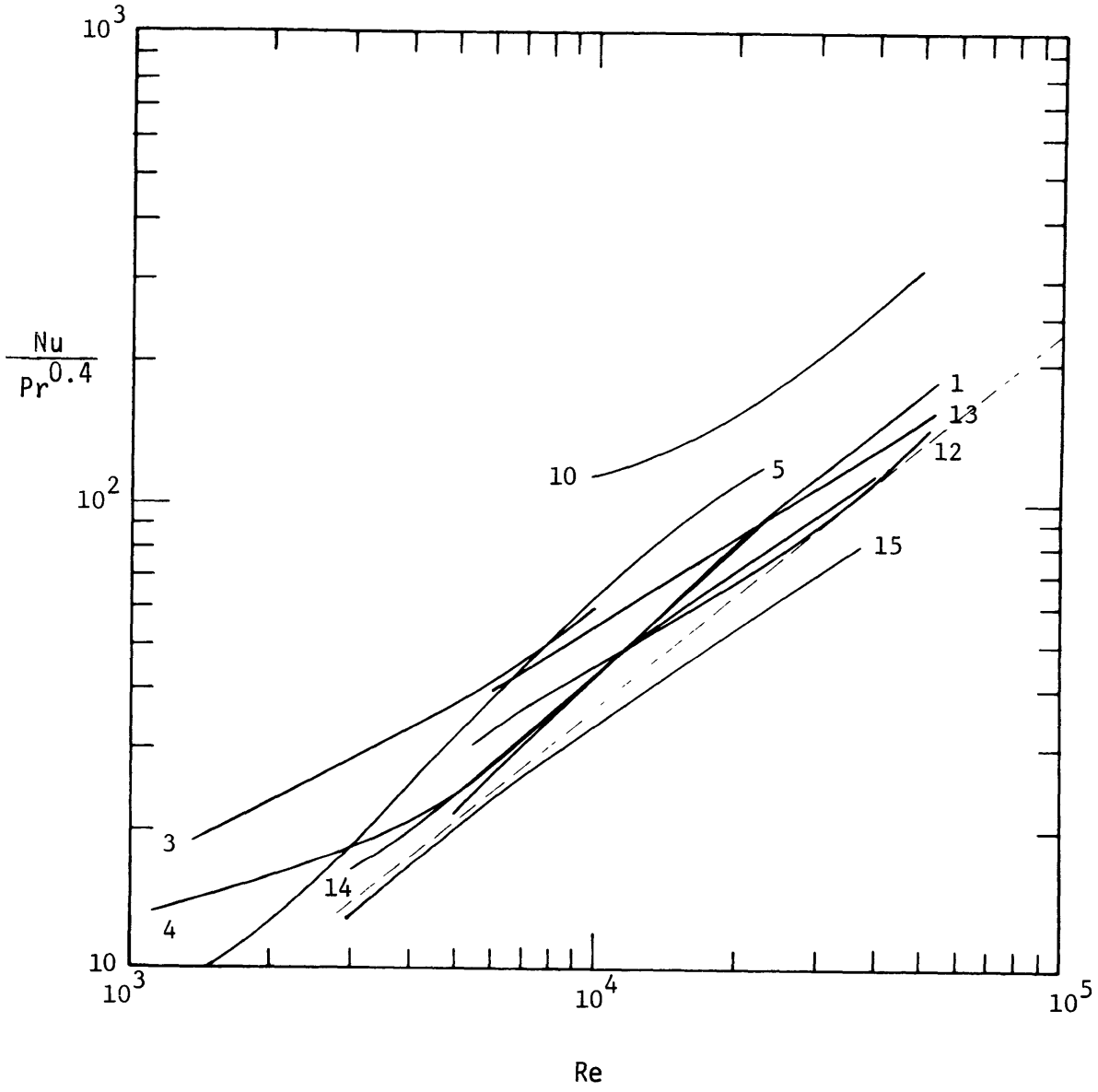

Fig. 20 Composite of Heat-Transfer Data for Internally Finned Tubes Based on Equivalent Diameter and Effective Heat-Transfer Area

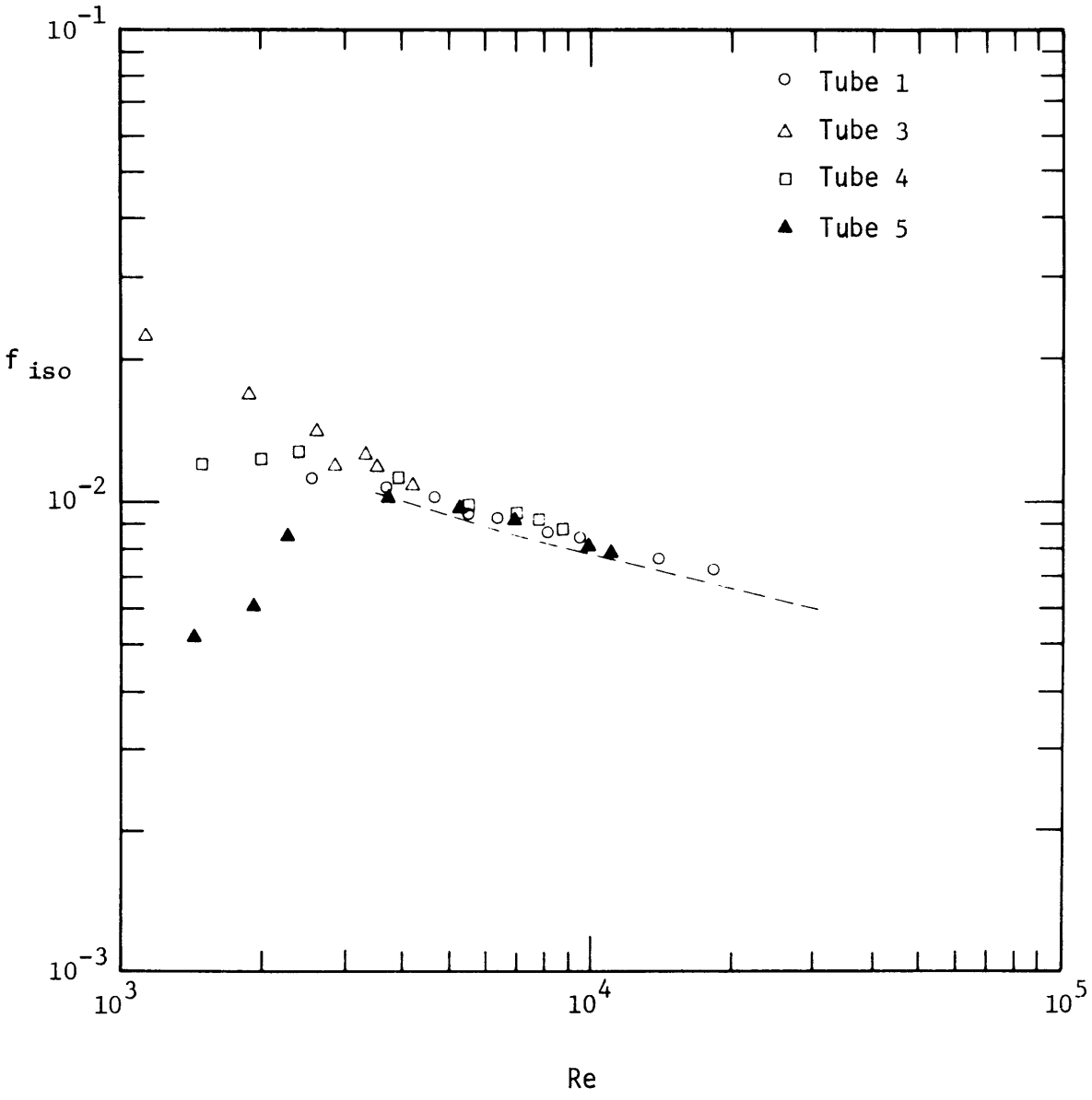

Fig. 21 Adiabatic Pressure Drop Data for Internally Finned Tubes

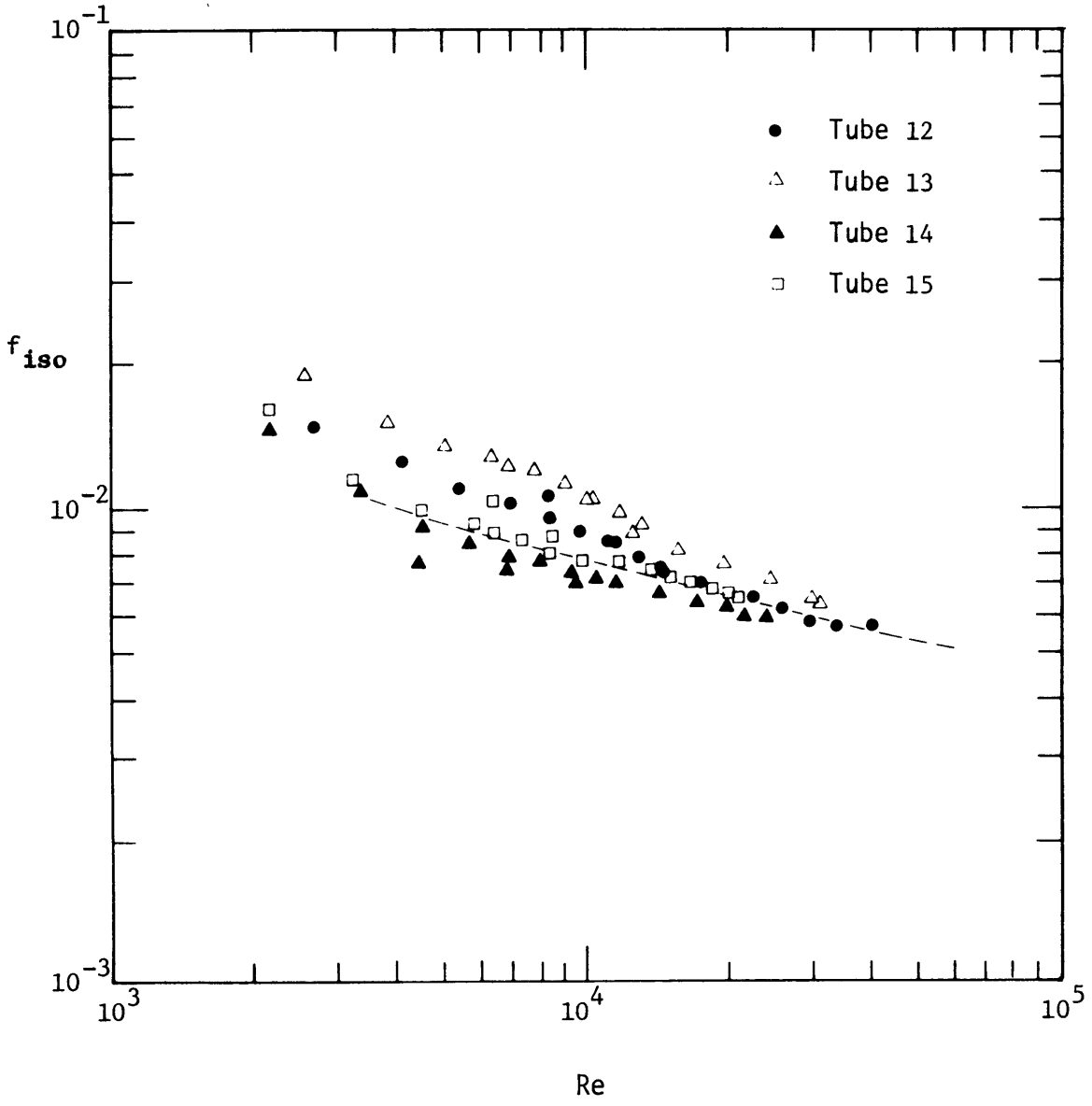

Fig.22 Adiabatic Pressure Drop Data for Internally Finned Tubes

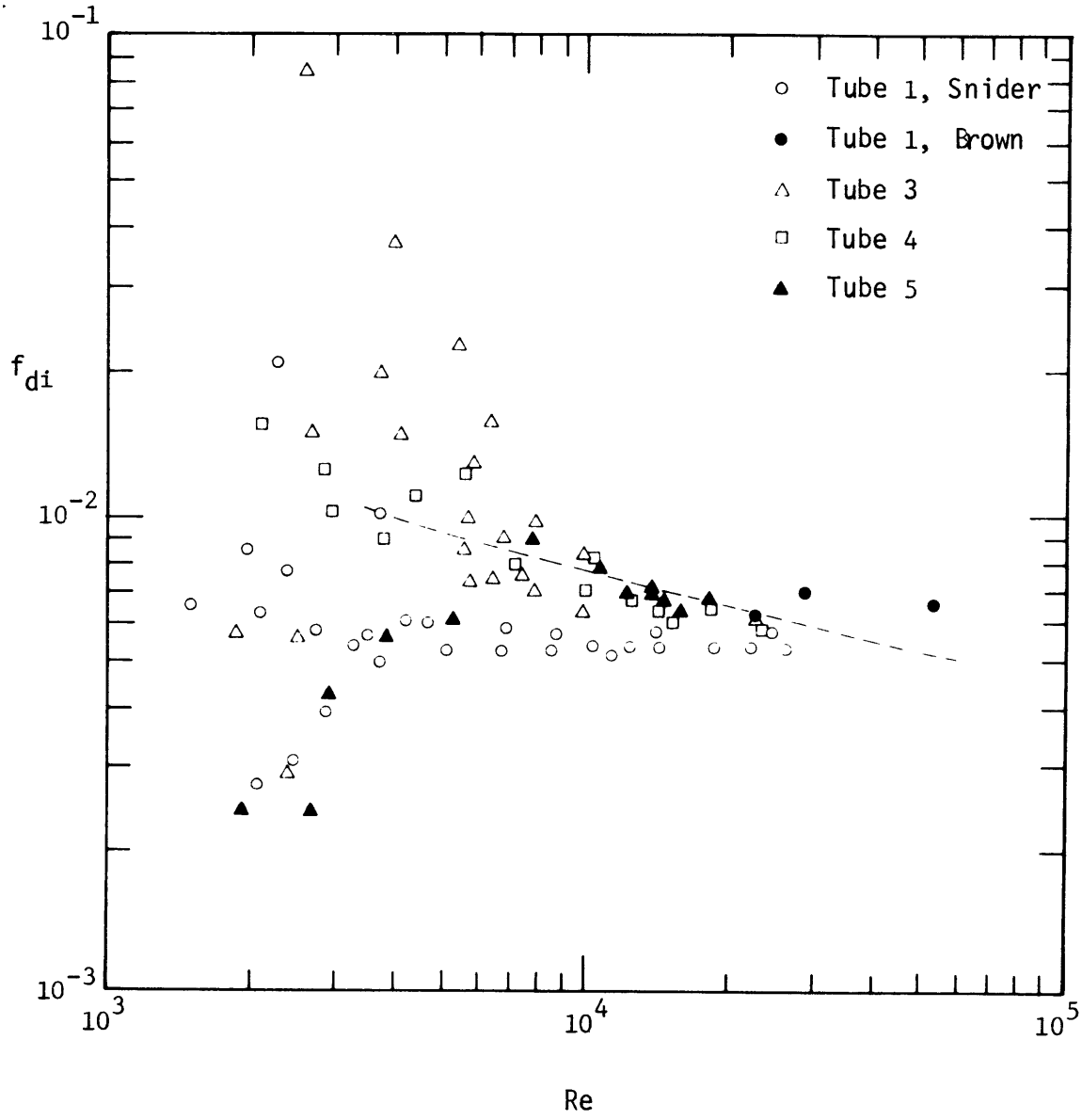

Fig. 23 Diabatic Pressure Drop Data for Internally Finned Tubes

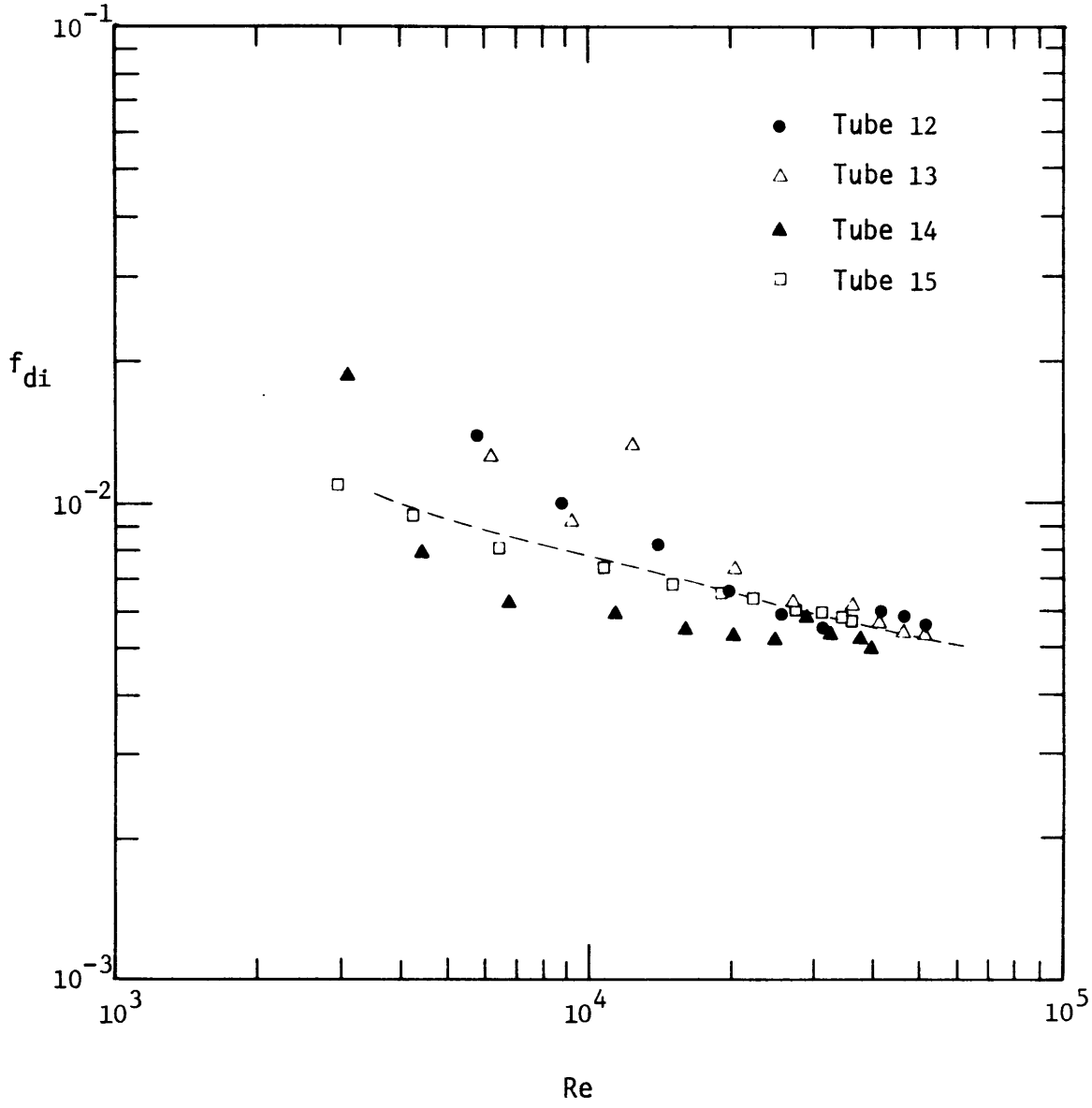

Fig. 24 Diabatic Pressure Drop Data for Internally Finned Tubes

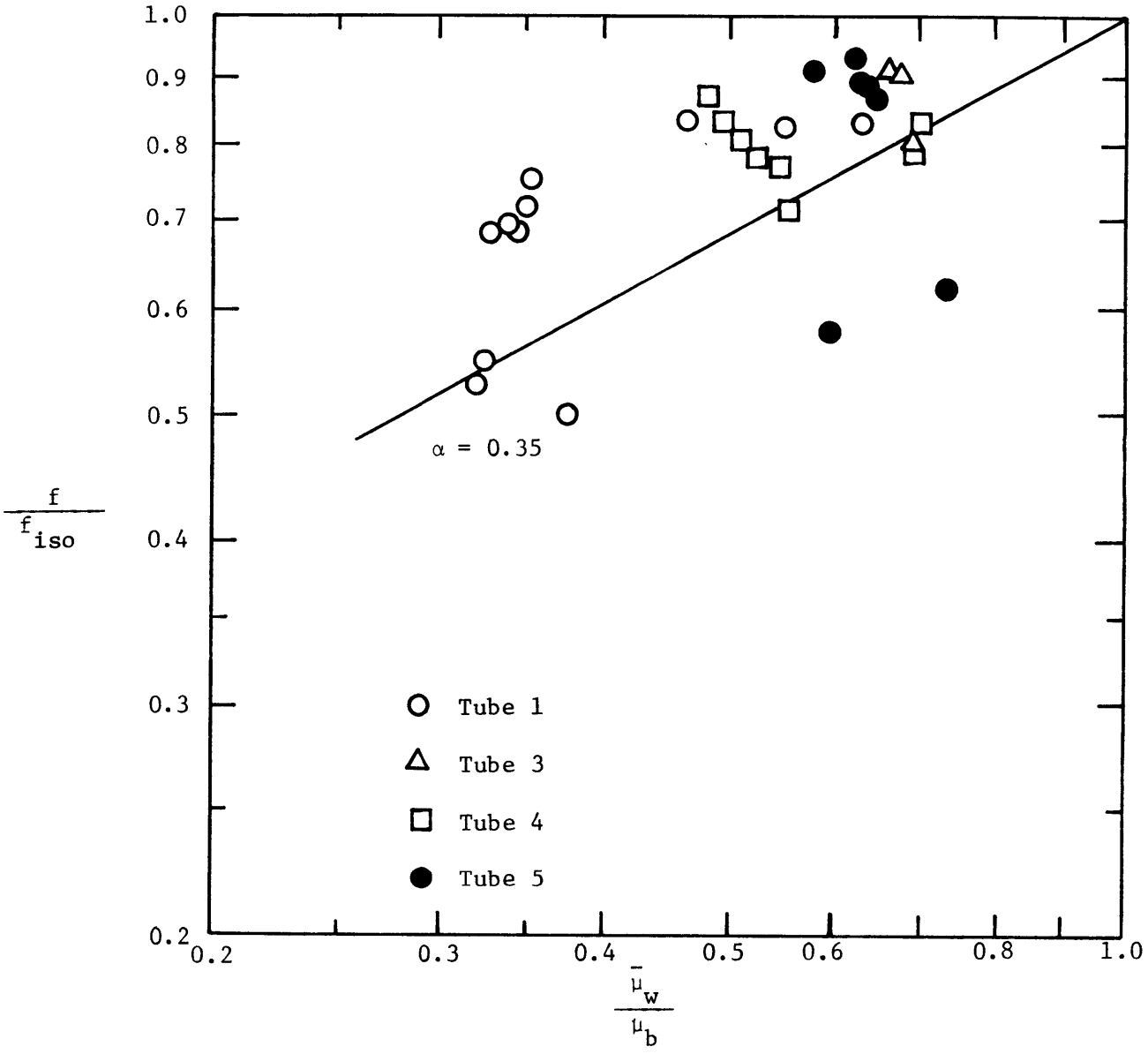

Fig. 25 Correlation of Non-isothermal Friction Factors for Internally Finned Tubing

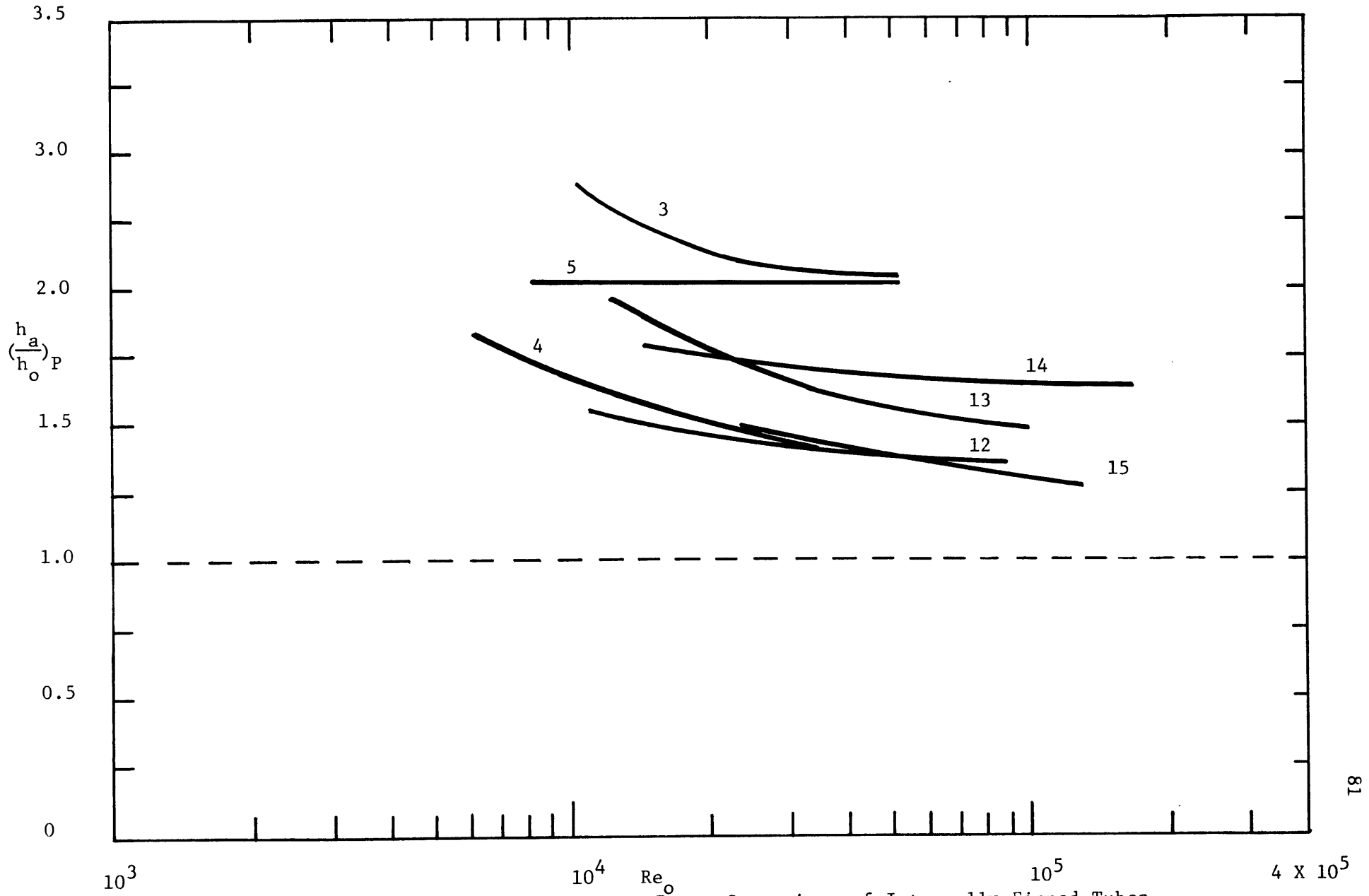

Fig. 26 Constant Pumping Power Comparison of Internally Finned Tubes

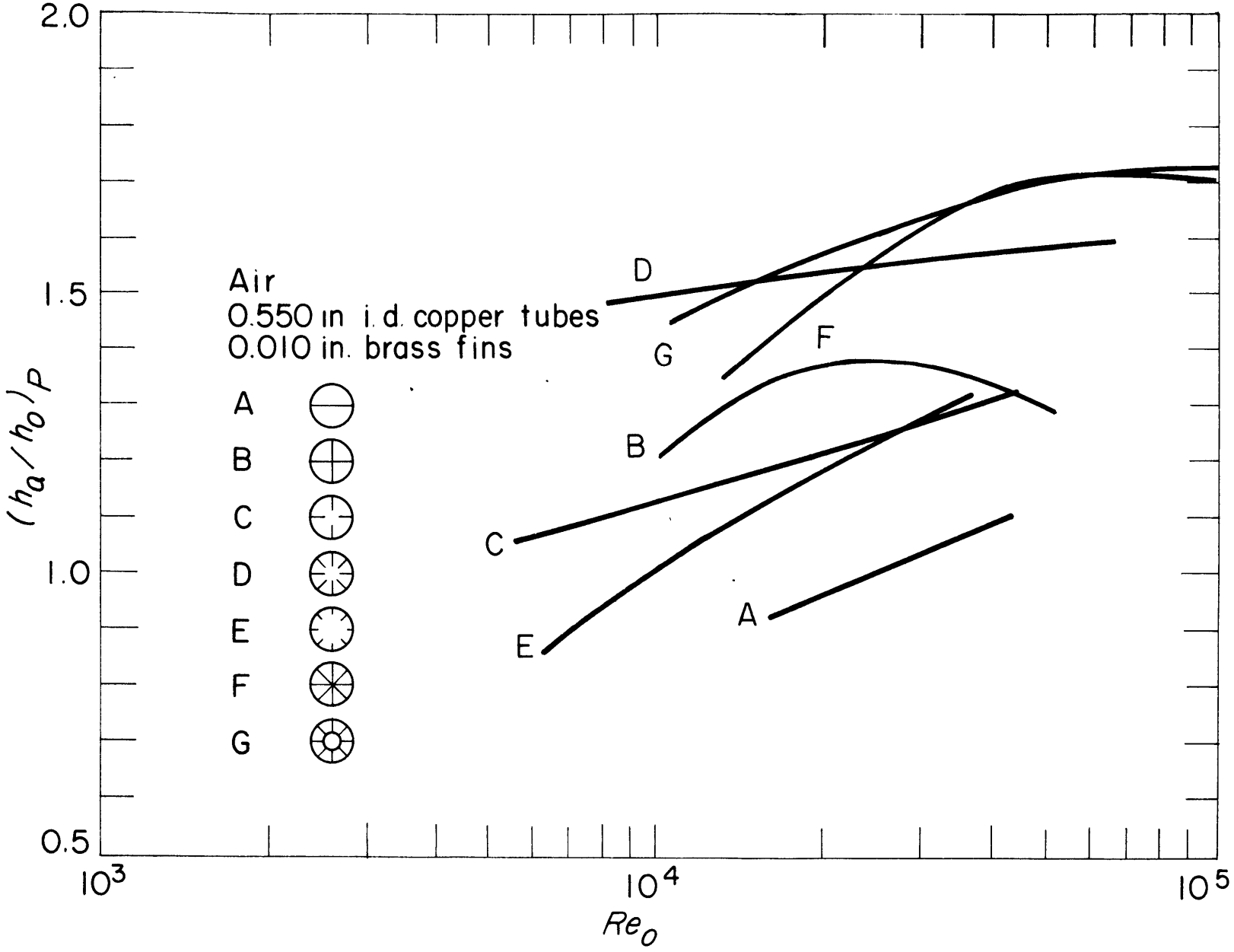

Fig. 27 Constant Pumping Power Comparison for Internally Finned Tubes Tested by Hilding and Coogan

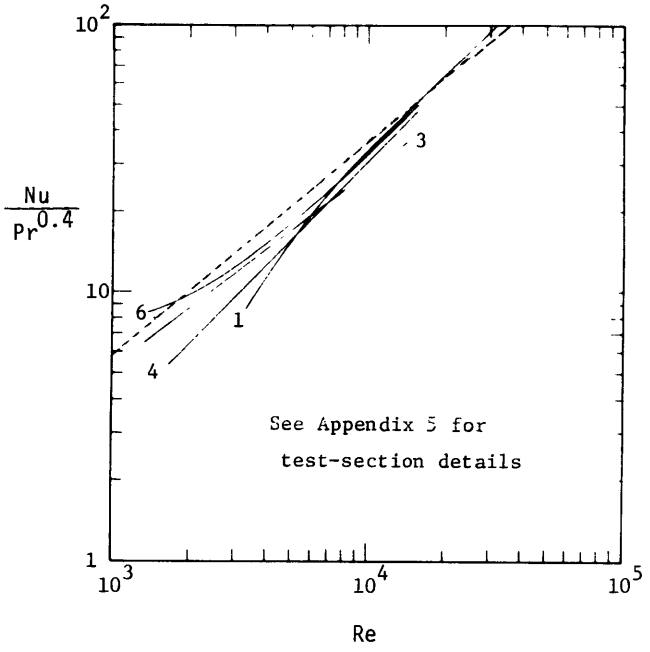

Fig. 28 Heat-transfer Data of Hilding and Coogan (26)

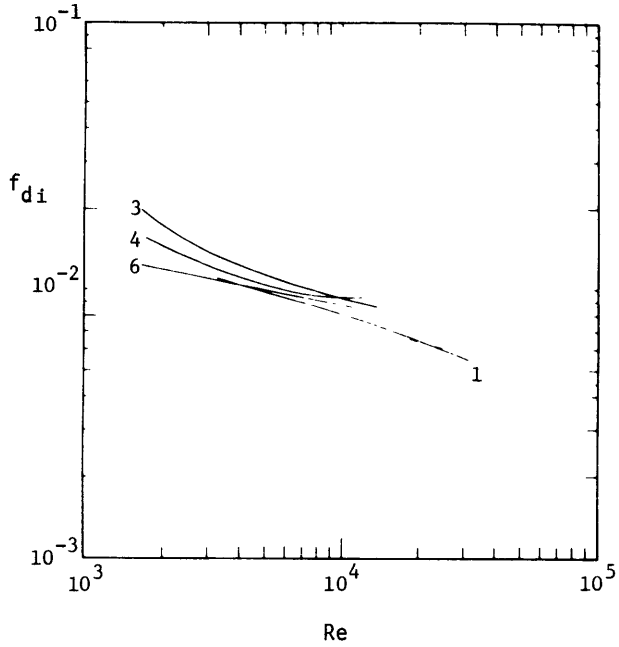

Fig. 29 Pressure Drop Results of Hilding and Coogan (26)

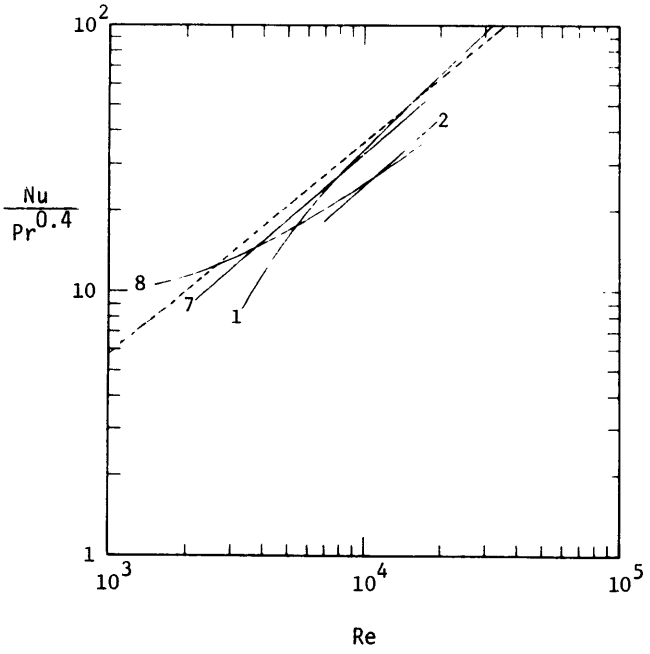

Fig. 30 Heat-transfer Data of Hilding and Coogan (26)

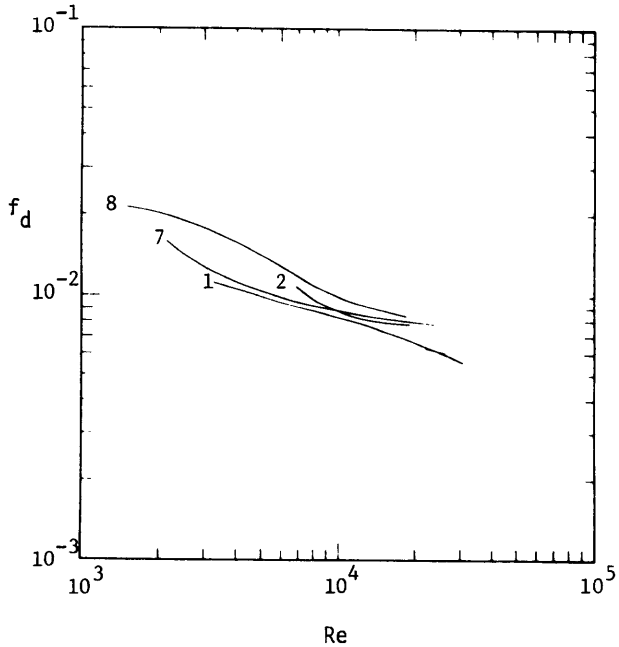

Fig. 31 Pressure Drop Results of Hilding and Coogan (26)

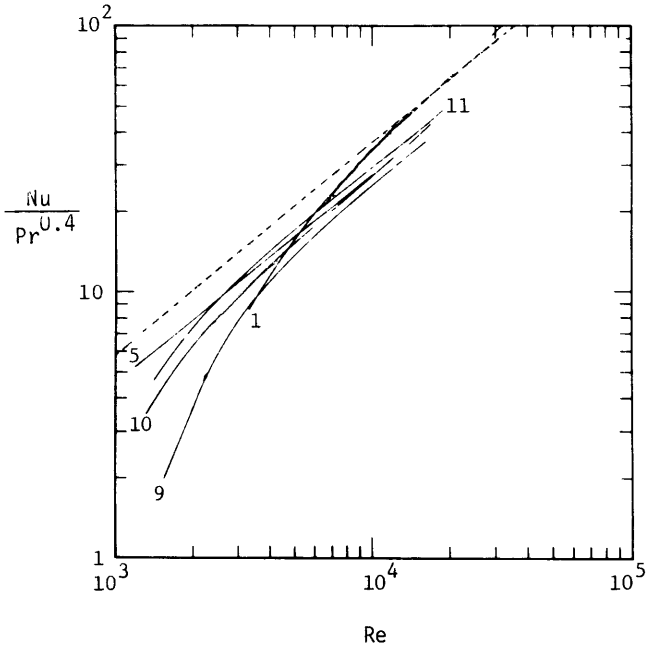

Fig. 32 Heat-transfer Data of Hilding and Coogan (26)

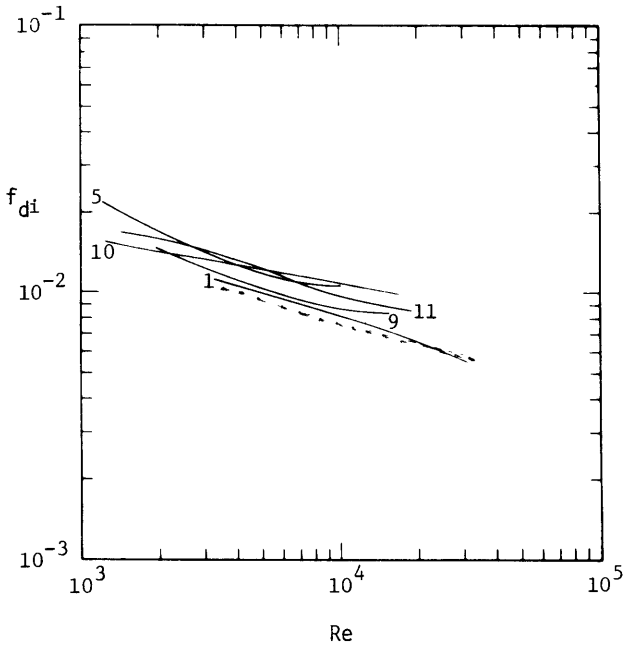

Fig. 33 Pressure Drop Results of Hilding and Coogan (26)

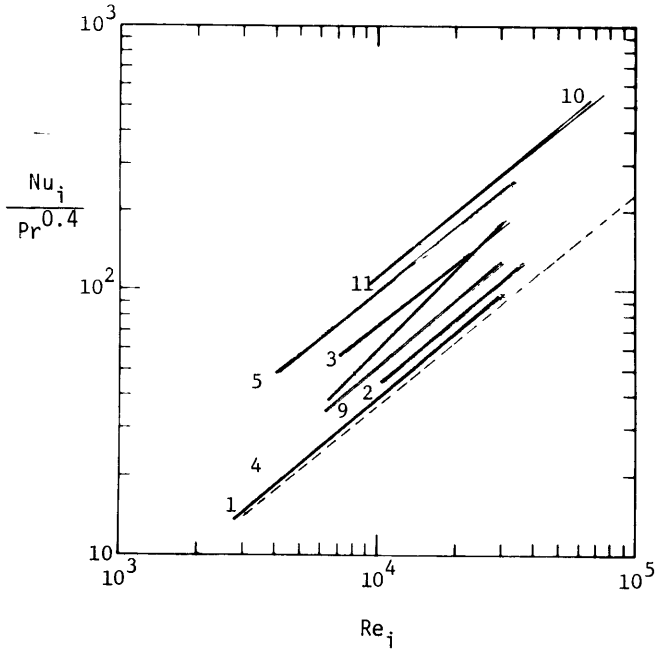

Fig. 34 Heat-transfer Data of Hilding and Coogan (26) for Continuous Fin Tubes (Based on the Nominal Diameter and Heat-Transfer Area)

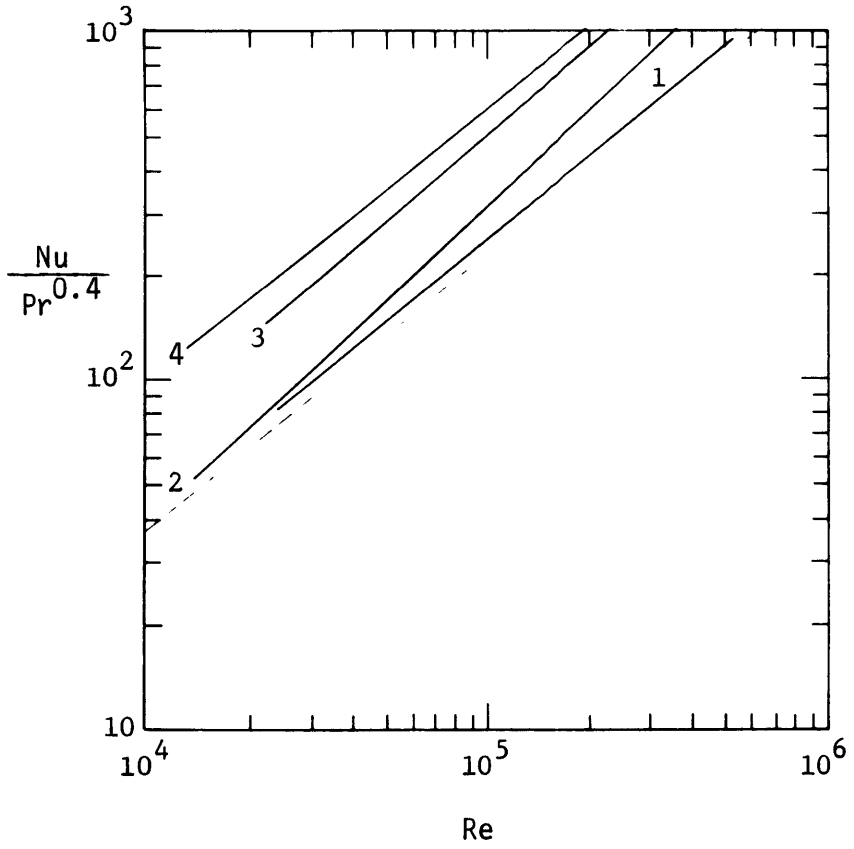

Fig. 35 Heat transfer Results of Dipprey and Sabersky [3]

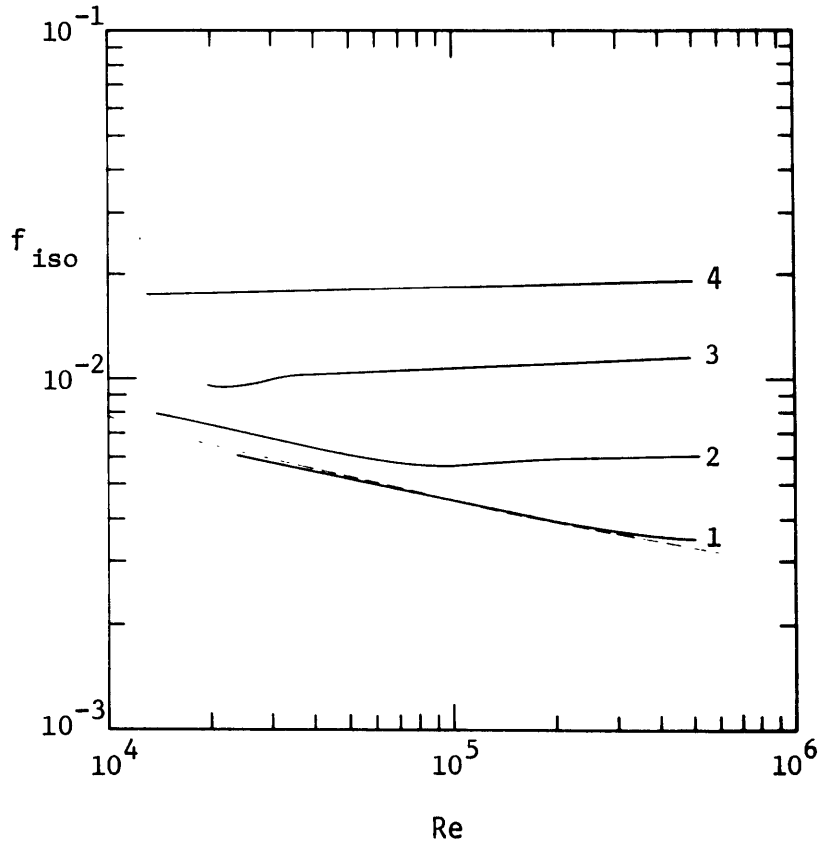

Fig. 36 Pressure Drop Results of Dipprey and Sabersky [3]

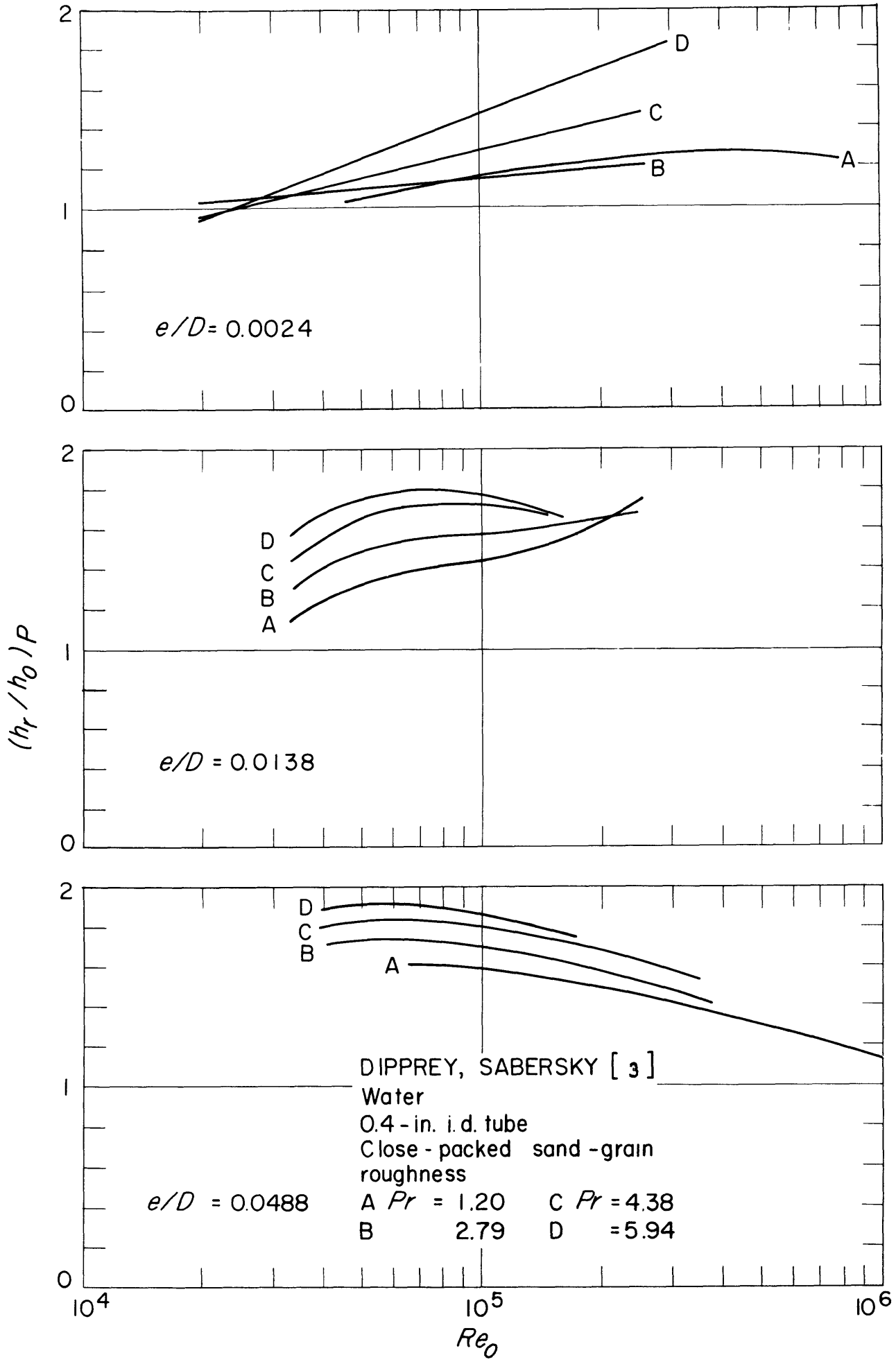

Fig. 37 Performance of Tubes with Sand-grain Type Roughness

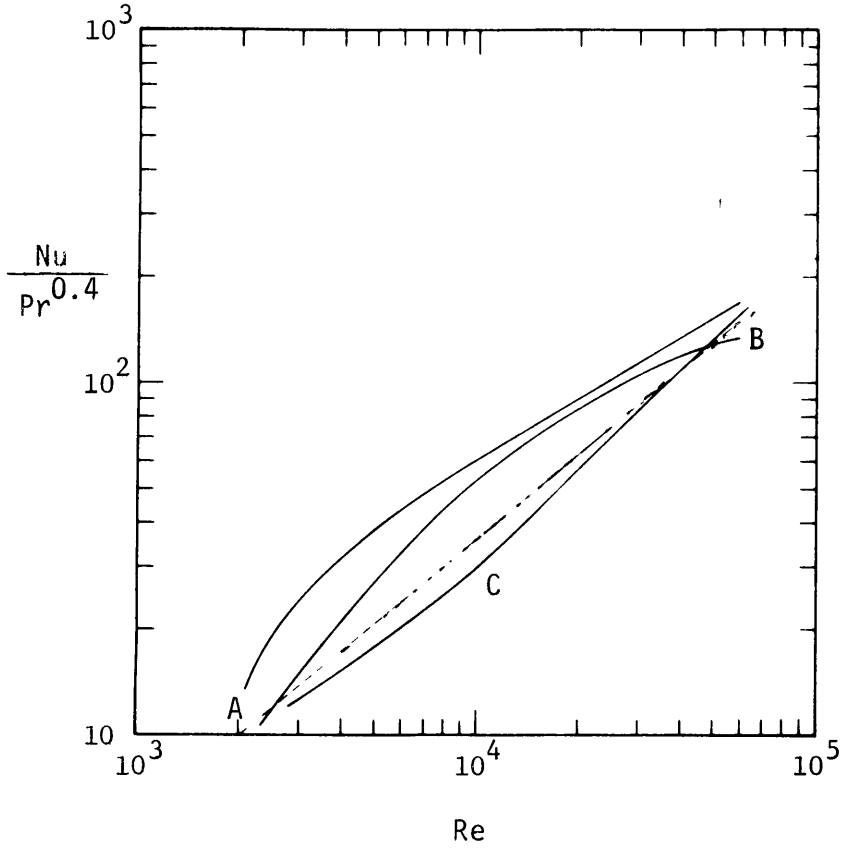

Fig. 38 Heat transfer Data of Cope [33]

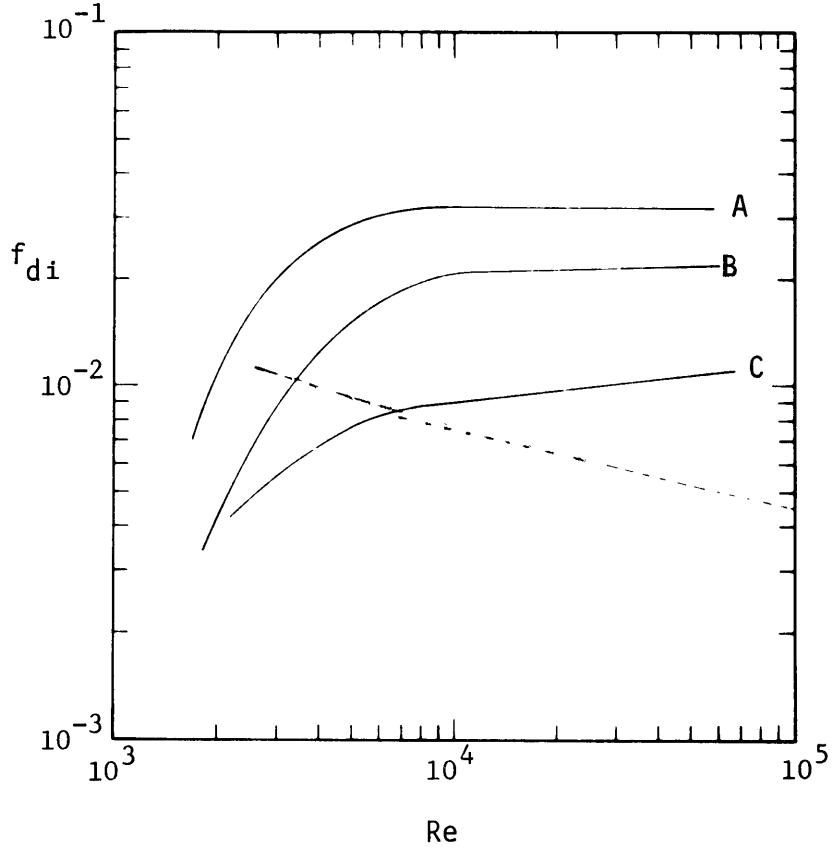

Fig. 39 Pressure Drop Data of Cope [33]

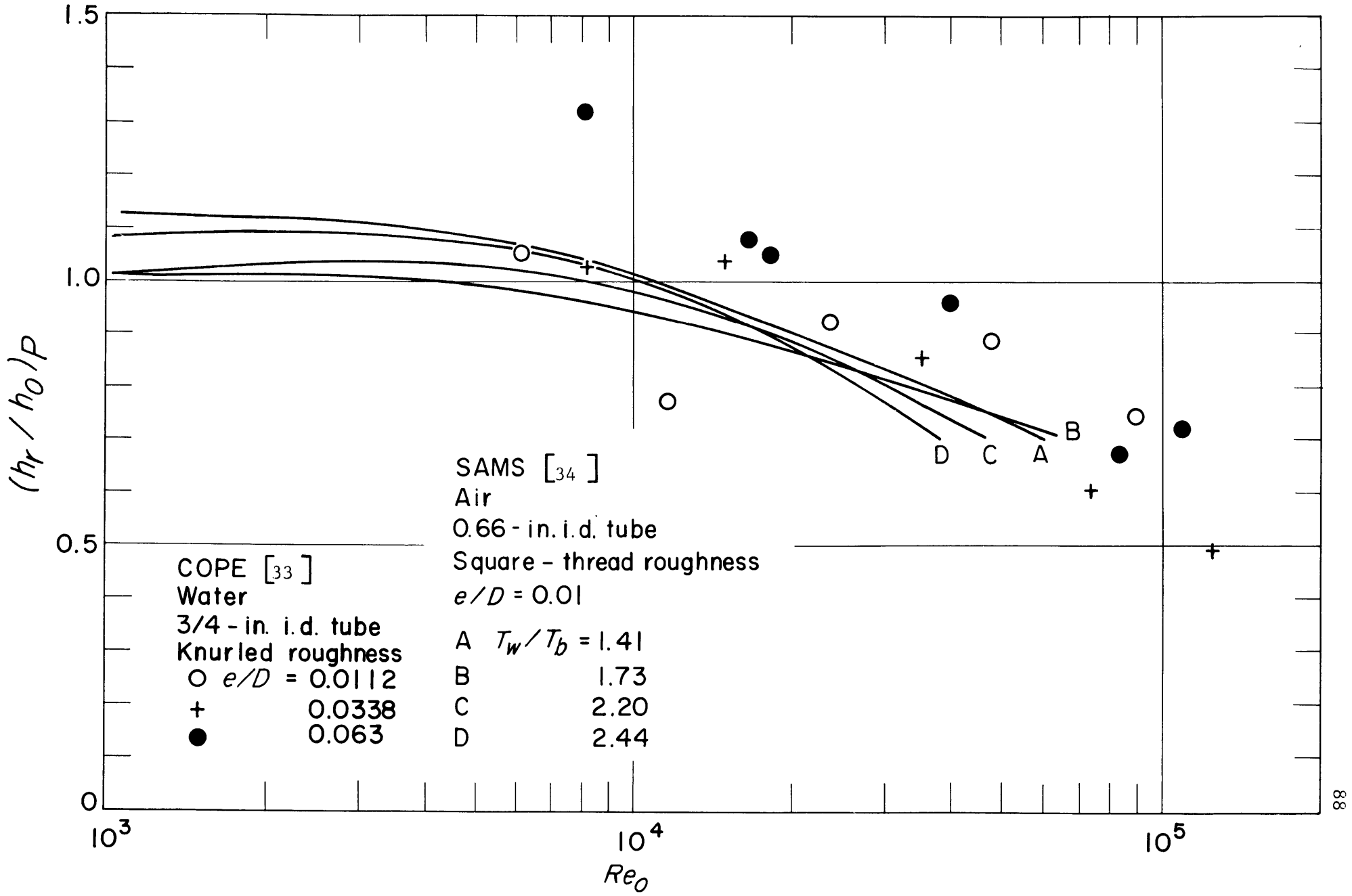

Fig. 40 Performance of Tubes with Machined Roughness

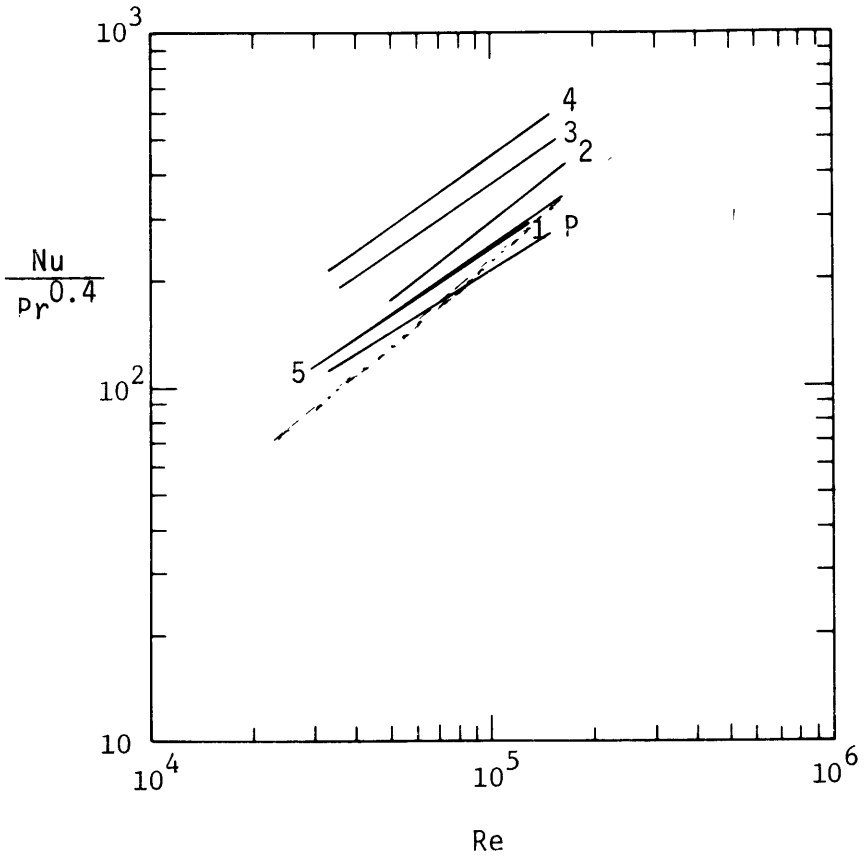

Fig. 41 Heat-transfer Data of Brouillette et al. [35]

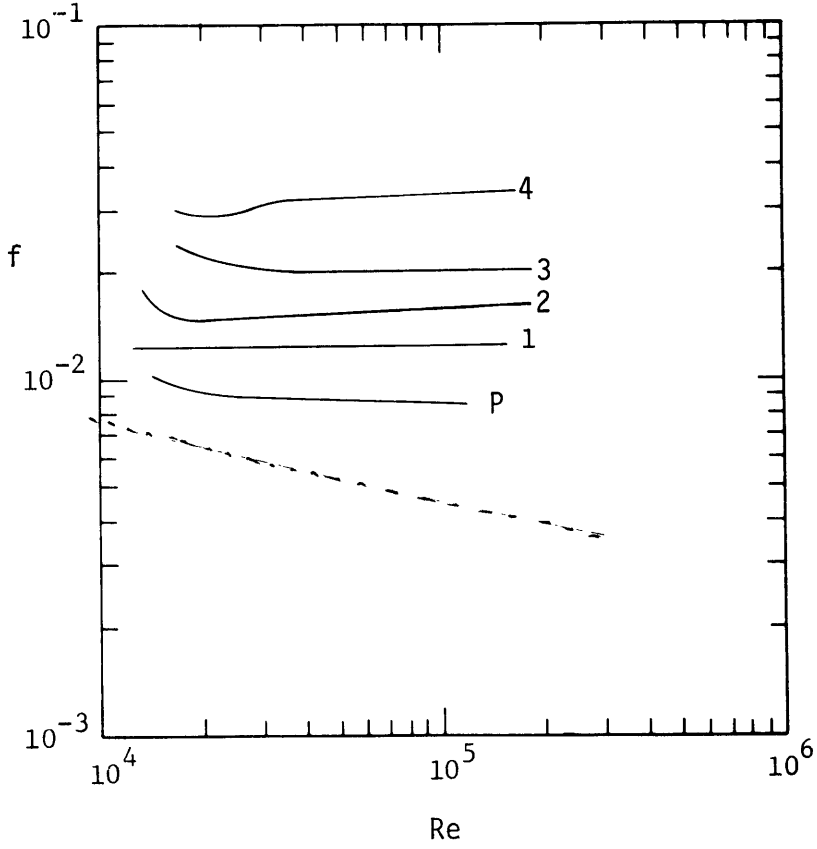

Fig. 42 Friction Factor Data of Brouillette et al. [35]

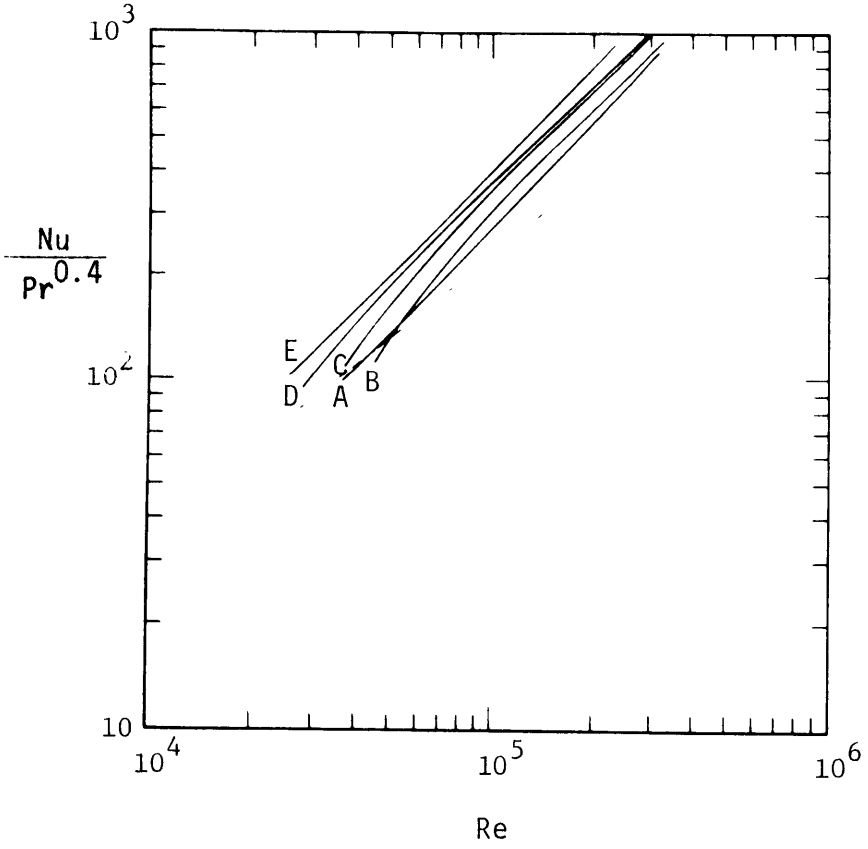

Fig. 43 Heat transfer Data of Teverovskii [36]

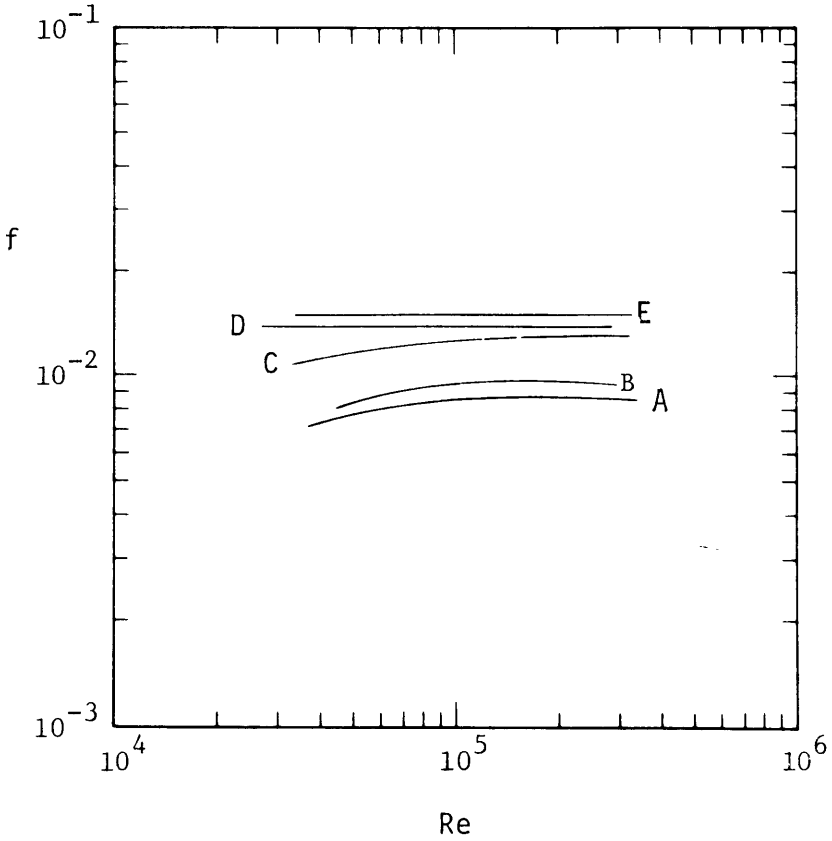

Fig. 44 Friction Factor Data of Teverovskii [36]

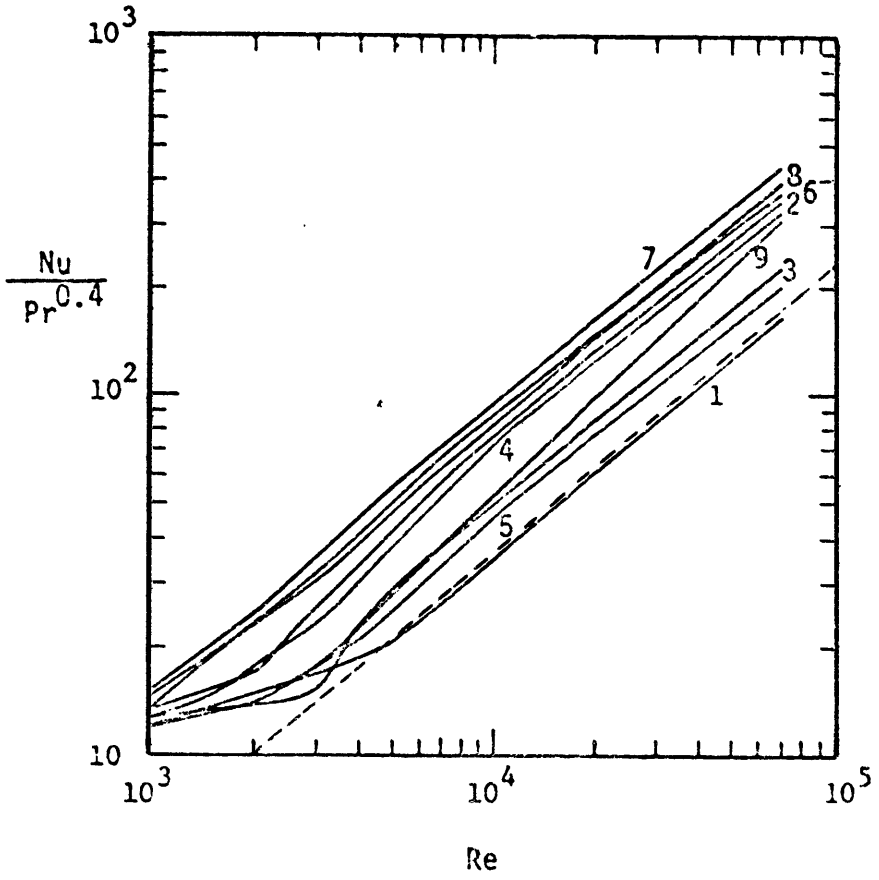

Fig. 45 Heat transfer Results of Nunner [31]

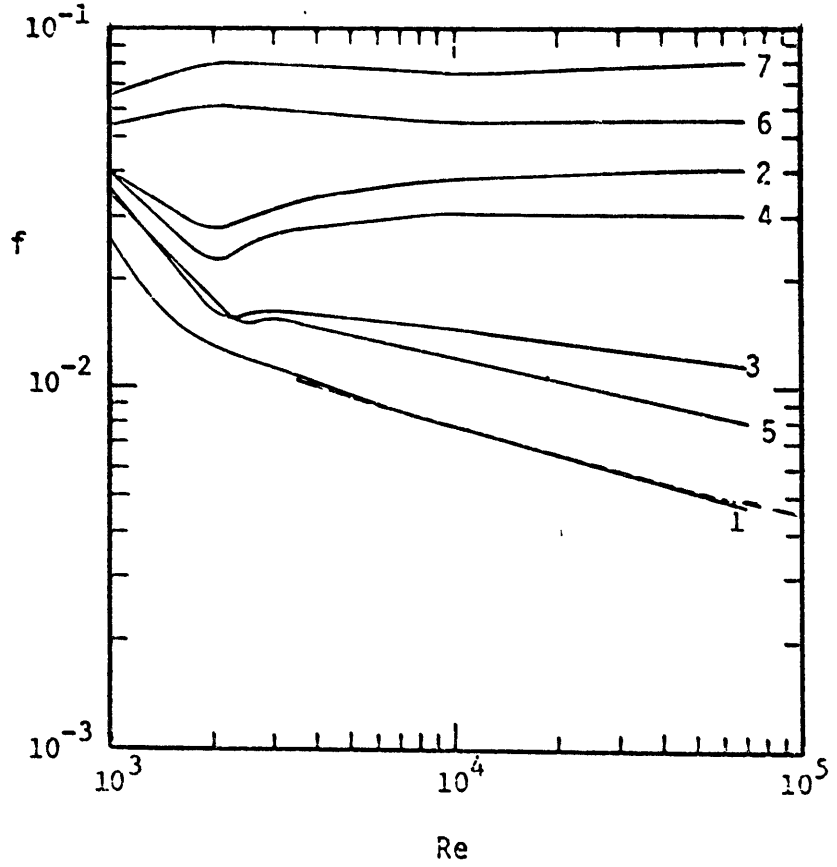

Fig. 46 Pressure Drop Results of Nunner [31]

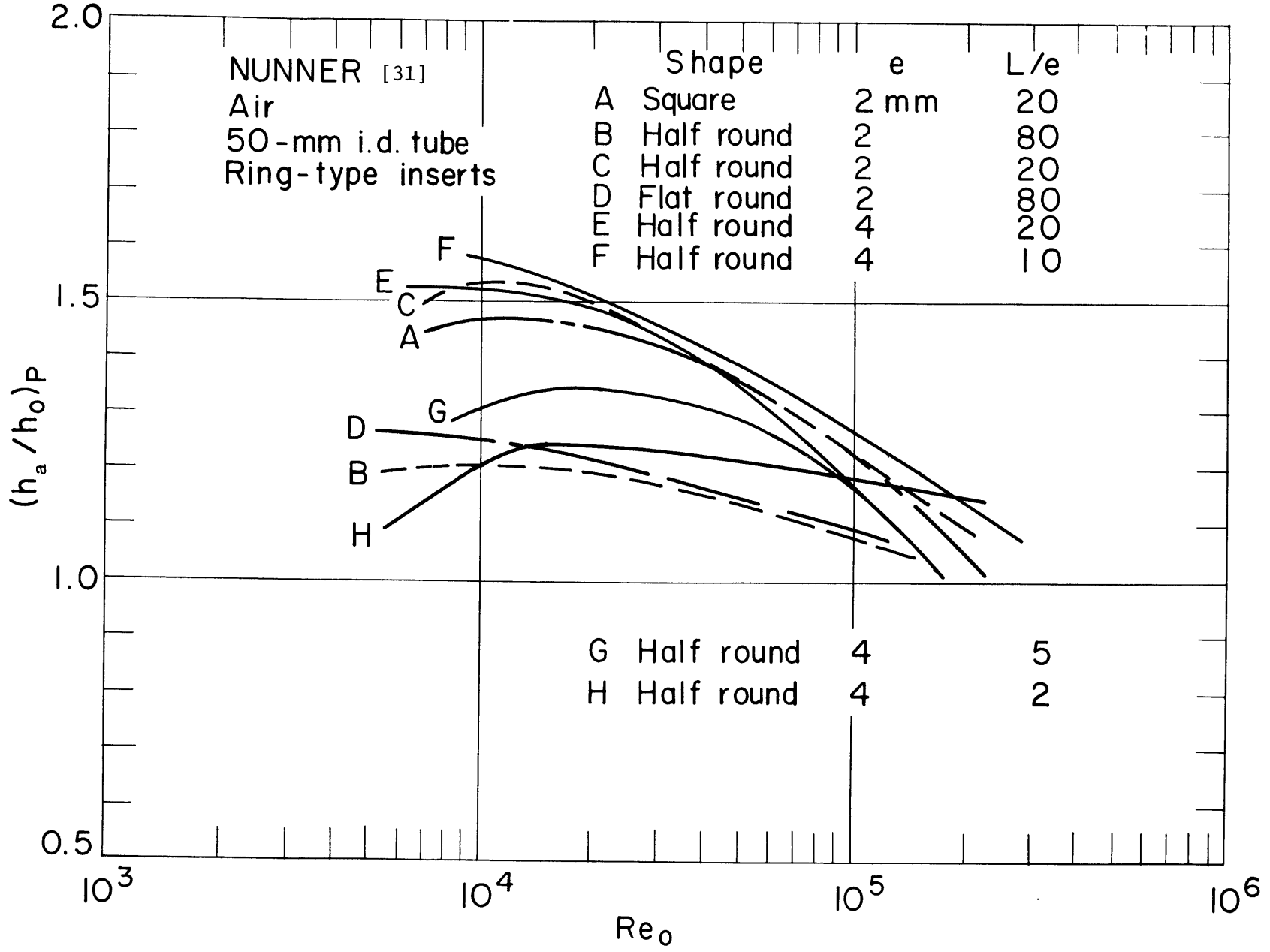

Fig. 47 Performance of Tubes with Small Ring-Type Inserts

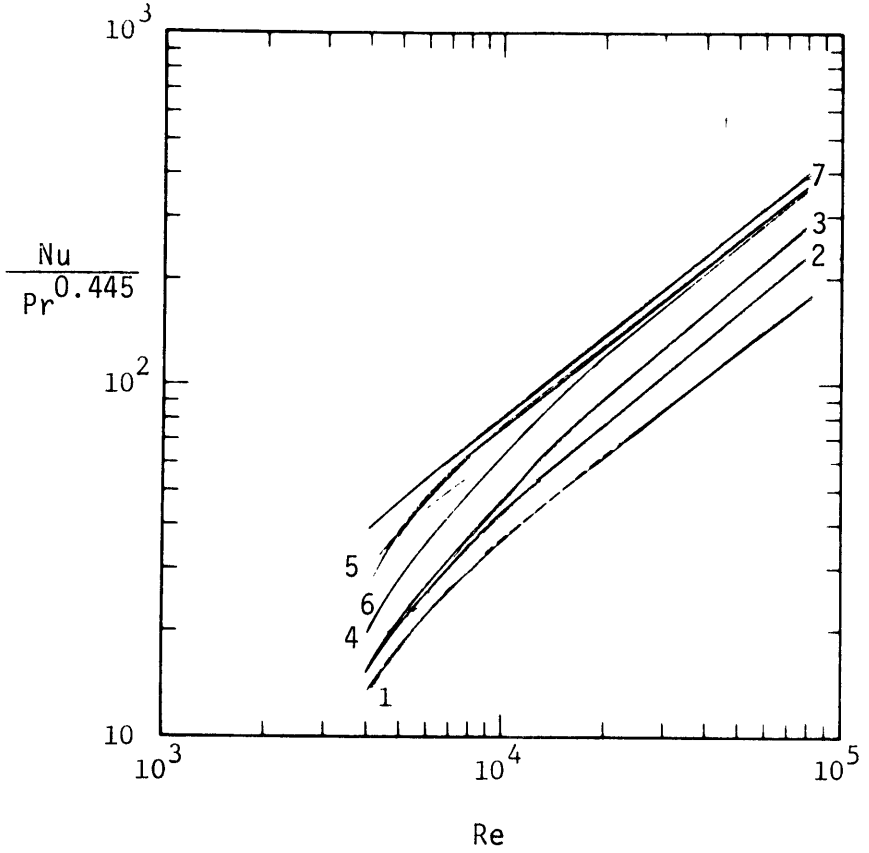

Fig. 48 Heat-transfer Results of Kalinin, et al. [40]

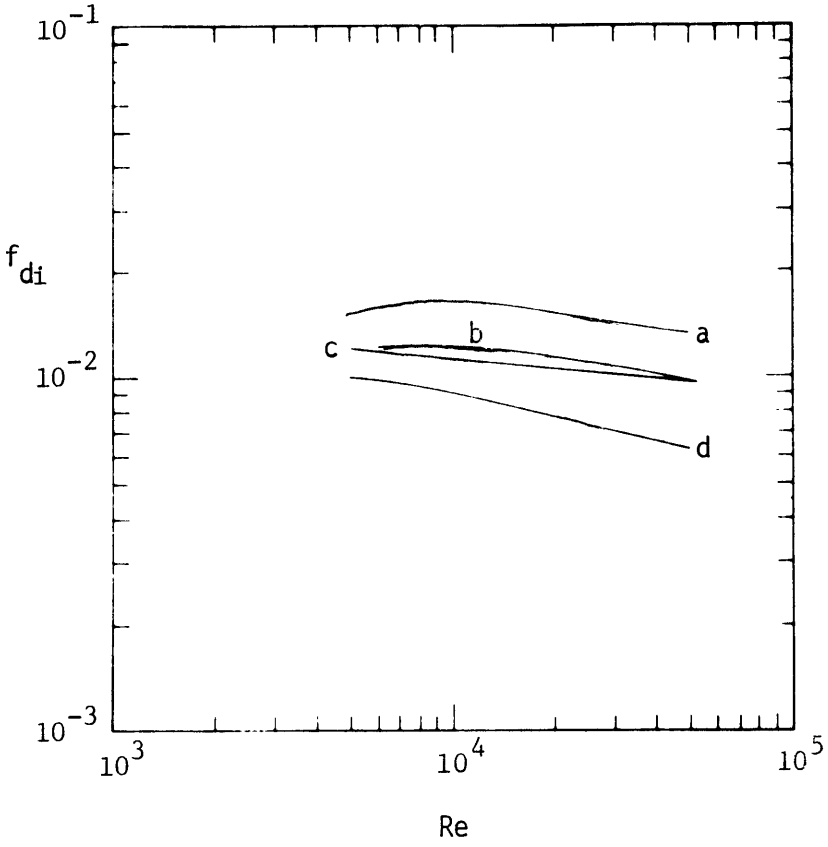

Fig. 49 Pressure Drop Results of Kalinin, et al. [40]

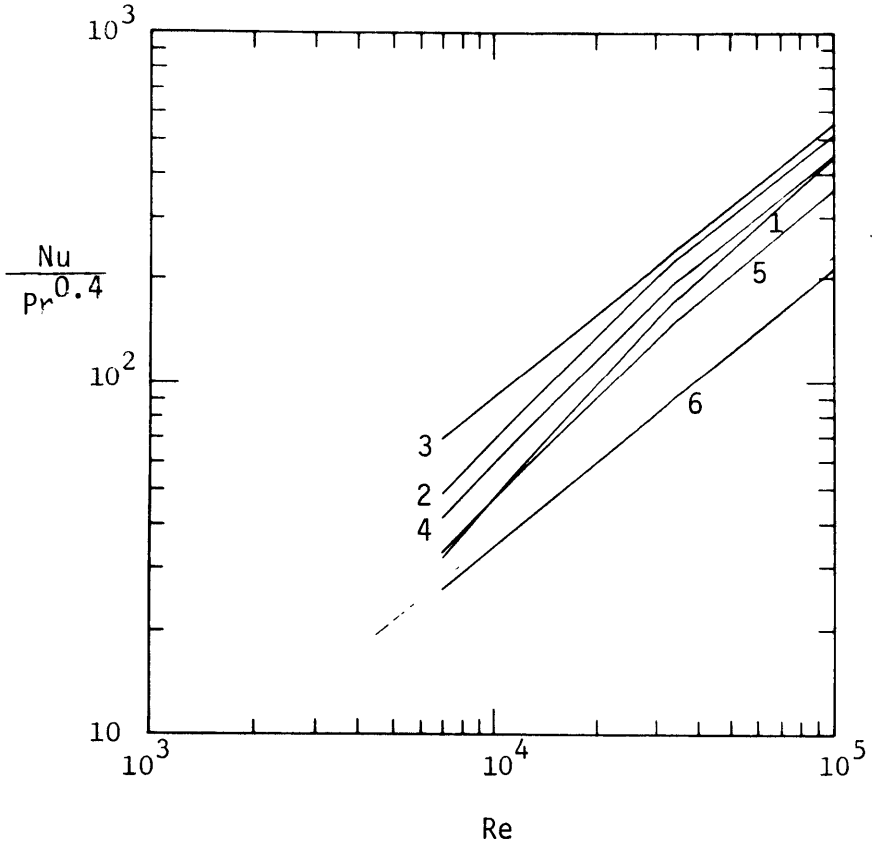

Fig. 50 Heat-transfer Results of Webb [41]

Pr = 0.71

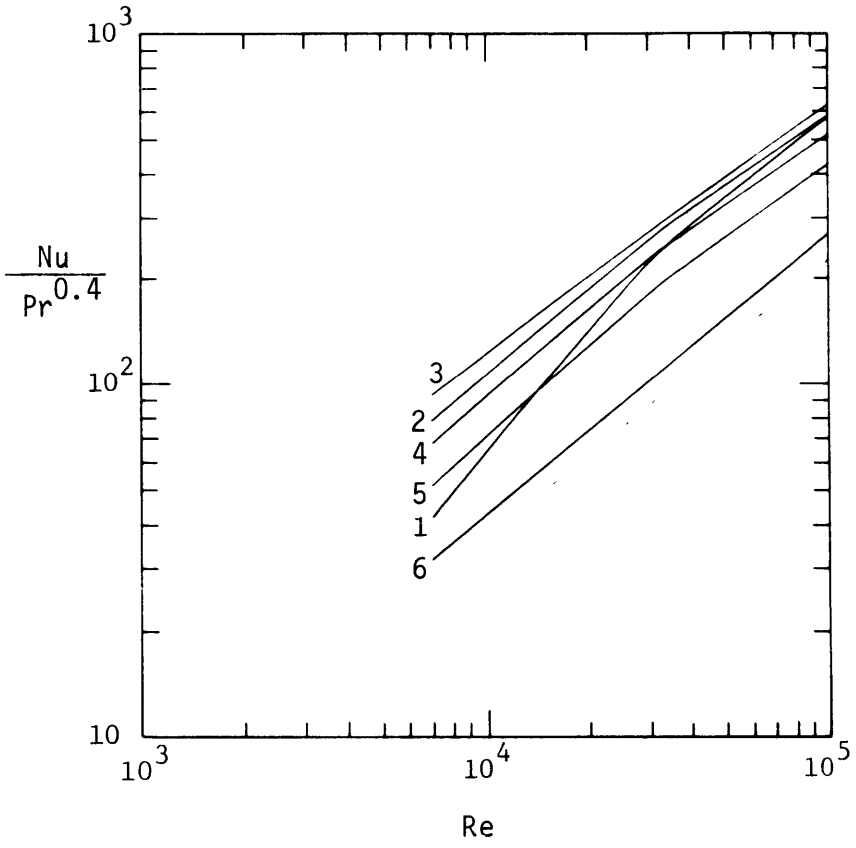

Fig. 51 Heat-transfer Results of Webb [41]

Pr = 5.10

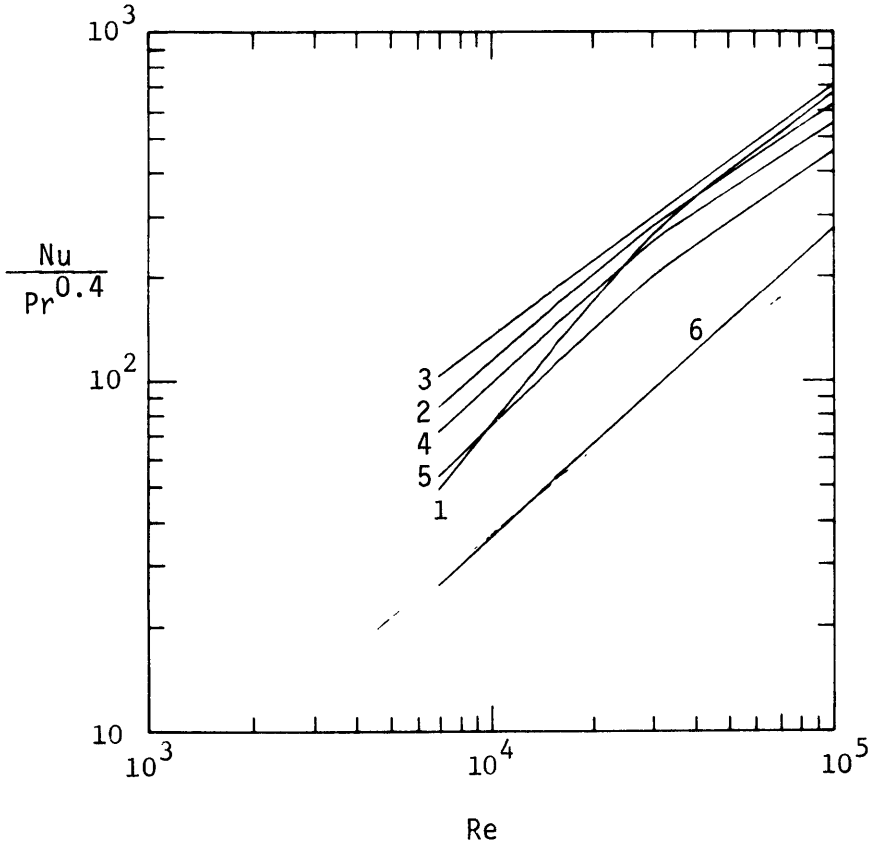

Fig. 52 Heat-transfer Results of Webb[41]

Pr = 21.7

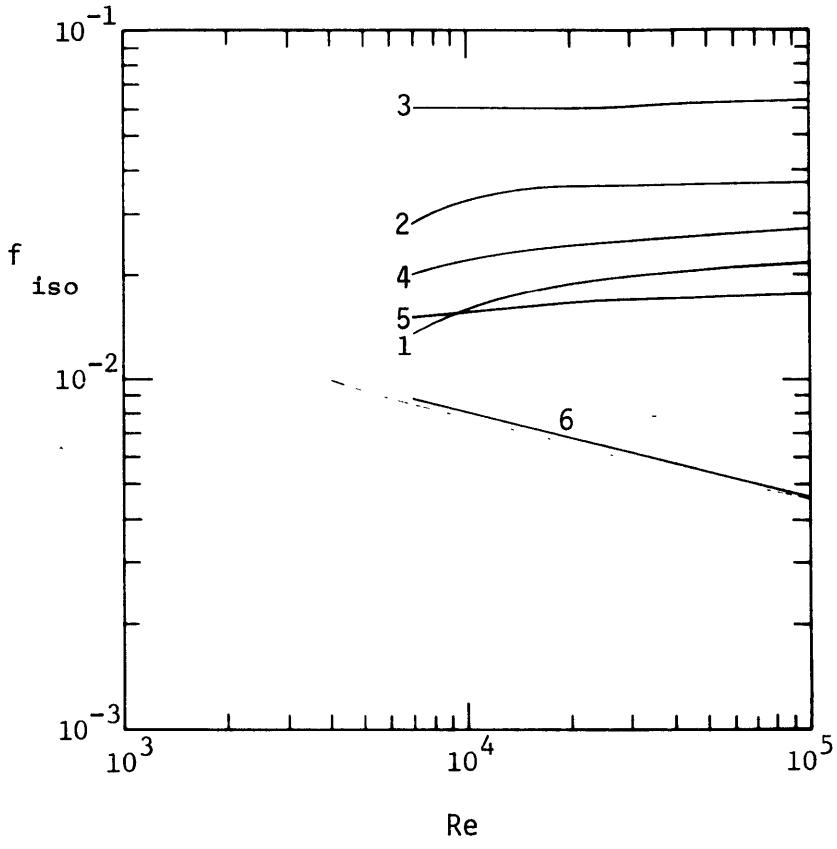

Fig.53 Pressure Drop Results of Webb[41]

Pr = 0.71

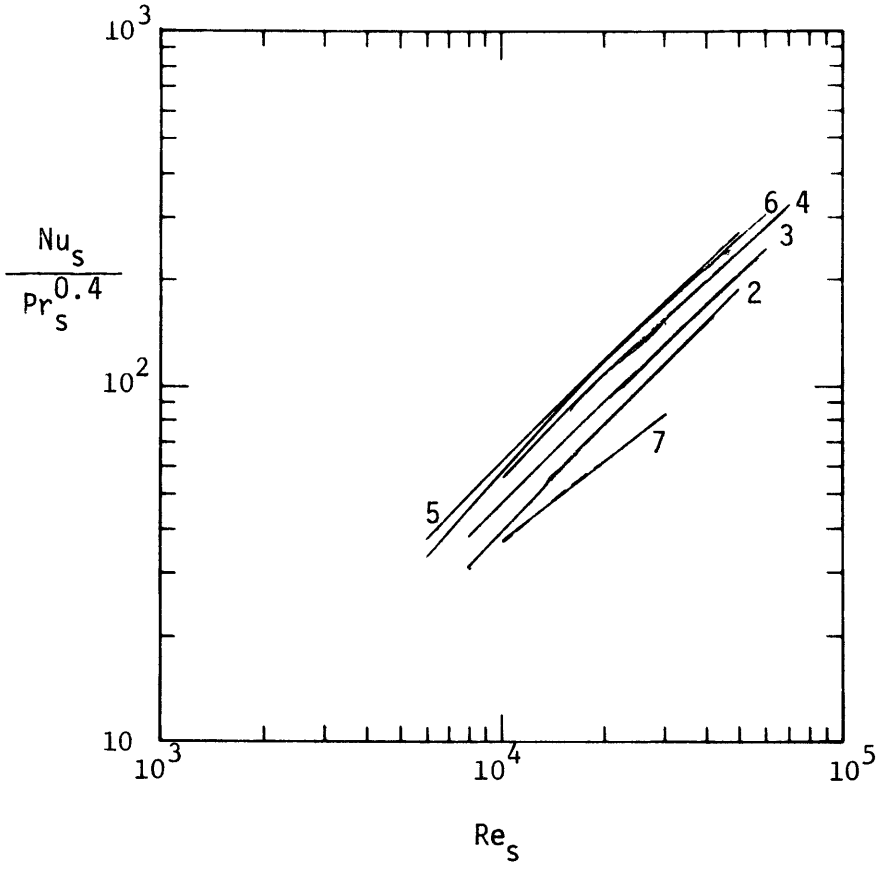

Fig. 54 Heat-transfer Results of Sams [44]

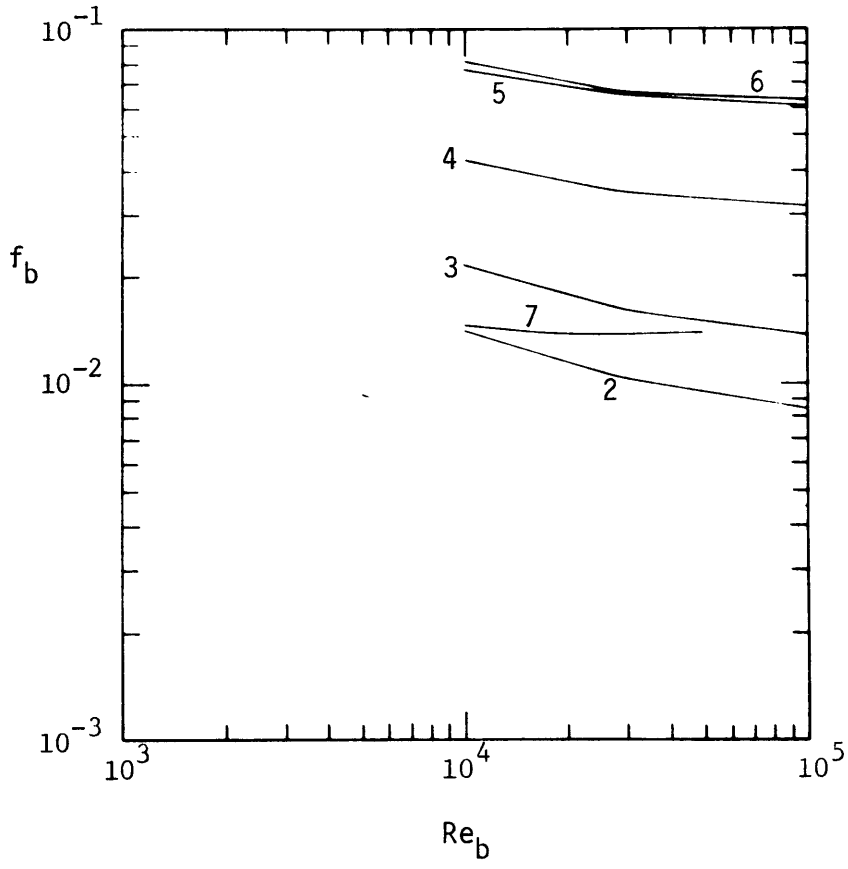

Fig. [55] Friction Data of Sams [44]

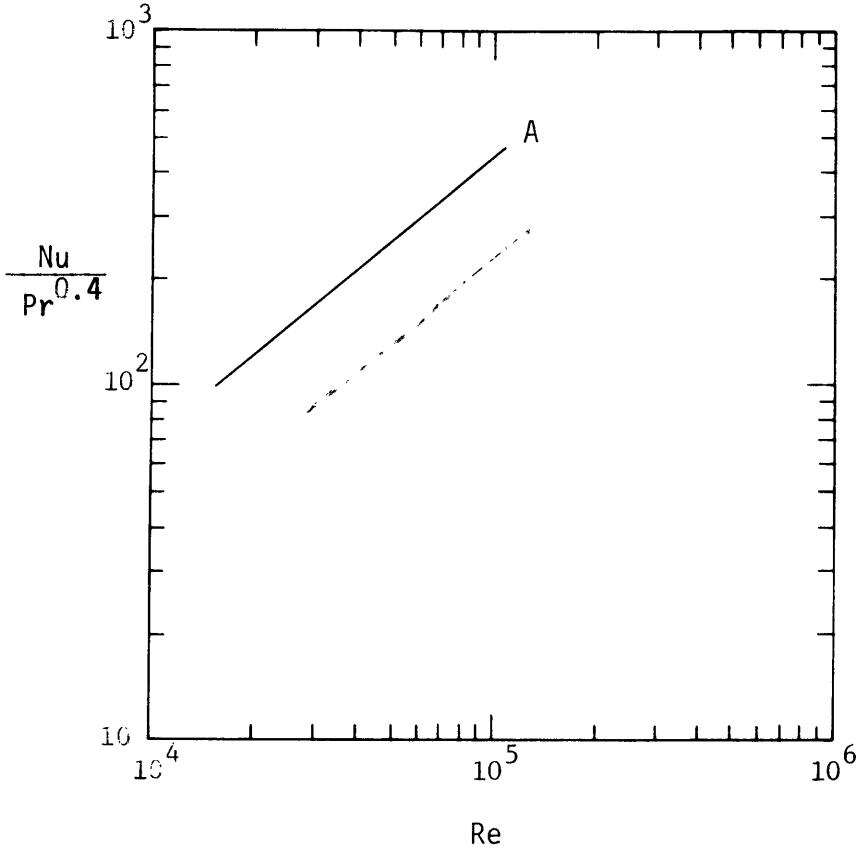

Fig. 56 Heat-transfer Results of Eissenberg [48]

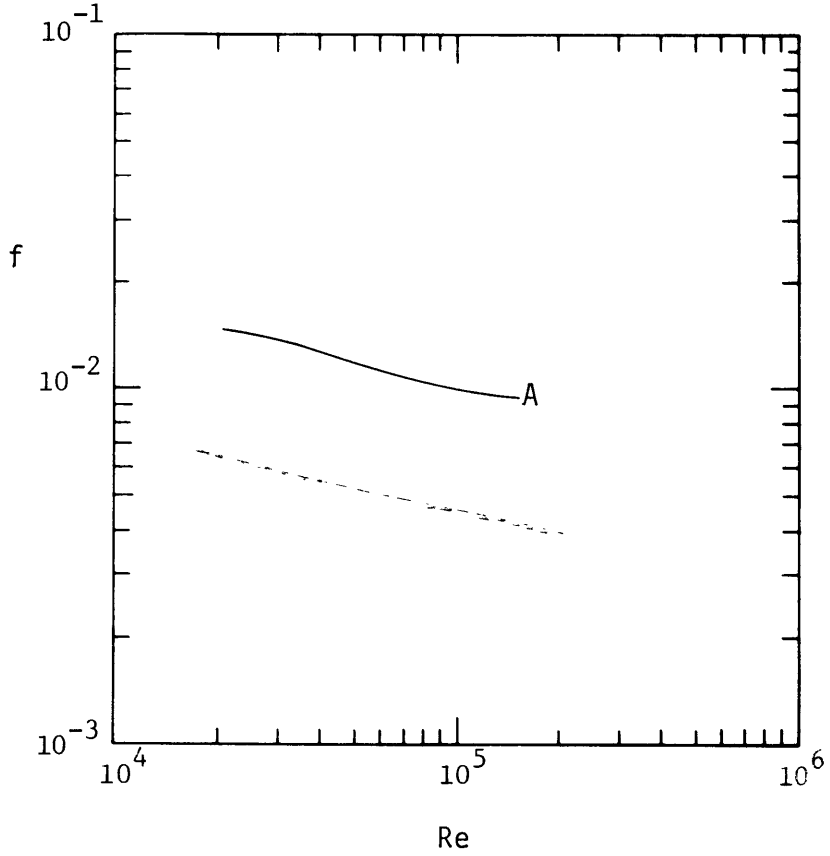

Fig. 57 Friction data of Eissenberg [48]

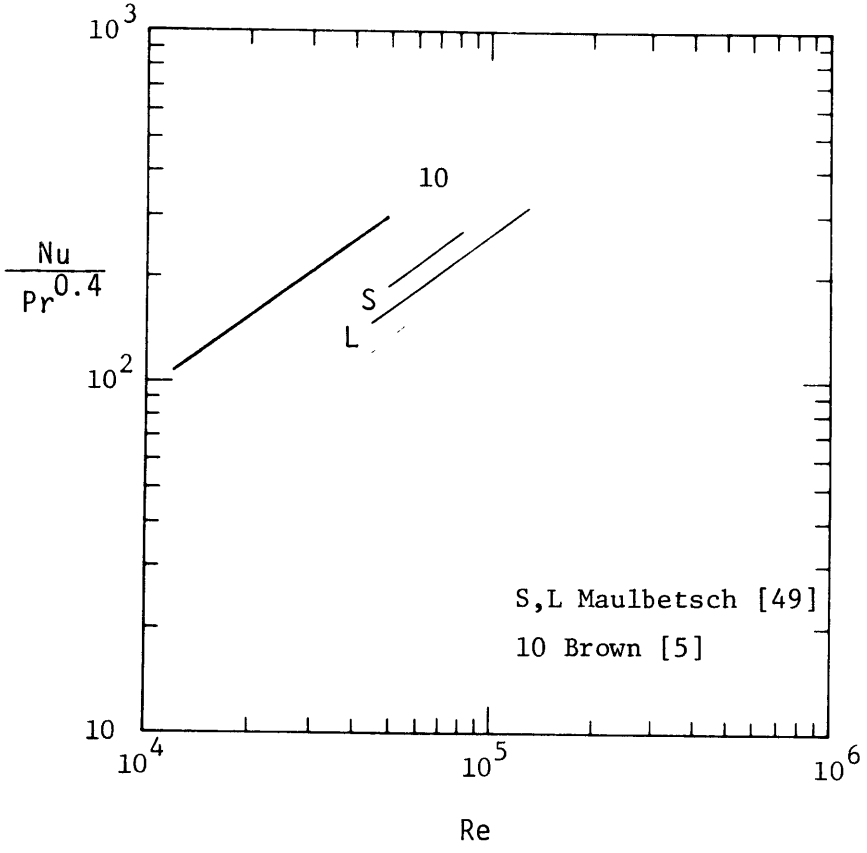

Fig. 58 Heat-transfer Data for Convoluted Tubes

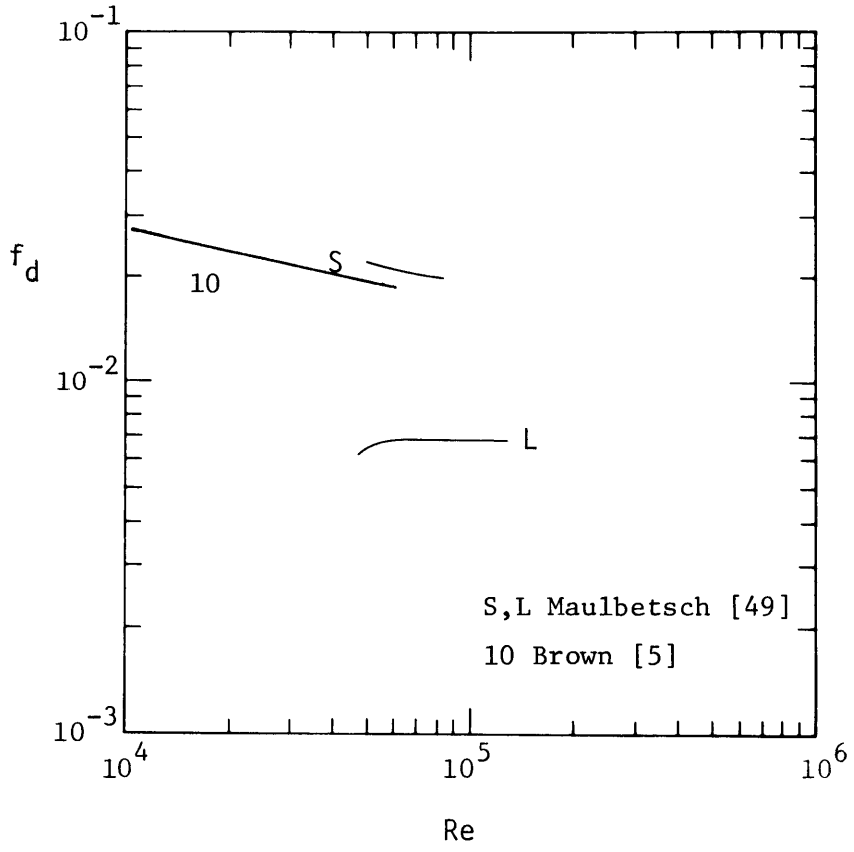

Fig. 59 Friction Data for Convoluted Tubes